Aalto University
School of Engineering

Timo Viitanen

Estimating the Validated Training Envelope of Simulators Used in Upset Prevention and Recovery Training

Thesis submitted for examination for the degree of Master of Science in Technology.

Helsinki, November 27th, 2017
Supervisor: Professor Pentti Kujala
Advisor: M.Sc. (Tech.) Olli Hänninen

Aalto-yliopisto
Insinööritieteiden korkeakoulu

Aalto-yliopisto, PL 11000, 00076 AALTO
www.aalto.fi

Diplomityön tiivistelmä

Tekijä Timo Samuli Viitanen		
Työn nimi Lentokoulutussimulaattoreiden validoidun lentoarvoalueen arviointi epätavallisten lentotilojen koulutusta varten		
Laitos Sovelletun mekaniikan laitos		
Pää-/sivuaine Lentotekniikka / virtausmekaniikka		**Koodi** Kul-34
Työn valvoja Professori Pentti Kujala		
Työn ohjaaja(t) Diplomi-insinööri Olli Hänninen		
Päivämäärä 27.11.2017	**Sivumäärä** 100 + 10	**Kieli** Englanti

Tiivistelmä

Lennonaikainen hallinnanmenetys on aiheuttanut kaupallisessa ilmakuljetuksessa enemmän kuolonuhreja kuin mikään muu onnettomuustyyppi kuluneen vuosikymmenen aikana. Kyseisen onnettomuustyypin ennaltaehkäisy on noussut yhdeksi tärkeimmistä lentoturvallisuuden kehityskohteista.

Euroopan lentoturvallisuusvirasto EASA ja Yhdysvaltain ilmailuhallinto FAA ovat reagoineet tilanteeseen uusilla vaatimuksilla, tarkoituksenaan varmistaa lentokoulutuksen antavan lentäjille valmiuksia välttää epätavallisia lentotiloja ja tarvittaessa suorittaa oikaisu. Tässä yhteydessä myös lentokoulutuksessa käytettäviä simulaattoreita koskeviin vaatimuksiin on tehty merkittäviä muutoksia. Aikaisemmin hyväksytyiltä simulaattoreilta ei ole vaadittu samaa realismin tasoa lentokoulutuksessa tavallisesti saavutetun lentoarvoalueen ulkopuolella.

Tämän diplomityön tavoitteena on selvittää epätavallisten lentotilojen koulutusta koskevien viranomaisvaatimusten nykytila ja lähitulevaisuuden näkymät, sekä tutkia kuinka vaatimustenmukaisuus voidaan osoittaa jo koulutuskäyttöön hyväksyttyjen simulaattoreiden kohdalla – tarkoittaen käytännössä simulaattorin lentomallin validointia oikeasta lentokoneesta mitattua koelentodataa vasten.

Diplomityö koostuu kirjallisuusselvityksestä, sekä kahdesta tapaustutkimuksesta. Ensimmäinen tapaustutkimus toteutettiin aineistoanalyysinä julkisesti saatavilla olevasta liikennelentokoneen koelentodatapaketista, tavoitteena tutkia miltä lentoarvoalueelta on tyypillisesti käytettävissä aerodynaamista dataa simulaattorin mallinnusta varten, sekä tutkia mitkä aerodynaamiset stabiliteettiderivaatat ovat oleellisimpia simulaattorin lentomallin vaatimustenmukaisuuden arvioinnin kannalta.

Toisessa tapaustutkimuksessa määritettiin lentokoulutusorganisaatioympäristössä käytössä olevalle simulaattorille epätavallisten lentotilojen koulutuksessa vaadittu validoitu lentoarvoalue. Tutkimuksessa selvitettiin simulaattorin lähdekoodista ja ohjelmistokuvauksista lentomallin sisältämän aerodynaamisen datan kattama arvoalue. Validoitu lentoarvoalue selvitettiin kokeellisella testauksella, verraten simulaattorin vastetta saatavilla olevaan koelentodataan. Tapaustutkimuksen asetelma vastaa tyypillistä hankalaa tapausta, jossa valmistajan tuotetukea ei ole enää saatavilla.

Avainsanat CAT, FFS, FSTD, LOC-I, QTG, UPRT, lentokoulutus, upset, validointi

Aalto University
School of Engineering

Aalto University, P.O. BOX 11000, 00076 AALTO
www.aalto.fi

Abstract of master's thesis

Author Timo Samuli Viitanen

Title of thesis Estimating the Validated Training Envelope of Simulators Used in Upset Prevention and Recovery Training

Department Department of Applied Mechanics

Major/minor Aeronautical Engineering / Fluid Dynamics **Code** Kul-34

Thesis supervisor Professor Pentti Kujala

Thesis advisor(s) M.Sc. Olli Hänninen

Date 27.11.2017 **Number of pages** 100 + 10 **Language** English

Abstract

Loss of control in-flight has been the most significant contributor fatal accidents in commercial air transport over the last decade. The mitigation of this accident type has been raised as one of the top safety priorities in commercial civil aviation.

As a reaction to the circumstances, the European Aviation Safety Agency and the Federal Aviation Administration of the United States have issued new provisions in effort to ensure that flight training provides pilots with the necessary knowledge and skill-set required to detect, avoid and, when needed, recover from aeroplane upset situations. Consequently, the qualification requirements for flight training simulators have been adapted to match this renewed type of training. Until recently, previously qualified simulators have not been required to demonstrate realistic fidelity outside of the normal training envelope.

The objectives of this master's thesis are to examine the status of the current and foreseeable regulatory framework related to upset prevention and recovery training, and to study how previously qualified simulators may be demonstrated compliant with the novel provisions.

This thesis is conducted by means of a literature study and two case studies. In the first case study an aerodynamic data package of a large transport aeroplane is examined in order to assess the ranges of aerodynamic data typically available for a simulator flight model, and to underline the essential aerodynamic stability derivatives that are required to evaluate the fidelity of a simulator flight model.

The second case study focuses on determining a validated training envelope for a previously qualified simulator, currently in use in flight training organisation environment. The range of the aerodynamic data encompassed within the simulator flight model was uncovered by examining the source code and software documentation of the simulator. Finally, a flight validated envelope was constituted by means of experimental testing and matching the response of the simulator with available flight test data. The problematics of this case study correspond to the typical challenging case in the industry, where support from the manufacturer is no longer available for an older device.

Keywords CAT, FFS, FSTD, LOC-I, QTG, UPRT, flight training, upset, validation

Acknowledgements

This thesis was written during the course of 2017 on free time without external funding.

First, I would like to express my gratitude to senior inspector M.Sc. Olli Hänninen, for originally introducing me to this truly interesting topic, and for his dedication and overwhelming expertise while advising the writing of this thesis.

Furthermore, I would like to thank Professor Pentti Kujala for supervising the thesis, and Seppo Ampio and Hannu Savinainen of the Finnish Aviation Academy for their help with the second case study.

I would also like to thank all my friends and my colleagues at the Finnish Transport Safety Agency for their support and understanding during this busier period of my life, as well as everyone in the Polyteknikkojen Ilmailukerho for enabling breaks from the daily grind, especially during the past gliding season.

Finally, a special word of thanks goes to my family, for the continuous support and encouragement, which they have always provided for me.

Helsinki, November 27th, 2017

Timo Samuli Viitanen

Table of Contents

Symbols

c_{D_0}	[-]	Drag force derivative with zero α
c_{D_q}	[-]	Drag force derivative with respect to q
c_{D_α}	[-]	Drag force derivative with respect to α
$c_{D_{\dot{\alpha}}}$	[-]	Drag force derivative with respect to $\dot{\alpha}$
c_{l_p}	[-]	Rolling moment derivative with respect to p
c_{l_r}	[-]	Rolling moment derivative with respect to r
c_{l_β}	[-]	Rolling moment derivative with respect to β
c_{L_0}	[-]	Lift force derivative with zero α
$c_{L_{\dot{q}}}$	[-]	Lift force derivative with respect to $\dot{q}$
c_{L_α}	[-]	Lift force derivative with respect to α
$c_{L_{\dot{\alpha}}}$	[-]	Lift force derivative with respect to $\dot{\alpha}$
c_{m_0}	[-]	Pitching moment derivative with zero α
$c_{m_{\dot{q}}}$	[-]	Pitching moment derivative with respect to $\dot{q}$
c_{m_α}	[-]	Pitching moment derivative with respect to α
$c_{m_{\dot{\alpha}}}$	[-]	Pitching moment derivative with respect to $\dot{\alpha}$
c_{n_p}	[-]	Yawing moment derivative with respect to p
c_{n_r}	[-]	Yawing moment derivative with respect to r
c_{n_β}	[-]	Yawing moment derivative with respect to β
$c_{n_{\dot{\beta}}}$	[-]	Yawing moment derivative with respect to $\dot{\beta}$
c_{Y_p}	[-]	Side force derivative with respect to p
c_{Y_r}	[-]	Side force derivative with respect to r
c_{Y_β}	[-]	Side force derivative with respect to β
$c_{Y_{\dot{\beta}}}$	[-]	Side force derivative with respect to $\dot{\beta}$
$\bar{c}$	[m], [ft]	Wing mean aerodynamic chord
C_D	[-]	Drag force coefficient
$C_{D_{Basic}}$	[-]	Basic drag force coefficient
$[C_D]_M$	[-]	Drag force coefficient at Mach number
C_l	[-]	Rolling moment coefficient
C_L	[-]	Lift force coefficient
$C_{L_{Basic}}$	[-]	Basic lift force coefficient
$C_{L_{max}}$	[-]	Maximum lift force coefficient
$C_{L_{ref}}$	[-]	Reference lift force coefficient
C_m	[-]	Pitching moment coefficient
$C_{m_{.25_{Basic}}}$	[-]	Basic pitching moment coefficient (c.g.=.25MAC)
C_n	[-]	Yawing moment coefficient
C_Y	[-]	Side force coefficient
F	[N]	Force
F_{aero}	[N]	Net force from aerodynamic model
F_{enigne}	[N]	Net force from engine model
F_l	[-]	Ground effect lateral control factor
$F_{l_{\dot{\beta}}}$	[-]	Ground effect sideslip factor

$F_{m_{GE}}$	[-]	Ground effect control factor
F_n	[-]	Ground effect lateral control factor
$F_{n_{\dot{\beta}}}$	[-]	Ground effect sideslip factor
$F_{undercarriage}$	[N]	Net force from gear model
F_x	[N]	Force about x body axis
F_y	[N]	Force about y body axis
F_z	[N]	Force about z body axis
F_D	[-]	Ground effect lateral control factor
F_{Y_β}	[-]	Ground effect sideslip factor
g	[m/s²]	Acceleration equivalent to standard gravity
g_x	[m/s²]	Gravity about x body axis
g_y	[m/s²]	Gravity about y body axis
g_z	[m/s²]	Gravity about z body axis
h	[m], [ft]	Altitude
I	[kgm²]	Moment of inertia
K	[-]	Coefficient interpolation factor
KIAS	[kts]	Knots Indicated Airspeed
L	[Nm]	Total moment about x body axis
M	[Nm]	Total moment about y body axis
m	[kg]	Mass
Ma	[-]	Mach number
MAC	[m], [ft]	Mean Aerodynamic Chord
N	[Nm]	Total moment about z body axis
n	[-]	Load factor
n_z	[-]	Normal load factor about z body axis
p	[rad/s]	Roll rate (about x body axis)
p_s	[rad/s]	Roll rate (about x body stability axis)
$\dot{p}$	[rad/s²]	Roll acceleration (about x body axis)
q	[rad/s], [deg/s]	Pitch rate (about y body axis)
$\dot{q}$	[rad/s²]	Pitch acceleration (about y body axis)
r	[rad/s]	Yaw rate (about z body axis)
r_s	[rad/s]	Yaw rate (about z body stability axis)
$\dot{r}$	[rad/s²]	Yaw acceleration (about z body axis)
t	[s]	Time
T	[Nms]	Total angular momentum
TAS	[kts]	True Airspeed
u	[m/s]	Velocity along x body axis
$\dot{u}$	[m/s²]	Acceleration along x body axis
v	[m/s]	Velocity along y body axis
$\dot{v}$	[m/s²]	Acceleration along y body axis
V	[m/s], [kts], [ft/s]	Airspeed
V_A	[m/s], [kts]	Manoeuvring airspeed
V_{MCA}	[m/s], [kts]	Minimum control speed (air)
V_{NE}	[m/s], [kts]	Never-exceed airspeed
V_{ref}	[m/s], [kts]	Reference speed
V_{stall}	[m/s], [kts]	Stall speed
V_{S1}	[m/s], [kts]	Stall speed in clean configuration
w	[m/s]	Velocity along z body axis

$\dot{w}$	[m/s²]	Acceleration along z body axis
X	[N]	Force about x body axis
$\dot{x}$	[m/s]	Velocity
$\ddot{x}$	[m/s²]	Acceleration
Y	[N]	Force about y body axis
Z	[N]	Force about z body axis
α	[rad], [deg]	Angle of attack
$\dot{\alpha}$	[rad/s], [deg/s]	Angle of attack rate
$\alpha_{F.R.L.}$	[rad], [deg]	Angle of attack relative to fuselage reference line
α_{max}	[rad], [deg]	Critical angle of attack
$\alpha_{W.D.P.}$	[rad], [deg]	Angle of attack relative to wing datum plane
β	[rad], [deg]	Angle of sideslip
$\dot{\beta}$	[rad/s], [deg/s]	Sideslip rate
δ_f	[rad], [deg]	Angle of flap deflection
δ_e	[rad], [deg]	Angle of elevator deflection
Δ	[-]	Change of quantity
ΔC_{D_α}	[-]	Change of drag force coefficient due to α
ΔC_{L_α}	[-]	Change of lift force coefficient due to α
$\Delta C_{l_{StallBreak}}$	[-]	Rolling moment coefficient at the stall break
ΔC_{m_α}	[-]	Change of pitching moment coefficient due to α
$\eta_{F.R.L.}$	[rad], [deg]	Stabiliser angle relative to fuselage reference line
θ	[rad], [deg]	Pitch angle
ϕ	[rad], [deg]	Bank angle
ψ	[rad], [deg]	Heading angle

Abbreviations

AC	Advisory Circular
AFM	Aeroplane Flight Manual
AMC	Acceptable Means of Compliance
ATPL(A)	Airline Transport Pilot License (Aeroplane)
AURTA	The Airplane Upset Recovery Training Aid
CAME	Conservation of Linear Momentum Equations
CAT	Commercial Air Transport
CFD	Computational Fluid Dynamics
CG	Centre of Gravity
CLME	Conservation of Angular Momentum Equations
CPL(A)	Commercial Pilot Licence (Aeroplane)
CRM	Crew Resource Management
CS-FSTD(A)	Certification Specifications for Aeroplane Flight Simulation Training Devices
CS-SIMD	Certification Specifications for Simulator Data
EASA	The European Aviation Safety Agency
EC	The European Communities
ECAM	Electronic Centralised Aircraft Monitor
EU	The European Union
FAA	The Federal Aviation Administration
FAR	Federal Aviation Regulation
FF	Free Flight
FFS	Full Flight Simulator
FPE	Flight Path Equations
F.R.L.	Fuselage Reference Line
FSTD	Flight Simulation Training Device
GE	Gravity Equations
GM	Guidance Material
IATA	The International Air Transport Association
ICAO	The International Civil Aviation Organisation
ICATEE	The International Committee for Aviation Training in Extended Envelopes
IOS	Instructor Operating Station
JAA	The Joint Aviation Authorities
JAR	Joint Aviation Requirements
KE	Kinematic Equations
LOCART	The Loss of Control Avoidance and Recovery Training Initiative
LOC-I	Loss of Control, In-Flight
LOFT	Line-Oriented Flight Training
MOFT	Manoeuvre-Oriented Flight Training
MPL	Multi-Crew Pilot Licence
MQTG	Master Qualification Test Guide
MSL	Mean Sea Level
NASA	The National Aeronautics and Space Administration
NPA	Notice of Proposed Amendment
OEM	Original Equipment Manufacturer

OSD	Operational Suitability Data
PANS-TRG	Procedures for Air Navigation Services - Training
Part-ORO	Organisation Requirements for Air Operations
PRD	Primary Reference Document
PSD	Power Spectral Density
QTG	Qualification Test Guide
RAeS	The Royal Aeronautic Society
RMT	Rulemaking Task
SARPs	Standards and Recommended Practices
SME	Subject Matter Expert
SOC	Statement of Compliance
SOQ	Statement of Qualification
UN	The United Nations
UPRT	Upset Prevention and Recovery Training
VDR	Validation Data Roadmap
W.D.P.	Wing Datum Plane
WP	Work Package

1 Introduction

1.1 Motivation

On February 12th 2009 a scheduled domestic passenger aeroplane stalled during approach in Buffalo, United States, and crashed in low visibility and heavily icing conditions. The National Transportation Safety Board of the United States concluded, after investigation, that crew fatigue was likely a contributing factor, and that "*the probable cause of this accident was the captain's inappropriate response to the activation of the stick shaker, which led to an aerodynamic stall from which the aeroplane did not recover."* [1]

Less than four months later on June 1st 2009 a scheduled passenger flight from Rio de Janeiro, Brazil to Paris, France perished in the Atlantic Ocean after experiencing temporary inconsistencies between the indicated airspeed readings during cruise flight. Several pitot probes were obstructed by ice crystal build-up as the aeroplane had entered a cumulonimbus cloud. According to the final report on the accident, "*in less than one minute after autopilot disconnection, the aeroplane exited its flight envelope following inappropriate pilot inputs*." [2]

Loss of control in-flight (LOC-I) accidents represent the highest risk to fatal accidents and hull losses in commercial civil aviation. This accident type accounts on average for more than one quarter of all casualties in scheduled commercial air transport. The International Civil Aviation Organisation (ICAO) has raised the prevention of LOC-I type accidents as a top safety priority. [3]

The aforementioned two accidents, Colgan Air flight 3407 and Air France flight 447, drew wide attention among the industry and authorities toward deteriorating manual flying skills and the adequacy of international flight crew training standards at the turn of the decade. Consequently, during recent years, the regulatory framework has been adapted to include requirements for additional training throughout a professional pilot's career, with the emphasis on early detection and correct application of recovery procedures in an impending upset situation.

Much of this training utilises the use of flight simulators, which consist of mathematical models of aeroplanes based on flight test data of their actual counterparts. As all civil aeroplanes are flight tested for their intended use – with only a limited level of additional control abuse, the behaviour of these training devices can be validated to match the behaviour of the real aircraft only in a limited range of flight regimes. [4]

Along this novel stance, the nature of utilisation of simulators in flight training has increasingly shifted from the normal operating envelope toward flight regimes bordering and in some cases even exceeding the edges of the flight tested envelope of an aeroplane. As a result, a necessity to define those borders of the flight envelope that still sufficiently represents reality, has emerged for those devices – that, in some cases, are used in a manner they were not initially designed for. This master's thesis focuses to analyse the issue and to provide a set of means to determine a validated training envelope for certain flight simulators.

1.2 Objectives and limitations of the thesis

The main objectives of this thesis are to summarise the background and requirements for simulator conducted upset prevention and recovery training in commercial air transport, and to produce means to assess the suitability of certain flight simulation training devices for such training. The first-mentioned objective is addressed through a literature study, focusing on the rationale behind upset training programmes, the challenges related to them, and the current and foreseeable state of the relevant regulatory framework.

The latter objective is addressed through two case studies, with the first being a parametric study of the contents of an aerodynamic data package, namely for a simulated flight model of the Boeing 747-100, with the intent of underlining the significant parameters, that define the fidelity of the flight model with sufficient accuracy. The Boeing 747 is a representative example of a long range very large jet airliner, cruising at transonic speeds and high altitudes.

In the second case study a simulator of the Beechcraft Super King Air 300, in use by a flight training organisation, is examined through testing and documentation research, in order to outline a validated training envelope for the device. This Level CG Full Flight Simulator serves as an example of an older device with grandfathered privileges, but nevertheless a solid customer base, being subject to new requirements and the qualification certificate holder faces the challenge to demonstrate compliance. The King Air 300 is a popular business and utility twin-turboprop, and as a slower and much smaller aircraft represents the other end of the scale compared to the Boeing 747.

Furtherly, considerations are made to find the best practices on how the qualification certificate holder may determine the acceptable limits of fidelity of flight models of different devices with varying sources of validation data, in order to successfully accommodate those devices into their upset training syllabi.

To provide the Reader with a coherent overall picture, it was found necessary to present a general overview of the technical basics of applicable flight simulation training devices; therefore Chapter Three is dedicated to this topic.

This thesis is limited to type-specific aeroplane simulators used by training organisations and air carriers to conduct initial and recurrent upset prevention and recovery training for commercial air transport pilots, who operate in multi-crew environment. The related authority requirements are studied especially from a European standpoint, although reflecting the developments in the trendsetting industry of the United States, as well as on the global level set by the ICAO, an agency of the United Nations.

The parametric study of the Boeing 747 aerodynamic flight model is conducted with free-air assumption, excluding effects of icing, ground operations and effects of simulated malfunctions leading to unsymmetrical flight conditions.

The effects of compressible aerodynamics, ground operations and control surface malfunctions were neglected in the case study of the Beechcraft King Air 300.

1.3 Research questions

According to guidance material to the current European Organisation Requirements for Air Operations (GM4 ORO.FC.220&230), a Level C, CG, D or DG Full Flight Simulator may be used to conduct upset recovery training exercises, if the training is conducted completely within the Validated Training Envelope (VTE) of the device. Regardless, the current regulations or guidance materials neither provides an exact definition for the term "Validated Training Envelope", nor means to determine such an envelope for a particular device. The background of upset training, the related regulatory basis, and the classification of flight simulation training devices are further discussed in Chapter Two.

The primary research questions of this master's thesis are intertwined with the term Validated Training Envelope of a Level C, CG, D or DG Full Flight Simulator. As the European regulations concerning provision of upset training are expected to expand in the near future – and possibly accommodate requirements for full-stall training – it is also essential to study in a broader context how the limits of satisfactory fidelity for a simulated flight model used in upset training may be assessed. This thesis will therefore address the following research questions:

- What is the status of current and foreseeable upset training provisions?
- What are the primary limitations of utilising simulators in such training?
- By which parameters should a simulator training envelope be defined?
- How should the Validated Training Envelope be determined for a previously qualified simulator, if support from the manufacturer is no longer available?

2 Aeroplane upset and upset mitigation strategies

2.1 Definition and causes of aeroplane upset incidents

Aeroplane upset is often erroneously perceived as being solely a stall related event. The ICAO has defined upset as an unintentional in-flight condition, in which an aeroplane exceeds the parameters normally experienced in line operations or training. More specifically, an aeroplane is considered to be in an upset condition when the pitch of the aeroplane unintentionally exceeds 25 degrees nose up or 10 degrees nose down, when the bank of the aeroplane unintentionally exceeds 45 degrees, or when the airspeed is inappropriate for the conditions. [5] Recently a broader definition has also been introduced by the AURTA, according which an aeroplane upset is "*an undesired airplane state characterized by unintentional divergences from parameters normally experienced during operations*". [6] Without appropriate and timely intervention by the pilot, aeroplane upsets are likely to lead to loss of control in-flight.

Not all aeroplane upset occurrences involve an aerodynamic stall, but an unintentional stall is a form of upset regardless of attitude, due to the criteria of being at an inappropriate airspeed for the conditions. [7] Nonetheless, stalls are a dominating contributor to LOC-I accidents, partially due to the tendency of a sudden roll-off, which may cause a distracted pilot to counter the roll through opposite aileron inputs, as what happened in the Colgan 3407 crash. The problematics of this issue are further elaborated in Chapter 2.5. Another common pilot error in an impending stall situation is to intuitively apply more thrust, which results in an unexpected nose-up moment in an aeroplane with engines installed below the wing. The correct counteraction in such a situation is to solely reduce the angle of attack, followed by the stabilisation of the aeroplane attitude. [8]

Causes of aeroplane upset incidents can be induced by environmental phenomena, systems-anomalies, flight crew, or a combination of all three. Environmental causes may include different forms of turbulence, windshear, microbursts, thunderstorms, mountain wave and icing. Systems-anomalies-induced occurrences are primarily related to flight instruments, autoflight systems or flight controls. Pilot-induced causes may include for example manual handling errors, instrument misinterpretation, distraction, vertigo or spatial disorientation. [9] According to a study conducted by the NASA, pilot-induced loss of control is by far the most important category to address within the LOC-I phenomenon. [10]

The above mentioned manual handling errors refer to inappropriate flight control inputs applied by the flight crew in response to abnormal events or flight regimes. It has been widely recognised, that the increasing level of cockpit automation has gradually shifted the focus away of teaching and practicing the basic stick-and-rudder manual flying skills and toward teaching the skills required to use and manage that automation. Additionally, some airline policies encourage the use of automation whenever possible during flight. This constantly growing reliance on automation has had an undesired impact on flight crews in the form of deteriorating manual flying skills. [10]

Psychological factors have a major significance in upset related events and have contributed to several LOC-I accidents. The effect of surprise or startle caused by unexpected changes may affect cognition and lead to delayed or irrational behaviour. In threatening situations the human mind tends to look for an immediate course of action, which is usually based on habit patterns and past experience. This kind of impulsive behaviour may become life threatening in an aeroplane upset situation, especially if there is no previous experience outside of the normal flight envelope.

During the past 10 years nearly 44 percent of all fatalities in commercial jet air transport have been caused by LOC-I accidents. Majority of these accidents involved an aerodynamic stall. The second highest cause of fatalities was controlled flight into terrain, with less than 21 percent of all fatalities. [11] The investigations have usually revealed a combination of several factors leading up to a loss of control, while the triggering event has very often been an external environmental factor, mainly meteorological, but potentially air traffic related in the form of wake turbulence. The three most common phases of flight when LOC-I accidents occurred during the period of 2010 to 2014 were initial climb, approach and cruise in the respective order. [12]

2.2 Upset related safety initiatives

In 2009 the British Royal Aeronautic Society (RAeS) launched an initiative in support with the ICAO to investigate the LOC-I phenomena and to provide recommendations of potential improvements and guidance material to mitigate such events; International Committee for Aviation Training in Extended Envelopes, or ICATEE was formed. The focus of ICATEE was to deliver a long-term strategy to reduce LOC-I accidents through enhanced upset prevention and recovery training (UPRT). [13]

In 2011 the Federal Aviation Administration (FAA) of the United States commissioned a rulemaking committee to develop upset prevention and recovery training methodologies. A year later, the European Safety Agency (EASA), the FAA and the ICAO combined efforts in what eventually became known as the Loss of Control Avoidance and Recovery Training (LOCART) initiative, where civil aviation authorities, pilot representatives, aeroplane manufacturers and subject matter experts were engaged in focused discussions to address the associated challenges. [5]

A data analysis conducted alongside this initiative revealed that the most frequently-identified cause of LOC-I accidents was pilot-induced, typically resulting from application of improper procedures – including inappropriate flight control inputs, spatial disorientation, poor aeroplane energy management, distraction and improper training. There were also found to be several records of successful recoveries from upset situations, and many other occurrences where a developing upset situation was effectively avoided. Accurate analysis of the situation by the flight crew and the timely and correct application of preventive/recovery techniques were found to be the key elements for successful recovery in most of these occurrences, but it was also found that some existing practices were either ineffective or even acted as an aggravating factor for upset in inappropriate responses by some flight crews. One example of such a practice is to emphasise minimal loss of altitude by minimising the reduction of angle of attack in an approach-to-stall

situation. Reducing the angle of attack should have the highest priority in such an event. [5]

ICATEE and LOCART have both finalised their observations and recommendations. The discoveries resulting from these initiatives turned attention toward enhancing the existing flight crew training programmes. A fundamental concept debated was the provision of upset prevention and recovery training throughout a professional pilot's career. Based on this work, the ICAO adopted several amendments to its norms, including UPRT requirements and recommendations to multi-crew pilot licencing (MPL) and commercial pilot licencing (CPL(A)), additional requirements for type rating, and requirements for recurrent training of pilots. Flight simulators are extensively utilised in these enhanced training programmes. [14]

2.3 Regulatory framework and supporting material

The ICAO is an agency of the United Nations, established to manage the administration and governance of the Convention on International Civil Aviation in 1944. Its role in international civil aviation is to provide global norms, known as Standards and Recommended Practices (SARPs), and policies for the member states to standardise their national regulations and aviation operations. SARPs are published in the form of annexes to the Chicago Convention. With 191 members and 190 of the 193 UN members, virtually all civil aviation authorities are committed to the ICAO objectives.

Following the LOCART initiative, the ICAO has amended Annex 1 (Personnel Licensing) and Annex 6 (Operation of Aircraft) to the Chicago Convention to include requirements for upset prevention and recovery training. A new chapter was added to the PANS-TRG (Procedures for Air Navigation Services - Training) to provide procedures for authorities, operators and training organisations to meet the new UPRT requirements introduced in Annex 1 and Annex 6. Additionally, a *Manual on Aeroplane Upset Prevention and Recovery Training*, also referred as the Document 10011, was published as support material for the new chapter in PANS-TRG. Document 10011 is further discussed in Chapter 2.3.1.

In comparison to the ICAO level, the regulatory framework in the European Union is notably more complex. The member states of the EU are bound by the "Basic Regulation" (EC) No 216/2008 of the European Parliament and of the Council, which establishes a European Aviation Safety Agency and sets a regulatory framework on common rules in the field of civil aviation. The basic regulation is supported by a set of implementing rules, consisting of so called "Cover Regulations", containing a short introductory regulation and annexes thereto – called "Parts", which contain the technical requirements for the implementation.

The basic regulation and its implementing rules are considered as hard law, being legally binding by definition. For each implementing rule there have also been published "Guidance Material" (GM) to assist the reader in complying, and "Acceptable Means of Compliance" (AMC) to serve as a means to fulfil the requirements. In addition, "Certification Specifications" (CS) are published as technical standards for aircraft, equipment and appliances. AMCs, GMs and CSs, are considered to be non-binding rules,

or soft law. The relevant European regulations for Full Flight Simulators used in upset prevention and recovery training are shown in Figure 1.

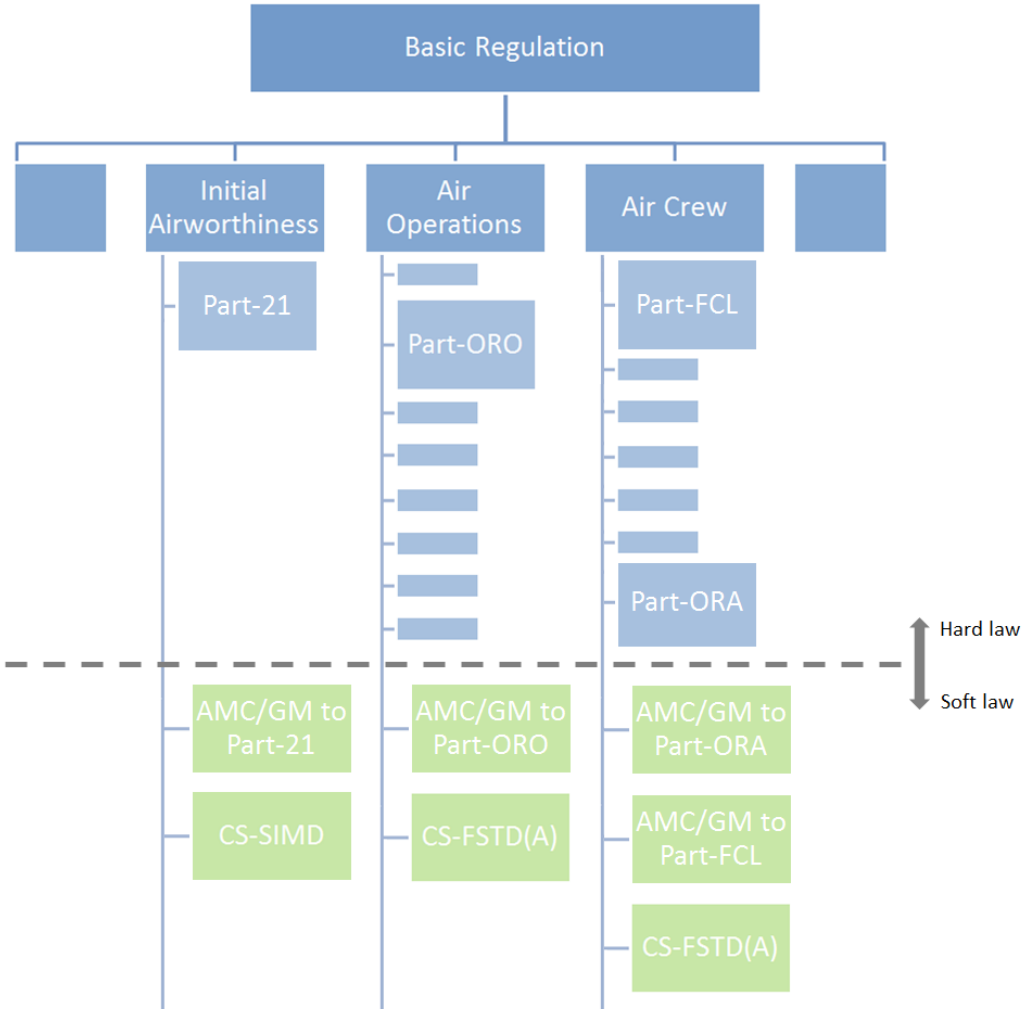

Figure 1 The relevant European regulations for upset prevention and recovery training and the use and qualification of flight simulation training devices

Part-21 of Commission Regulation (EU) No 748/2012 sets the implementing rules for the initial airworthiness of aircraft and related products, parts and appliances. In addition with the CS-SIMD (Certification Specifications for Simulator Data), these rules include requirements for flight simulator data packages provided by manufacturers of new aircraft types.

The implementing rules for technical requirements and administrative procedures related to air operations are laid down in Commission Regulation (EU) No 965/2012 and its parts. Training and checking programmes of flight crew and the use of flight simulation training devices by air operators are included in Part-ORO (Organisation Requirements for Flight Operations) of this regulation.

Commission Regulation (EU) No 1178/2011 contains the implementing rules for technical requirements and administrative procedures related to civil aviation aircrew. The relevant parts of this regulation are Part-ORA (Organisation Requirements applicable to Air Crew) and Part-FCL (Flight Crew Licencing), the first covering the organisation requirements for FSTD qualification certificate holders, and the latter covering the use of FSTDs in flight crew licencing level training.

Certification specifications for aeroplane flight simulation training devices (CS-FSTD(A)) describes the technical requirements a new FSTD has to comply in order achieve a certain level of qualification and to maintain that level. Older devices approved under the provisions of previous regulations may however retain their qualification level by grandfather rights. European regulations concerning the technical requirements of Full Flight Simulator used in upset recovery training are further discussed in chapter 2.4.3.

In the context of delivering UPRT, the most relevant EU regulations are doubtlessly encompassed within Part-ORO and Part-FCL, and the AMC's and GM's related to them, as well as CS-FSTD(A). The EU regulations concerning upset related training are further discussed in chapter 2.3.3.

All aviation activities in the United States are governed by the Federal Aviation Regulations (FAR), positioned under Title 14 of the Code of Federal Regulations and administrated by the FAA. The FARs are organised into sections called parts; the relevant regulations concerning the use and qualification of FSTDs in the United States are Part 60, Part 61 and Part 121. The FAA also publishes advisory circulars (AC) as additional guidance to comply with the regulations. Advisory circulars are informative in nature, describing guidelines and best practices. The FAA provisions concerning upset training are further discussed in chapter 2.3.4.

2.3.1 ICAO manual on upset prevention and recovery training

In 2014 the ICAO published Document 10011, titled as Manual on Aeroplane Upset Prevention and Recovery Training, which provides means of compliance for a training programme by which states can fulfil the new UPRT requirements in Annexes 1 and 6 to the Convention on International Civil Aviation. It is emphasized that such a programme should satisfy three distinctive objectives:

- to provide heightened awareness of threats,
- to enable effective avoidance at early indication of a potentially threatening situation, and
- to enable effective and timely recovery from a realised upset condition.

The two major components of UPRT programmes are academic and practical training. Academic training is training that focuses in studying and reasoning to enhance knowledge levels, in this case designed to provide pilots "*with the knowledge and awareness needed to understand the threats to safe flight and the employment of mitigating strategies"*. [5]

Practical training is further divided into two sub-components: on-aeroplane training and simulator training. It places an emphasis on developing specific practical or technical skills, in this case to "*effectively employ upset avoidance strategies and, when necessary, to effectively recover the aeroplane to the originally intended flight path*". [5]

On-aeroplane training would be conducted in light aeroplanes during licensing level (CPL(A) or MPL) training for the pilot to develop the "*knowledge, awareness and experience of aeroplane upsets and unusual attitudes, and how to effectively analyse the event and then apply correct recovery techniques*". This non-type-specific training would provide a general frame of reference for upset situations, transferrable to FSTD environment later in training. [5]

Finally, simulator training on specific or generic aeroplane types would be used to build "*knowledge and experience, and apply these to the multi-crew CRM environment, at all stages of flight, and in representative conditions, with appropriate aeroplane and system performance, functionality and response*". [5]

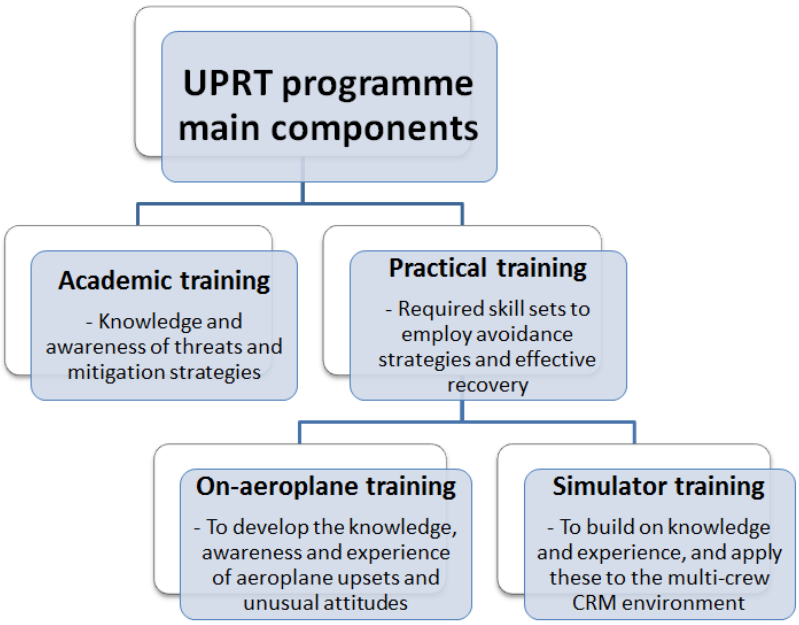

Figure 2 Main components of an ICAO-proposed UPRT programme

The ICAO has presented an integrated approach to upset prevention and recovery training, in which the above-mentioned training resources are identified and re-enforced throughout a pilot's career by utilising the existing training infrastructures. This concept is illustrated in Figure 3. Academic upset training would be provided continuously, starting from licensing level training and extending to the end of the career. Hands-on experience from authentic upset situations and correct recovery techniques would be gained from on-aeroplane training during initial licensing level. Finally, type-specific simulator based practical upset training would be provided during type rating training, as well as recurrent training in the forms of line-oriented flight training (LOFT) and manoeuvre-oriented flight training (MOFT).

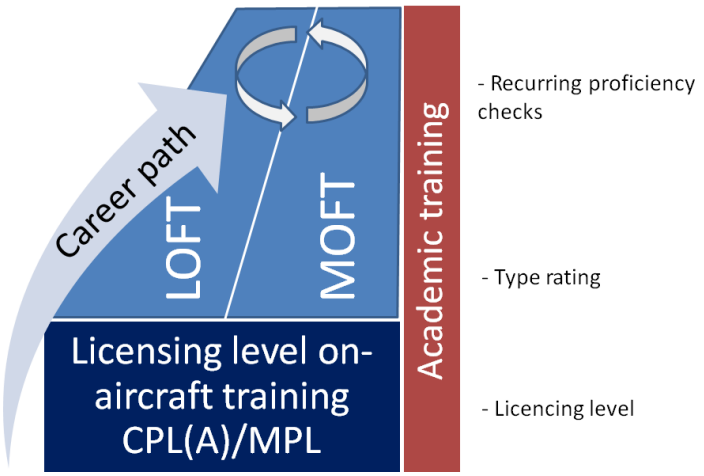

Figure 3 Integrated UPRT concept

The main goal of academic training is to instil the understanding that an upset situation is a natural threat, and that automation may not always help to prevent such occurrences. It is recommended that the academic training sessions should be directly related to – and held prior to practical training sessions with care taken to minimise the delays between. Academic training administered during type rating and recurrent training would provide a comprehensive recapitulation of the core subjects taught during licencing level training, as well as type-specific knowledge to be applied during practical simulator training. [5]

On-aeroplane upset training should not be focused on type-specific performance, but instead to introduction of general principles which may be applied to a broader range of aeroplanes. This training should be utilised to fill in the gap caused by limitations in simulator motion cueing and reduced emotional response, such as startle, in order to demonstrate the full range of conditions experienced in an actual upset recovery situation. On-aeroplane upset training differs notably from aerobatic training from human factors point of view, and therefore these two should not be considered synonymous; the primary objective of aerobatic flight training is to execute pre-planned manoeuvres with precision, whereas upset recovery training should focus on stabilisation of the aeroplane after a spontaneous abnormal event. Aerobatic training does not sufficiently address to the effects of startle, nor the analytical reasoning required for quick and correct determination of the required recovery action in a high stress situation. [5]

In practical stall training emphasis should be placed upon immediate actions after recognising the condition and that recovery is always performed in the same manner regardless to the manner by which the stall condition was entered. During on-aeroplane training the pilots should be introduced to both approach-to-stall conditions as well as developed aerodynamic stall conditions. However, due to fidelity limitations, the ICAO recommends that aerodynamic stall training with simulators should only be carried out as carefully managed demonstrations using only such devices that are qualified for the training task. [5]

The role of simulator based UPRT is to permit training in operational conditions that would otherwise be dangerous or impractical to accomplish. During type rating training and recurrent operator training the utilisation of simulators would complement the skills and knowledge achieved in on-aeroplane training during licensing level. It is identified as a major concern that the delivery of UPRT should always adhere with the valid training envelope for a particular device. [5]

2.3.2 Airplane Upset Recovery Training Aid

The Airplane Upset Recovery Training Aid (AURTA) is a document published in the public domain, crafted by a working group composed of industry specialists and the United States government officials, initially published in 1998 with the goal of providing pilots the necessary academic knowledge to recognise and avoid impending upset situations, and to enhance their ability to recover from actualised upset situations. This document was revised in 2004 to address limitations and procedures involving components of transport category aeroplanes, such as vertical stabilisers and rudders, and subsequently in 2008 to address high-altitude slowdowns. The AURTA specifically addresses to swept-wing transport category aeroplanes with 100 seats or greater, although the information presented within the latest revision is applicable to most jet aeroplanes operating routinely in high-altitude environment. [9]

In 2017, as a result of an ICAO and industry led effort, the document was revised for the third time to include information on turboprop and smaller swept-wing aeroplanes. At the same time the content was integrated into a website form and re-titled as Airplane Upset Prevention and Recovery Training Aid. In the industry the AU(P)RTA has evolved into a standard reference on the subject and its latest revision is widely referenced in guidance materials provided by the ICAO, the EASA and the FAA as a recognised source for basis of academic training programmes, as well as for the design of practical training exercises. [6]

2.3.3 EASA requirements on simulator based upset training

Since April 2015 the European Part-ORO regulations have required air transport operators to provide academic and practical upset prevention training during type conversion courses and recurrent training programmes. According to the regulation, practical upset recovery training exercises, such as approach-to-stall, should be conducted in a flight simulator qualified for the training task. Full aerodynamic stalls or other exercises outside the Validated Training Envelope of the simulator should not be conducted. However, it may be confusing that the current technical requirements placed in the CS-FSTD(A) do not require any additional UPRT-specific qualifications for FSTDs, but the device must meet the standards of certain general qualification levels in order to be used in upset training. [15]

The European Union is still in the process of fully incorporating the previously mentioned ICAO amendments into the European regulatory framework. The EASA has scheduled rulemaking tasks RMT.0581 and RMT.0582 on “Loss of Control Prevention and Recovery Training” in its 2014-2019 Rulemaking programme. The requirements and provisions by these rulemaking tasks include simulator based UPRT for multi-pilot type rating courses,

requirements for continuous UPRT training programmes for CAT operators and requirements for simulator instructors. A Notice of Proposed Amendment (NPA 2015-13) concerning these rulemaking tasks was issued in September 2015 and the new training provisions are expected to take place in April 2018, followed by a one year transition period. In the EASA rulemaking process, an NPA is a drafting of a new rule, published for commenting by stakeholders. [13]

In this NPA the EASA proposed that upset recovery training should act as a prerequisite for the first issue of a single-pilot high-performance complex aeroplane type rating in multi-pilot operations and multi-pilot aeroplane type rating training courses. Recovery exercises of this training must be conducted in a type-specific simulator qualified for the training task, and should cover approach-to-stall situations and recovery from nose high and low attitudes at various bank angles. Requirements for full-stall and post-stall recovery exercises were not included at the time of the proposition, as aeroplane manufacturers were still considered to be in trial phase of demonstrating solutions to provide validated data in support of simulator based full-stall training. For the same reason the technical qualification requirements for flight simulation training devices listed in the CS-FSTD(A) were not yet amended to include full-stall behaviour. [16]

The effective technical requirements for the devices were however considered to not have kept up with the pace of technological advancements, or the upcoming training provisions. Therefore, in July 2016, the EASA commenced an additional rulemaking task RMT.0196 for the purpose of updating these requirements. Due to the complexity and volume of the issues to be addressed, this RMT was divided into three work packages (WP), each scheduled to produce an Agency Decision in three consecutive years, starting from 2017. Starting with the most urgent issues, the WP1 has proceeded to NPA phase in July 2017, as NPA 2017-13 was issued, and the first Agency Decision is expected in the fourth quarter of the year 2017. [17]

The main objectives of this first NPA are to make the qualification requirements encompassed in the CS-FSTD(A) compatible with the new UPRT requirements, to sharpen the competency requirements for FSTD inspectors, and to provide guidance material to assist stakeholders in assessing the suitability of each FSTD for specific training tasks. In this NPA an optional qualification based on special evaluation is proposed for those devices intended to be used for training in post-stall regime. This qualification is further addressed in Chapter 2.4.3. [18]

2.3.4 FAA requirements on simulator based upset training

Compared to Europe, more stringent requirements have already taken place in the United States. US Public Law 111-216, titled as Airline Safety and Federal Aviation Administration Extension Act of 2010, mandated all CAT operators to start conducting stall prevention training and, beginning in 2019, to conduct instructor-guided hands-on training on recovery from full-stall and stick-pusher activation. Air carriers are required to provide stall event training for pilots during the following career phases:

- Initial training,

- Transition training,
- Differences and related aircraft differences training,
- Upgrade training,
- Requalification training,
- Recurrent training.

[19]

The training methodology should follow a building block approach of first introducing academic understanding before progressing to practical application of those skills in a simulator. The FAA recommends air carriers to incorporate applicable sections of the AURTA on stall aerodynamics and high-altitude stalls into their academic training.

Simulator based stall prevention training may be provided as manoeuvre-based or scenario-based training; the first focusing on individual tasks, such as take-off, and the latter focusing on decision-making skills relating to stall prevention during line-oriented flight training. In scenario-based training the impending stalls may be induced for example by minor malfunctions, air traffic control instructions or unsuitably selected autopilot mode. The FAA encourages training providers to utilise the highest fidelity devices available for these training tasks, and requires the instructors to be familiar with the limitations of the particular devices in order to mitigate negative transfer of training. [20]

The focus of full-stall training should be on manoeuvre-based tasks, in which the pilot may be asked to call out some indications of the impending stall, but the response is deferred until directed to recover in order to experience the aeroplane's behaviour in full-stall regime. Stick-pusher training should be conducted as a repetitive exercise, until the pilot's reaction is to permit the reduction of angle of attack even at low altitudes. [20]

In 2016 the FAA issued a retroactive directive, the FSTD Directive 2 of Appendix A to Part 60, which imposes additional requirements for previously qualified simulators that are used to conduct certain training manoeuvres, such as full-stall demonstrations, under FAA approved training programmes. Such simulators will be required to be additionally qualified for those specific training tasks after March 12th 2019. These requirements are already effective for initial qualifications of new simulators. [21]

2.3.5 Examples of upset recovery training tasks

Current EASA provisions

The currently effective Part-ORO requirements include UPRT training provisions for European operators during conversion training and recurrent training. The required exercises for recurrent upset recovery training are listed in the respective AMC:

Table 1 Recurrent upset recovery exercises (AMC1 ORO.FC.220&230) [22]

Exercises		Ground Training	FFS Training
A.	**Recovery from developed upsets**		
1.	Timely and appropriate intervention	•	•
2.	Recovery from stall events, in the following configurations; - take-off configuration, - clean configuration low altitude, - clean configuration near maximum altitude, and - landing configuration during the approach phase.	•	•
3.	Recovery from nose high at various bank angles	•	•
4.	Recovery from nose low at various bank angles	•	•
5.	Consolidated summary of aeroplane recovery techniques	•	•

All of these exercises are required to be covered by a period not exceeding 3 years. It is further elaborated in the respective guidance material, that a "stall event" in this context refers to an approach-to-stall situation only, in which the aeroplane experiences one or more conditions associated with approach-to-stall or aerodynamic stall. Full aerodynamic stalls should not be conducted to avoid negative training due to insufficient fidelity. In other words the critical angle of attack should not be reached during these exercises, and the sideslip angle is likely to remain within a moderate region. [22]

Current FAA provisions

The guidance material issued by the FAA to fulfil the training provisions applicable to air carriers is divided into two Advisory Circulars: AC 120-111 *"Upset Prevention and Recovery Training*", and AC 120-109A "*Stall Prevention and Recovery Training*".

The Advisory Circular 120-111 describes the recommended academic and simulator training for aeroplane UPRT. The training tasks include recovery exercises from nose-high and nose-low situations, which should initially be practised as manoeuvre based training, followed by scenario based training. For the recovery from nose-high situations, pilots are instructed to push to achieve less than 1 g's. It is highlighted that special care must be taken in the use of rudder during upset prevention and recovery manoeuvres. Rudder is still effective in high angles of attack, and therefore it is important to guard against excessive inputs and control reversals. The instructor should provide feedback if the recovery was too aggressive, insufficiently positive, or if control inputs were excessive or cyclic with control reversals. After a successful recovery, the instructor should elucidate that the absence of g-load sensing may lead to a tendency to undercontrol recovery in the real aeroplane, when these loads are sensed. [19]

A recovery task from nose-high situation is described as follows. Either pilot should recognise and confirm the developing situation and announce "Nose High". Subsequently, the pilot flying should disconnect the autopilot, disable auto-throttle and apply as much nose-down control input as required to obtain a nose-down pitch rate. Thrust should be adjusted as required. When airspeed is sufficiently increasing, the pilot flying should

recover to level flight. Throughout the recovery, the pilot not flying should monitor airspeed and attitude, and announce any continued divergence. [19]

The Advisory Circular 120-109A, published in November 2015, contains guidelines for the implementation of stall prevention and recovery training by operators based in the United States. Stall prevention training may consist of manoeuvre based exercises, in which impending stalls should be trained in the following configurations:

- Take-off and manoeuvring configuration
- Clean configuration
- Landing configuration

Using the following conditions:

a) Level flight and turns using a bank angle of 15 to 30 degrees
b) Manual and automated flight
c) Visual and instrument flight conditions
d) High altitudes near the aeroplane's maximum altitude and low altitudes within 500 feet above ground level
e) Various weights and CG locations within aeroplane's limitations

[20]

Commonly for these exercises, the aeroplane's operational limitations should not be exceeded during recovering, hence the critical angle of attack should not be reached at any point and the sideslip angle should stay within a moderate region. Emphasis is laid on correctly and timely applied preventative actions, performed immediately after recognition of an impending stall. Momentary secondary stall warnings are tolerated, as long as the angle of attack is promptly reduced and the aeroplane's limitations are not exceeded.

A full-stall training manoeuvre is initiated by creating a situation that yields an unfavourable energy trend; this may be achieved by reducing thrust to less than adequate to maintain airspeed, or adjusting flightpath by changes to climb rate or entering turns. Upon pilot recognition of the impending stall, the instructor encourages to furtherly increase the angle of attack in order to reach full-stall, while highlighting the impending stall cues. When asked to recover by the instructor, the pilot should perform a smooth and deliberate reduction of angle of attack. Attention is paid to appropriate application of thrust, avoidance of secondary stalls, and thoughtful rudder and aileron control inputs. The simulator should be able to accurately demonstrate type-specific aural and motion cueing and reduced roll stability encountered in these flight regimes. In addition to very high angles of attack, also high sideslip angles may be reached during these exercises. [20]

2.4 Flight simulation training devices

2.4.1 Definition and classification

According to CS-FSTD(A), a flight simulation training device (FSTD) is defined as a training device which, in the case of aeroplanes, is a Full Flight Simulator (FFS), a Flight Training Device (FTD), a Flight and Navigation Procedures Trainer (FNPT), or a Basic Instrument Training Device (BITD). [23]

A Full Flight Simulator represents the highest fidelity of flight simulation training devices. Such device is a qualified full size replica of a specific type (make, model and series) aircraft cockpit, including all equipment and software necessary to represent the aircraft in ground and flight operations, a visual system providing an out of the cockpit view, and a motion cueing system. [24]

A Flight Training Device is a qualified full size replica of a set of instruments, equipment, panels and controls of a specific aircraft type in an open or enclosed cockpit configuration. There is no requirement for an FTD to be equipped with a motion cueing or visual system, and the equipment and software should represent the aircraft in ground and air operations to the extent of the systems installed in the device. [24]

Unlike FFS and FTD, a Flight Navigation Procedures Trainer does not usually represent a specific type of aircraft, but instead a generic cockpit environment of a class of aeroplane. FNPT's are typically used for obtaining instrument training credits. Finally, a basic instrument training device is a training platform for at least the procedural aspects of instrument flight, and it may for example consist of screen based instrument panels and spring loaded flight controls. [24]

Flight simulation training devices have qualifications based on their level of technical ability. For example a Level 1 FTD could be a device built for partial system training, having only one system fully represented, whereas a Level 2 FTD would have all systems of the specific aircraft type represented in an enclosed cockpit. Qualification levels of Full Flight Simulators goes from A to D, with D having the highest fidelity.

European FSTD operators have the right to retain the qualification level of older devices granted under a previous regulation of an EASA member state. These "Grandfather rights" are denoted by adding the letter G in the qualification level of the device; for example "FFS CG" would refer to a grandfathered Level C Full Flight Simulator. The pilot receives equal amount of training credits, regardless if the device is grandfathered or not. [24] Generally a grandfathered Full Flight Simulator has been designed for exactly the same training purposes as its modern counterpart of the same qualification level. As an example, the lists of required functions and subjective tests are almost identical between the current CS-FSTD(A), and aeroplane simulator evaluation requirements FAA AC 120-40a, issued in 1986. The differences lay in the capabilities of the devices; a modern simulator is able to represent reality with higher fidelity, and is therefore also subject to more stringent testing and tolerances during the qualification process. [24], [25]

2.4.2 Qualification process by the competent authority

Flight simulation training devices are subjected by authorities to an evaluation process, with the purpose of qualifying the flight simulator as an acceptable replication of the aeroplane. This process consists of an initial evaluation and subsequent recurrent evaluations. The initial qualification is achieved by inspecting and approving the validation data obtained from the flight test programme of the aeroplane, and subsequently comparing the performance of the device to this data.

The authority approved document produced during the process, referred as master qualification test guide (MQTG), contains test results, statements of compliance and other information to acknowledge that the device meets the requirements set for the applied qualification. Between each recurrent evaluation, qualification test guide (QTG) tests are progressively executed in order to demonstrate that the performance of the device is continuously, and within tolerances, matching to the validation data, and that there are no significant deviations from the MQTG.

The regulatory document which was the applicable technical regulation during the initial qualification is referred as the Primary Reference Document (PRD); all the required tests and tolerances to attain a certain qualification level are contained in the PRD. If a simulator has been grandfathered for such training, which has become subject of more stringent regulation, the device is still required to comply solely with the provisions set in the PRD. For new simulators qualified by aviation authorities under the European Union, the PRD is the CS-FSTD(A).

It is noteworthy that the fidelity of the aerodynamic model can only be tested under a limited set of flight conditions with reasonable effort. Therefore a representative set of samples is tested during the qualification process to provide sufficient confidence that the aerodynamic model behaves accordingly also between the sampled data points, within the envelope. This confidence may be strengthened by additional subjective testing, where a suitably qualified subject matter expert (SME) reflects the response of the device to his/her flight experience.

2.4.3 Full Flight Simulators used in upset recovery training

Until recent years, simulator requirements for stall manoeuvres were predominantly limited to evaluation of stall speeds at relatively low altitudes. Even in the current CS-FSTD(A), stall characteristics are required to be tested only in 2nd segment climb, approach and landing conditions. [24] As the typical training exercise was composed of an approach-to-stall situation, terminating at the first activation of stall warning, little emphasis was placed upon the fidelity of the simulation at angles of attack exceeding the initial stall warning. Consequently, the handling characteristics of previously approved simulators may not always provide the sufficient level of realism, required to teach the appropriate techniques for stall recognition and recovery from a stalled flight condition.
[25], [26]

Current EASA provisions

According to current European regulations for air operators, practical training of upset prevention can either consist of training conducted in an FSTD or an aeroplane, whereas practical training of upset recovery should solely consist of training in an FFS qualified for the training task. It is further elaborated that a Level C or D device is required for upset recovery training tasks and that all training should be conducted within the Validated Training Envelope of the device. [22] Level C equals to the second highest level of fidelity, fulfilling the general technical requirements listed in Table 2. Level D implies the highest qualification level, comprising enhanced sound and motion systems. [24]

Table 2 General technical requirements for Level C and D FFS devices (Appendix 8 to AMC1 FSTD(A).300) [24]

Qualification Level	General technical requirements
C	- An enclosed full-scale replica of the aeroplane cockpit/flight deck including simulation of all systems, instruments, navigational equipment, communications and caution and warning systems. - An instructor's station with seat should be provided. Seats for the flight crew members and two seats for inspectors/observers should also be provided. - Control forces and displacement characteristics should correspond to that of the replicated aeroplane and they should respond in the same manner as the aeroplane under the same flight conditions. - Validation test data should be used as the basis for flight and performance and systems characteristics. - Additionally ground handling and aerodynamics programming to include ground effect reaction and handling characteristics should be derived from validation flight test data. - A daylight/twilight/night visual system is required with a continuous, cross-cockpit, minimum collimated visual field of view providing each pilot with 180 degrees horizontal and 40 degrees vertical field of view. - A six-degrees-of-freedom motion system should be provided. - The sound simulation should include the sounds of precipitation and other significant aeroplane noises perceptible to the pilot and should be able to reproduce the sounds of a crash landing. - The response to control inputs should not be greater than 150 ms more than that experienced on the aeroplane. - Windshear simulation should be provided.
D	As for Level C plus: - Extended set of sound and motion buffet tests.

The term "Validated Training Envelope" is not defined or mentioned in the current technical requirements enclosed in the CS-FSTD(A).

Currently the EASA does not require separate qualifications for upset training, but regards a Full Flight Simulator qualified as Level C, CG, D or DG sufficient, as long as the training tasks do not exceed the capabilities of the device. The current European validation test requirements, as defined in the CS-FSTD(A), includes a stall characteristics test, starting with wings level at 1 g condition, with thrust at or near idle power. The time history data should include entry into stall, development of a full-stall and initiation of recovery. Stall warning should occur in the proper relation to stall and aeroplane specific characteristics, such as sudden pitch attitude change or sudden decrease of the load factor should be accurately replicated. For Level D devices, a separate test measuring approach-to-stall buffet, should also be conducted. There are no particular requirements to test combinations of high angle of attack and high sideslip angle, however steady state sideslips and engine out trim conditions are covered by separate validation tests. [24]

In addition to objective validation tests, the CS-FSTD(A) also lays down requirements for subjective tests, conducted by a suitably qualified person. These tests cover manoeuvres such as high angle of attack, approach to stall, stall warning initiation, buffet and g-break, performed at different aeroplane configurations. The subjective testing should also cover the flight envelope which may be reasonably achieved by a trainee, even though the device has not been approved for training in that area. [24] The possibility of a trainee being able to reach such flight regimes that are not approved for training, highlights the need to determine the Validated Training Envelope and to be able to detect when an excursion occurs.

Foreseeable EASA provisions

In the proposed revision of these requirements (NPA 2017-13 "*Update of flight simulation training devices requirements*"), it is described that this envelope should depict the confidence level of the simulation, depending on the degree of flight validation behind the aerodynamic modelling. This envelope should be presented with respect to angle of attack and sideslip angle, or by an equivalent method. It is furtherly proposed that the term "Validated Training Envelope", used in Part-ORO requirements should be replaced with the term "FSTD training envelope" for harmonisation with the corresponding FAA regulations. In the aforementioned NPA, it is also proposed that the general technical requirements for Level C and D devices, as listed in Table 2, should be amended to include a UPRT feedback mechanism for the instructor. [18] The proposed requirements concerning the FSTD training envelope and the IOS feedback mechanism is further discussed in Chapter 4.4.

The NPA 2017-13 also encompasses proposals to amend the qualification requirements for stall characteristics tests set in the CS-FSTD(A). The proposed tolerances for stall characteristics tests are listed in Table 3 – it is noteworthy how these tolerances are almost identical to the corresponding FAA requirements, already in force. [18]

Additional initial qualifications are proposed for all simulators used to conduct training manoeuvres at angles of attack beyond the activation of the stall warning system. Emphasis is placed upon the "*recognition cues, as well as the performance and handling qualities of*

a developing stall through the stall identification angle of attack and stall recovery". Due to limitations of available validation data, no strict tolerances are proposed for any parameter beyond the stall warning angle of attack, but instead a Statement of Compliance (SOC) defining the source data and methods used to develop the aerodynamic stall model is to be required. [18]

At minimum, the SOC should identify the sources of data used to develop the aerodynamic model, the FSTD training envelope with respect to angle of attack and sideslip angle where the aerodynamic model stays valid for training, and finally the type specific model characteristics. The aerodynamic model must incorporate the following model characteristics, where applicable per aeroplane type:

- degradation of the static/dynamic lateral-directional stability,
- degradation in control response (pitch, roll and yaw),
- uncommanded roll acceleration of roll-off requiring significant control deflection to counter,
- apparent randomness or non-repeatability,
- changes in pitch-stability
- stall hysteresis,
- Mach effects,
- stall buffet, and
- angle of attack rate effects.

An additional SOC is required, confirming that a qualified SME pilot, knowledgeable to the aeroplane type, has subjectively evaluated the aerodynamic stall model. The recognition cues and handling qualities from stall break through recovery should be sufficiently "representative", meaning that the type-specific level of fidelity is on such level that the training objectives can be satisfactorily accomplished. [18]

Current ICAO provisions

The fidelity requirements for Full Flight Simulators used in UPRT are addressed in Section 4 of the ICAO Document 10011, where it is presented that most FSTD's may be used satisfactorily for a significant portion of upset training not involving full-stalls, as long as the simulation remains within the valid training envelope. The valid training envelope is defined as the region of angle of attack and sideslip that is included in the flight envelope data provided by the original equipment manufacturer and used for the qualification of the simulator. For full-stall demonstrations the ICAO recommends the utilisation of a type-representative post-stall aerodynamic model. [5]

Current FAA provisions

Ahead of the EASA, the Federal Aviation Administration of the United States has recently placed requirements for additional qualifications for certain training tasks; Level C or D Full Flight Simulators, if used to conduct full-stall training, upset recovery training or airborne icing training under FAA approved training programmes, are subject to additional qualification criteria for those specific training tasks, regardless of the original qualification basis of the devices. [21] The required additional qualifications are based on

subjective and objective testing, and are realised as amendments to the Statement of Qualification (SOQ) of the simulator, reflecting the additional training tasks that the device is qualified to conduct. Previously qualified simulators used to conduct unusual attitude recovery tasks that do not exceed the pitch, bank angle or airspeed criteria of aeroplane upset are however exempt from this requirement. In case the operator elects not to apply for qualification of a Level C or D FFS for full stall training, the approach to stall training with such device will be restricted to tasks that terminate at the activation of the stall warning system. [27]

The aerodynamic modelling is required to be able to cover the angle of attack and sideslip range of all training tasks, and at minimum it should support an angle of attack range to ten degrees beyond stick-pusher activation, or the first distinctive indication that the aircraft has stalled. As appropriate to the specific aeroplane type, the high angle of attack modelling must demonstrate degradation in static and dynamic lateral-directional stability, degradation in control response, uncommanded roll response or roll-off, apparent non-repeatability, changes in pitch stability, Mach effects and stall buffet. The presence of these qualities must be declared in a Statement of Compliance. [21]

The associated objective evaluation of stall characteristics is only required for wings level second segment climb and approach or landing flight conditions. The specific tolerances and requirements for these tests are listed in Table 3. [21]

Table 3 Objective stall characteristics tests as required by the FAA, and as proposed in the EASA NPA 2017-13 [28], [18]

Variable:	**Tolerance / Requirement:**	
Approach to stall	**FAA**	**EASA NPA 2017-13**
Stall warning speed	± 3 kts	± 3 kts
Pitch angle	± 2.0°	± 2.0°
Angle of attack	± 2.0°	± 2.0°
Bank angle	± 2.0°	± 2.0°
Control inputs	Must demonstrate correct trend and magnitude	(Not mentioned)
Stall warning up to stall	**FAA**	**EASA NPA 2017-13**
Stall speed	± 3 kts	± 3 kts
Pitch angle	± 2.0°	± 2.0°
Angle of attack	± 2.0°	± 2.0°
Roll rate and yaw rate	Must demonstrate correct trend and magnitude	Must demonstrate correct trend and magnitude
Stick-pusher stick force	± 10 % or ± 2.2 daN	± 10 % or ± 2.2 daN
Angle of attack threshold for initial buffet	± 2.0°	± 2.0°
Stall break and recovery	Statement of Compliance required	Statement of Compliance required

Numerical tolerances are not applicable after reaching the critical angle of attack, i.e. full stall, but the simulator must demonstrate a correct trend throughout recovery.

In subjective testing the stall characteristics should be assessed by a qualified SME pilot with direct experience in stall characteristics of the specific aeroplane type. Additional objective testing is not required. The following stall entry points should be evaluated as necessary for training purposes:

- Stall entry at wings level, 1g;
- Stall entry at a constant altitude, turning flight of at least 25° bank angle;
- Power-on stall entry;
- Aircraft configurations of second segment climb, high altitude cruise, approach and landing.

[27]

The results of these tests must be declared in an SOC. In addition, where known limitations exist in the aerodynamic model for particular stall manoeuvres (e.g. aircraft configuration or stall entry methods), these limitation must be declared in the SOC. [28]

For upset manoeuvre training, the FAA also requires the simulator to have a feedback mechanism for the instructor, providing information on the FSTD's validation envelope, flight control inputs and aircraft operational limits. The validation envelope may be displayed as an angle of attack vs sideslip (α-β) envelope cross plot and it should display the expected fidelity with respect to the envelope that is validated against aerodynamic data for flaps up and flaps down configurations at minimum. Examples of α-β cross plots are illustrated in Figure 14 (Chapter 4.3). The instructor's display should show the trainee's flight control inputs during the recovery manoeuvre, including control forces and the flight control law mode for fly-by-wire aeroplane. In addition the simulated parameters of airspeed, load factor and angle of attack should be displayed with respect to the aeroplanes operational limits. [21]

2.5 Limitations of simulator training

2.5.1 Negative training and negative transfer of training

A major challenge associated with simulator based training is the potential of negative training, which "*unintentionally introduces incorrect information or invalid concepts, which could actually decrease instead of increase safety*". Negative training may, for example, be caused by improper simulation of the flight condition, improper behaviour of the simulator in the flight condition, improper feedback from the motion-, aural-, or visual ques, improper flight control loading and improper instruction. [5]

In history, negative simulator training has propagated to fatal consequences due to a flawed learning process. An example of such an occurrence is the American Airlines flight 587, which suffered a structural failure of the vertical stabiliser due to excessive rudder input by the pilot in response to wake turbulence. Elements of the advanced manoeuvring training programme implemented by the airline operator were found to be a contributing factor to

these rudder pedal inputs, as the motion cues experienced in simulator-conducted exercises had not correctly represented the lateral accelerations that are associated with full rudder deflections. [29], [30] The mitigation of negative training in UPRT programmes requires thorough risk assessment and expertise from both psychological and technical points of view.

Another important aspect to address is the process of training transfer, which describes the degree to which what was learned in the training environment is transferred to the job environment. Negative transfer of training may occur in the form of making inappropriate generalizations of a skill or knowledge to a situation on the job that does not equal the situation in training. [31] As an example, single-engine piston engine aeroplanes behave differently compared to large transport aeroplanes; a correctly learned skill in a small aeroplane inappropriately applied to a large aeroplane is a form of negative transfer of training.

It is of utmost importance that the potentials of negative training and negative transfer of training are recognised and prevented from realisation in all UPRT. Every deviating characteristic of the simulator does not necessarily lead to negative training, but in such situations the expertise of the instructor is of particular importance. The instructor should always be able to distinguish when the behaviour of the simulator differs significantly from that of the actual flight, and take necessary actions, such as briefing and debriefing the student or avoiding the occurrence, to ensure correct and effective outcome of the training.

2.5.2 Modelling of aerodynamic stall and flow separation

Excluding stalls, most level C or D Full Flight Simulators provide sufficient fidelity to cover a significant portion of upset training. However, the simulation near the critical angle of attack and in the post-stall regime is often deficient. If the simulation does not satisfactorily represent the aeroplane's behaviour at and beyond the critical angle of attack, training of aerodynamic stalls may result in misperceptions about such an event and the recovery experience. [5]

Previously only approach-to-stall training has been required from FSTDs, and therefore the simulator manufacturers did not necessarily concentrate on the aeroplane control and response characteristics which prevail during an aerodynamic stall. Type-specific flight test data is usually unavailable from full-stall and post-stall regimes, as flight test programmes do not generally cover those areas. A typical aeroplane in full-stall condition will experience reduced or even negative stability and diminished control effectiveness in comparison to the situation where the stall warning has initially occurred. Especially the tendency of wing roll-off during stall is rarely modelled accurately, even though being a typical response for a swept-wing transport aeroplane. As a result a flight simulator is often easier to recover from fully developed stall or post-stall regimes compared to the real aeroplane. Negative training associated to control characteristics during a stall is particularly hazardous, as it may lead the pilot to inappropriately try to control axes that are becoming unstable, instead of reducing the angle of attack first. [5]

In general, a dropping wing experiences higher angle of attack compared to its counterpart. When operating below full-stall condition, i.e. below the critical angle of attack, the

increment in angle of attack leads to higher lift produced by the dropping wing, which, in turn, counters the rolling motion of the aeroplane. In such case the aeroplane has positive roll stability. The roll may be further countered by the pilot with opposite aileron control, which further raises the angle of attack of the dropping wing. In a post-stall condition this behaviour changes significantly, as an increment in angle of attack results to reduced amount of lift, and opposite aileron control confusingly further escalates the rolling motion, as illustrated in Figure 4. This effect, known as negative roll damping, is very rarely modelled correctly in simulator flight models.

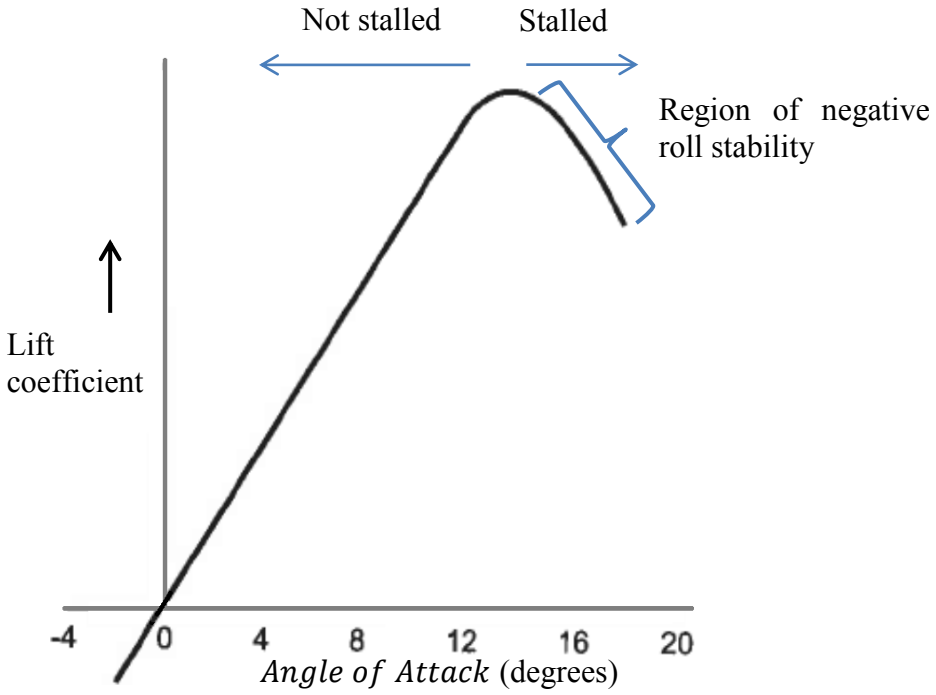

Figure 4 Region of negative roll stability

In a swept wing aeroplane the flow separation usually begins from the wing tip, causing the centre of pressure move forward. The resulting nose-up moment occurring in a progressing stall may not be correctly represented in simulators. Similarly the simulator behaviour in high altitude stalls may be unrepresentative; on a real swept-wing aeroplane the experienced stall angle of attack and pitch attitude may be noticeably lower in high altitudes due to compressibility effects. Previously considerably less attention has been paid to the validation of high altitude stall characteristics. [5] , [32]

In history there have been recurrent occurrences, where a transport aeroplane has entered dynamic stall during take-off or go-around, often followed by wing drop. Significant pitch rates, often accompanied by wing surface contamination, have been identified as common factors in these incidents. Research conducted on the phenomenon suggests that the effects of pitch rate, wing surface roughness and ground proximity are nonlinearly coupled, and therefore predictions based on superposition of their individual effects would likely lead to incorrect results. The physical mechanisms behind the dynamic stall phenomenon are related to viscous effects of accelerated flow, leading to a combination of pressure gradient

lag effects inside and outside of the boundary layer. As a result, the boundary layer near the leading edge on the upper wing surface becomes more resistant to flow separation during a rapid pitch-up manoeuvre, allowing the static stall angle of attack to be momentarily exceeded. This dynamic stall overshoot likely leads to abrupt and unsymmetrical flow separation triggered, for example, by free stream turbulence coupled with rigid body motion. Validation of simulator stall effects at ground proximity has been generally unfeasible, as there is no available flight test data for obvious reasons. The increasing possibilities of computational fluid dynamics (CFD) have, however, improved the research of unsteady aerodynamics at ground proximity. [33]

Another issue to address is the phenomenon of aerodynamic hysteresis experienced during a stall. As illustrated in Figure 5 by Yang et al., the reattachment of the airflow may occur at a noticeably lower angle of attack compared to that of the flow separation. Thus, the available lift force may be considerably different at a given angle of attack in different phases of the stall event, which in turn could possibly affect the recovery characteristics from stall or spin flight conditions. [34] The replication of stall hysteresis may be unrepresentative in the aerodynamic models of some simulators.

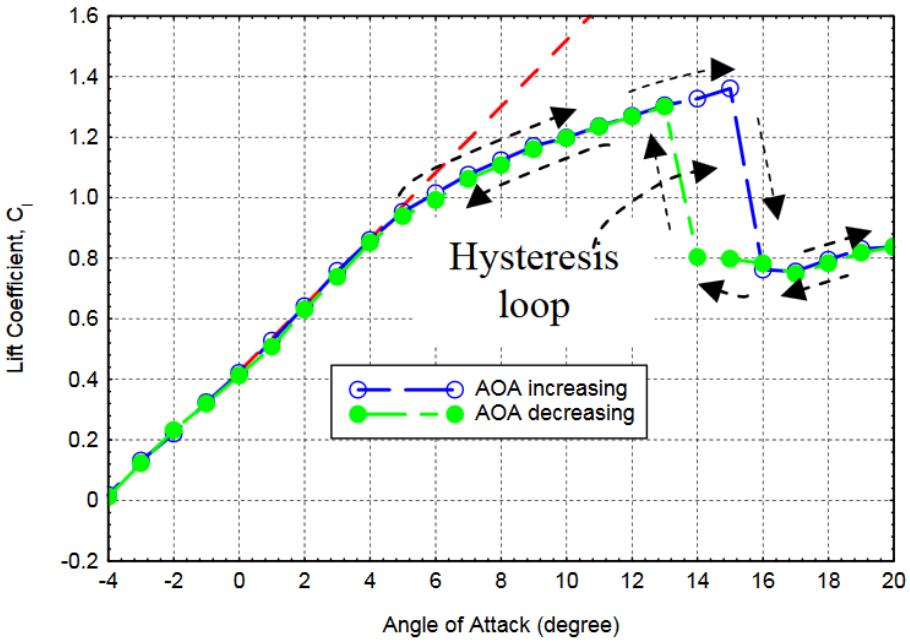

Figure 5 Stall hysteresis loop of a low-Reynolds number aerofoil [34]

No two real stalls are alike. This is due to the complex nature of turbulent flow and the abruptness of flow separation. The requirement for incorporating apparent randomness or non-repeatability of stall events into the aerodynamic model has only recently been introduced in the FAA regulations, and so far only proposed for the EASA regulations. Therefore it is likely that this aspect has been left to less attention in the implementation of aerodynamic models, at least in the case of older devices.

2.5.3 Modelling of icing effects

Reduced performance due to icing conditions has typically been modelled as a weight increase of the aeroplane in the simulator flight model. However, such a solution does not take into account the reduction of the critical angle of attack caused by ice build-up on the surface of the wing. In severe icing conditions on a real aeroplane, the stall event may occur earlier – or in some cases even before – with respect to the activation of stick shaker, whereas in the simulator the critical angle of attack would remain the same and the stick shaker would always provide the pilot with similar buffer for angle of attack prior to stall break.

New requirements are proposed in the EASA NPA 2017-13 to increase the fidelity of the airframe icing effects. Emphasis is placed upon type-specific recognition cues that should be based on data supplied by the OEM or other suitable analytically obtained data, and it is proposed that at least one icing model should be objectively tested to demonstrate that it generates the correct cues as necessary for training. [18]

2.5.4 Limitations of the motion system

The human self-motion perception is derived from the combination of the visual system, the vestibular system, the tactile sense and the sense of the relative position of the neighbouring parts of the body. Even the highest fidelity motion systems are able to provide only momentary ques instead of replicating sustained g-forces. Therefore it should be carefully considered how to avoid negative training when replicating experiences which require g-awareness. In an actual upset situation the pilot may be floating up against restraints or pushed down against the seat, making it more difficult to apply proper control inputs. There may also be unsecured items flying around the cockpit in an actual situation, potentially causing startle and distraction. [5]

The somatogravic illusion is a disorienting vestibular illusion, occurring during prevailing linear accelerations, when a pilot has no clear visual reference. In such an illusion the pilot may for example falsely perceive acceleration as climbing, deceleration as descending, or levelling from climb as an abrupt nose-up motion. The somatogyral illusion is a similar illusion, causing false sensations of rotation. [35] These illusions have contributed to several aeroplane upsets and fatal LOC-I accidents, especially during low altitude go-around manoeuvres. An example of such an accident is the Gulf Air flight 072. [36] The motion systems of current simulators are incapable of delivering such sustained accelerations that are required to replicate these illusions. In May 2017, the EASA has published NPA 2017-06 "*Loss of control or loss of flight path during go-around or other flight phases*", which contains elements to address the issue through amendments in certification specifications of large aeroplanes. [37]

Another source of potential negative training is the simulation of the buffet, which is an essential cue for the pilot in an approach-to-stall situation. In some situations, such as severe wing icing, aerodynamic buffet may be the first indication the pilot receives of an impending stall. In aerodynamic models the g-threshold of the start of the buffet may be inappropriate, the buffet may occur in wrong order in relation to other stall warnings, or the buffet cues may mispresent those of the actual flight. [5] According to Advani et al., it was recognised by ICATEE that the power spectral density (PSD) analysis, which is

currently used to validate simulator motion buffets, may not be the most appropriate method to assess this dynamic flight condition. [29]

The intensity of the simulator motion buffet during stall is generally milder compared to the real aeroplane. In a real stall the buffet may be so severe that the pilot has difficulties in reading the instruments or reaching the selectors of the instrument panel. According to Allerton, "*the generation of high-frequency accelerations by six hydraulic jacks would be very demanding of the bandwidth of the actuators increasing significantly the cost of the motion platform) and would also place additional requirements on on-board systems, to ensure their immunity to vibrations (increasing the cost of electronic equipment installed in the simulator cabin*)". [38] Additionally, the technical requirements set in the CS-FSTD(A) requires only approach-to-stall, and not full-stall validation of aerodynamic buffet. As an example, a QTG full stall test of a Level D Full Flight Simulator of the Airbus A350 – a particularly modern device – displayed a prominent difference in the buffet intensity in some regions of the spectrum between the simulator and flight test data. However, the simulator fulfilled the qualification provisions, as there are no specific requirements set for validation of the full stall buffet characteristics. [39]

3 Technical basics of flight simulators

3.1 Main components of a Full Flight Simulator

Different ground based devices have been used as an aid to flight training since the first decades of the 20th century. The Second World War saw extensive use of training devices to train very large numbers of pilots and crew for increasingly complex operations and procedures. Some of these devices were accurate mock-ups of real aircraft, some incorporated functional instrumental navigation, and some rudimentarily mimicked aircraft motion. Shortly afterwards the direct ancestors of the modern flight simulator were introduced, as the post-war development of analogue computers made the technology available to compute the responses to aerodynamic forces instead of empirical duplication of their effects. Being fully analogue in the beginning, the use of flight simulators became an integral part of commercial airline operations in the 1960's, and by the end of the decade the capability of digital computers had improved to such a level that they could be considered to replace analogue computers in real-time simulation. Since the 1970's the basic configuration of flight simulation training devices has remained much the same, while the overall fidelity of the simulation has constantly improved especially in the fields of motion and visual cues. [40]

At the heart of a modern flight simulator are the equations of motion. They take inputs from pilot controls, aerodynamic terms, environmental terms and engine terms and compute them to variables such as forces, moments, attitude, position and motion of the simulated aircraft. These equations are updated tens or hundreds times per second and each time new values of forces and moments are applied to the aircraft, constituting to the flight model of the simulator. Aerodynamic data, engine data and details of features - such as undercarriage - are needed to describe the behaviour of the specific aircraft at each state. This data is usually stored in lookup tables and functions, and, in case of Full Flight Simulators, consists of engineering data and actual flight test data obtained from the aircraft manufacturer. [38]

Allerton (2009) has illustrated the main components of a typical flight simulator in Figure 6. Several arrows in the figure represent a bi-directional link, as many terms are a function of variables such as angle of attack, Mach number or altitude. [38]

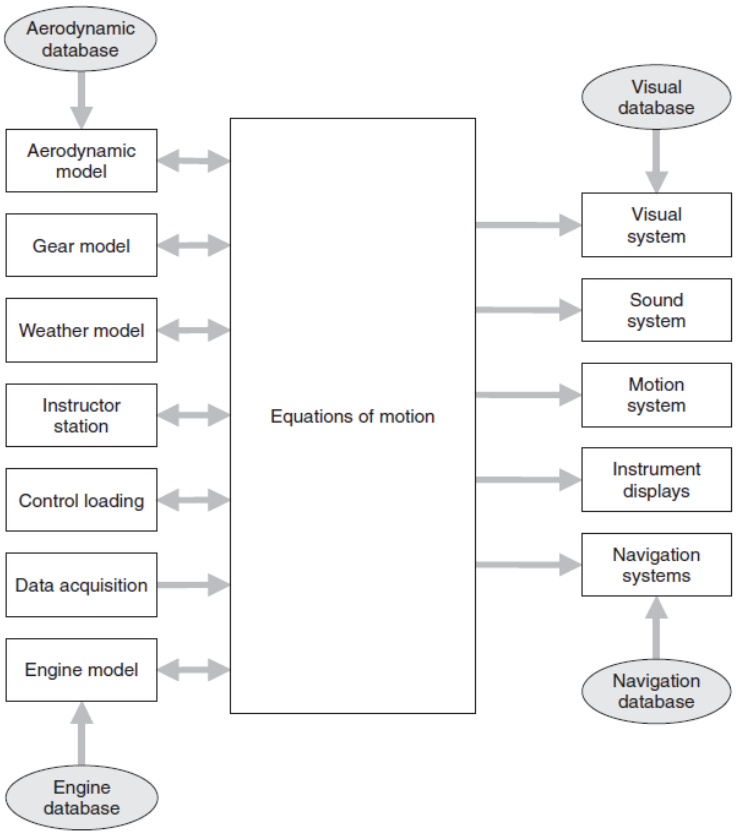

Figure 6 Organisation of a flight simulator [38]

The aerodynamic model is among the most critical elements of a flight simulator, as it enables the computation of aerodynamic forces and moments of the aircraft. It reproduces lift, drag and moments about all three axes acting on the aeroplane. Aerodynamic terms are derived as functions of the state of the aircraft - for example lift coefficient as a function of the angle of attack - and specific aerodynamic coefficients, such as stability derivatives, which are defined in the aerodynamic database. An error in modelling the aerodynamics may fail the qualification of the simulator and therefore the quality of the aerodynamic database is of particular importance. [38], [41]

Similarly as the aerodynamic model, the engine model requires access to variables computed in the flight model, as the behaviour of an engine is dependent of the state of the aircraft. Rather than as a thermodynamic model, the engine is modelled through engine dynamics to derive thrust, fluid flows, pressures and rotational speeds. The state-dependent engine dynamics are defined in the engine database, and the engine model is often as detailed as the aerodynamic model. Engine failure modes are tested extensively in the flight simulator qualification process. [38]

The aerodynamic data and engine data are provided as data packages typically by the manufacturer, containing several thousand graphs of aerodynamic and engine variables as functions of other variables. This data is usually obtained by a combination of flight test data and engineering data, such as wind tunnel tests and computational fluid dynamics. In addition the data package contains extensive amount of validation data for the simulator developer to compare the simulator performance with actual aircraft data. The data

packages produced by aircraft and engine manufacturers are of a high commercial value and usually protected by confidential agreements between manufacturers and simulator developers. Therefore, there are very few detailed data packages available in the public domain. [38]

Data acquisition of a Full Flight Simulator may consist of several hundred inputs, as the flight deck of the simulator is an exact replica of the aircraft. In addition to the primary flight controls, every lever, selector, knob and switch is interfaced to appropriate simulator modules. [38]

The atmospheric variables are computed in the weather model. In addition to air pressure, air density and air temperature, also winds and turbulence are modelled. According to Allerton there are two universally adopted models for atmospheric turbulence, the Dryden model and the Royal Aircraft Establishment model. Hazardous conditions, such as wind-shear, microburst, icing and heavy rain are also simulated in higher fidelity weather models. [38]

The visual system provides real-time images of the simulated outside world from the pilot point of view. The pilot eye position and orientation is calculated from the equations of motion, and rendered to a scene typically 60 times per second. [38] A Level C or D Full Flight Simulator is required to be equipped with a visual system comprising of continuous, cross-cockpit, collimated visual field of view providing each pilot with 180 degrees horizontal and 40 degrees vertical field of view. [24]

Sounds act as important cues for the pilot, and therefore the sounds created by the flight simulator must be consistent with the sounds heard in an actual aircraft. There are two general methods to generate cockpit sounds in a flight simulator sound system: to record actual aircraft sounds or to analyse and synthesize waveforms of each sound. The latter method is more commonly adopted. [38] There are several aural cues and aural warnings related to a developing aeroplane upset situation. As an example extracted from the flight crew operating manual of the Airbus A320 family, the following upset related aural cues are incorporated in the Electronic Centralised Aircraft Monitor (ECAM) of the aeroplane: [42]

Table 4 Upset related aural warnings incorporated in the ECAM of the A320 family [42]

Aural warning	**Meaning**
Continuous repetitive chime	Aircraft in dangerous configuration or limit flight conditions (e.g. stall, overspeed), or system failure altering flight safety
Cricket + “STALL” (synthetic voice)	Stall, permanent warning as long as a correct angle of attack is not recovered
“SPEED, SPEED, SPEED” (synthetic voice)	Current thrust is not sufficient to recover a positive flight through pitch control
“PITCH, PITCH” (synthetic voice)	The aircraft pitch attitude is becoming excessive during flare and landing

In addition, the sound of the passing airflow acts as an indication of the airspeed.

Flight simulation training devices used in upset prevention and recovery training are required to be equipped with a six-degrees-of-freedom motion system. The accelerations are calculated in the flight model and passed to the motion system, which tries to mimic the accelerations with hydraulic actuators. The only positive G available from the motion platform is the vertical heave, which is constrained by the length of the actuators – typically 2 - 3 meters. The angular motion is typically restricted to 30 - 40° due to the legs of the motion platform. These constraints can be relaxed to some degree by deceiving the human brain by for example slowly leaking away motion without the pilot noticing. Visual cues from the visual system strengthen the feel of motion experienced by the pilot. [38] In addition to aural cues, there are strong motion cues related to upset situations on a real aeroplane; for example vibrations in a developing aerodynamic stall.

The control loading is modelled by attaching motion-resisting actuators to the flight controls of the simulator. In primary controls the resistance is usually varying with airspeed. During last two decades electrical drive motors have become available as an alternative to hydraulic actuators in simulator control loading systems. [38]

3.2 Mathematical model of an aeroplane

As presented by Rolfe, the equations of motion which govern the motion of an aeroplane have the generic form

$$\ddot{x} = F/m \tag{1}$$

where $\ddot{x}$ is the acceleration of the aeroplane, F is the applied force, and m is the mass. The mathematical model of the aeroplane is embodied in the definition of F, and it primarily consists of the relationship between air reactions and motion of the aeroplane relative to the air – the aerodynamic model. Engine thrust and landing gear ground contact supply additional forces and moments to the mathematical model. Thus,

$$F = F_{aero} + F_{engine} + F_{undercarriage} \tag{2}$$

Flight simulation is fundamentally the generation of these forces and solutions to the equations of motion. [41]

Mathematical modelling for flight simulation has similarities with the basics of aeroplane stability and control theory, but there are also some significant differences. Classical stability and control analysis assumes a trimmed state, a local equilibrium, about which equations of motions can be linearized, and once linear equations are available, examines the stability of motion after a disturbance from trim. This approach allows only small disturbances from the equilibrium state before the model becomes invalid, and therefore does not fulfil the requirements of many simulation tasks. [41]

The conventional notation of the three components of force, moment, linear and angular velocity acting on an aeroplane is illustrated in Figure 7. Origin O is fixed in the aeroplane and no particular set of axes are assumed. [41]

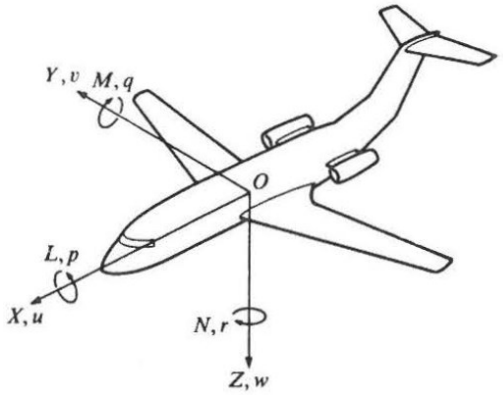

Figure 7 Notation of forces, moments and velocities [41]

The equations of motion of a rigid aeroplane in still air, with any system of axes fixed in and rotating with the aeroplane, may be expressed as force equations

$$\begin{aligned} m(\dot{u} + qw - rv) &= F_x + mg_x \\ m(\dot{v} + ru - pw) &= F_y + mg_y \\ m(\dot{w} + pv - qu) &= F_z + mg_z \end{aligned} \tag{3}$$

and moment equations

$$\begin{aligned} I_x\dot{p} - I_{yz}(q^2 - r^2) - I_{zx}(\dot{r} + pq) - I_{xy}(\dot{q} - rp) - \left(I_y - I_z\right)qr &= L \\ I_y\dot{q} - I_{zx}(r^2 - p^2) - I_{xy}(\dot{p} + qr) - I_{yz}(\dot{r} - pq) - (I_z - I_x)rp &= M \\ I_z\dot{r} - I_{xy}(p^2 - q^2) - I_{yz}(\dot{q} + rp) - I_{zx}(\dot{p} - qr) - \left(I_x - I_y\right)pq &= N \end{aligned} \tag{4}$$

which constitute to so called total force equations. With the reasonable assumption, that a conventional civil aeroplane has a symmetrical mass distribution with respect to the fore-and-aft plane of symmetry, the terms I_{yz} and I_{xy} become zero. Thus the moment equations become more compact

$$\begin{aligned} I_x\dot{p} - I_{zx}(\dot{r} + pq) - \left(I_y - I_z\right)qr &= L \\ I_y\dot{q} - I_{zx}(r^2 - p^2) - (I_z - I_x)rp &= M \\ I_z\dot{r} - I_{zx}(\dot{p} - qr) - \left(I_x - I_y\right)pq &= N \end{aligned} \tag{5}$$

The most common method to define the orientation of an aeroplane in space is to use a sequence of three angles, known as the Euler attitude angles. These angles are the heading angle ψ, the pitch angle θ and the bank angle ϕ. Then a set of axes $Ox_oy_oz_o$ with origin O fixed in the aeroplane, initially aligned with earth reference axes as datum, are brought into alignment with the body-fixed axes Oxyz with a specific sequence of rotations. [41]

The rotation sequence is illustrated in Figure 8, with the sets of axes labelled successively $x_oy_oz_o$, $x_1y_1z_1$, $x_2y_2z_2$, xyz. The heading angle ψ and bank angle ϕ can take values from the range of $\pm\pi$, whereas the pitch angle θ is in the range of $\pm\pi/2$. [41]

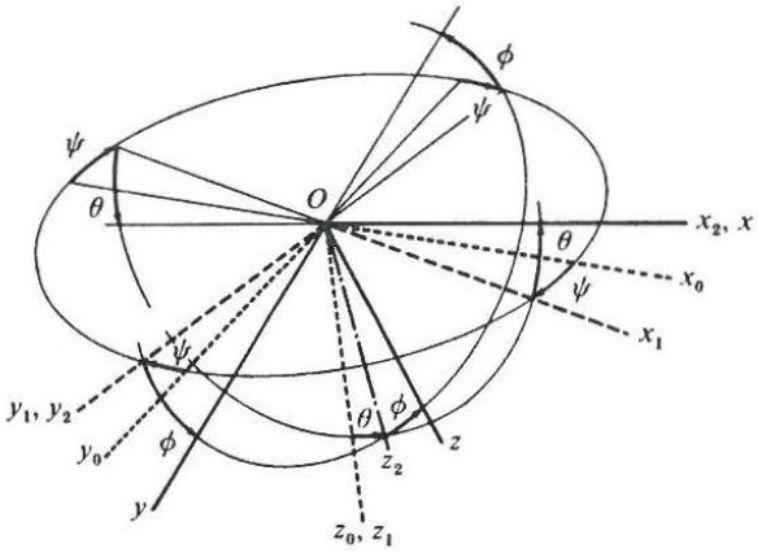

Figure 8 Euler attitude angles and sequence of rotations [41]

It should be noted that $\dot{\phi} = p$ only when $\theta = 0$ and $\dot{\theta} = q$ only when $\phi = 0$. Therefore it is necessary to define the relationship between the rates of change of the Euler attitude angles and the components of angular velocity of the aeroplanes body axes. So called gimbal equations are widely used:

$$\begin{aligned} \dot{\phi} &= p + q \sin\phi \tan\theta + r \cos\phi \tan\theta \\ \dot{\theta} &= q \cos\phi - r \sin\phi \\ \dot{\psi} &= q \sin\phi \frac{1}{\cos\theta} + r \cos\phi \frac{1}{\cos\theta} \end{aligned} \tag{6}$$

The inverse of these equations is:

$$\begin{aligned} p &= \dot{\phi} - \dot{\psi} \sin\theta \\ q &= \dot{\theta} \cos\phi + \dot{\psi} \sin\phi \cos\theta \\ r &= -\dot{\theta} \sin\phi + \dot{\psi} \cos\phi \cos\theta \end{aligned} \tag{7}$$

In the special case of pitch angle θ being ±90° the expressions for $\dot{\phi}$ and $\dot{\psi}$ become indeterminate in gimbal equations, as $\tan\theta = \pm\infty$ and $\cos\theta = 0$. If such manoeuvres, where pitch angle reaches ±90°, are avoided, the gimbal equations may be used without difficulty. For the simulation of aerobatics or similar rough manoeuvres, an alternative method of deriving the aeroplane attitude angles is required. [41] There is no intent to reach pitch attitudes of ±90 degrees during the manoeuvres required by the current UPRT provisions, and therefore this issue does not generally cause problems. Singularities may be completely avoided by utilising an alternative method, which is presented later in this chapter without going further into detail, as this is not a significant issue within the scope of this thesis.

Transformation of variables between body and earth axes is usually handled with the help of direction cosines. The transformation may be expressed as:

$$\begin{bmatrix} x \\ y \\ z \end{bmatrix} = \begin{bmatrix} l_1 & l_2 & l_3 \\ m_1 & m_2 & m_3 \\ n_1 & n_2 & n_3 \end{bmatrix} \begin{bmatrix} x_0 \\ y_0 \\ z_0 \end{bmatrix} \tag{8}$$

where x, y and z represents the three components of a variable – for example velocity – in body axes, and x_0, y_0, z_0 the corresponding components in earth axes. The earth axes components in terms of body axes components may be expressed with the inverse relation:

$$\begin{bmatrix} x_0 \\ y_0 \\ z_0 \end{bmatrix} = \begin{bmatrix} l_1 & m_1 & n_1 \\ l_2 & m_2 & n_2 \\ l_3 & m_3 & n_3 \end{bmatrix} \begin{bmatrix} x \\ y \\ z \end{bmatrix} \tag{9}$$

The direction cosines can be expressed in terms of the Euler attitude angles by:

$$\begin{aligned} l_1 &= \cos\theta \cos\psi \\ l_2 &= \cos\theta \sin\psi \\ l_3 &= -\sin\theta \\ m_1 &= \sin\phi \sin\theta \cos\psi - \cos\phi \sin\psi \\ m_2 &= \sin\phi \sin\theta \sin\psi + \cos\phi \cos\psi \\ m_3 &= \sin\phi \cos\theta \\ n_1 &= \cos\phi \sin\theta \cos\psi + \sin\phi \sin\psi \\ n_2 &= \cos\phi \sin\theta \sin\psi - \sin\phi \cos\psi \\ n_3 &= \cos\phi \cos\theta \end{aligned} \tag{10}$$

A more complex alternative to the Euler equations is the quaternion method, which does not suffer from singularities when the pitch angle reaches ±90°. The quaternion method utilises the fact that a frame of axes Oxyz may be brought into coincidence with a reference frame $Ox_oy_oz_o$ by a single rotation about a fixed axis in space, making angles A, B, C with the reference frame. Thus, the orientation of the frame Oxyz is defined by the four parameters of A, B, C and the rotation angle D. [41]

These relations are constituted into a transformation matrix, which is furtherly simplified by a change of variables from the original four parameters to a set of quaternion parameters. These quaternions may be derived from the body axis components of angular velocity p, q, r, or from the Euler angles ψ, θ, ϕ. Transformation of variables between body axes and earth axes is achieved by the use of direction cosines, and the Euler angles are still required for example for the use of display on the pilot's instruments. [41]

Several sets of axes are required as frames of reference for the solving of equations of motion, aerodynamic forces, moments and aircraft attitude. These can be classified either as body axes fixed with the aircraft, or earth axes, also referred as inertial axes. There are typically multiple body axes, having their x-axis aligned with a geometric feature, such as the fuselage reference line (F.R.L.), the wing datum plane (W.D.P.), or the principal inertia axis. For example for the same model, $\alpha_{W.D.P.}$ could be used for defining the aerodynamic forces and moments, and $\alpha_{F.R.L.}$ for axis transformations and all other uses. The difference between $\alpha_{W.D.P.}$ and $\alpha_{F.R.L.}$ is synonymous to the wing incidence angle, typically a few degrees. [41]

In addition to attitude angles which define the aircraft's orientation with respect to earth axes, the aircraft's incidence angles that define the direction of the airflow with respect to the body axes are required for the calculation of aerodynamic forces and moments. Generally these incidence angles are expressed in the form of so called aerodynamic angles, namely angle of attack α and sideslip angle β:

$$\tan\alpha = w/u \qquad \sin\beta = v/V \tag{11}$$

where α lies in the range of ±π and takes the sign of w, and β lies in the range of ±π/2 and takes the sign of v. [41]

The requirement to perform a variety of manoeuvres involving substantial variation in angle of attack over a wide speed range calls for the aerodynamic model to have a detailed representation of the aerodynamic forces and moments. These forces and moments may have to be expressed as functions of one or more of the following:

- angle of attack,
- airspeed / Mach number,
- rotation rates,
- altitude,
- centre of gravity position,
- ground proximity,
- geometry / aeroplane configuration. [41]

Typically these forces and moments are constituted from dimensionless aerodynamic coefficients, which are furtherly composed as a sum of effects of stability and control derivatives. These derivatives describe the response of a force or a moment with respect to changes in stability related parameters or control surface deflections. The stability and control derivatives are either tabulated, or expressed as functions with respect to relevant variables. As an example, Figure 9 illustrates the basic lift coefficient $C_{L_{Basic}}$ as a function of angle of attack per flap configuration in the aerodynamic data package of a Boeing 747 transport aeroplane. All these data plots originating from actual flight tests are transformed – possibly manually, into a tabular form in order to implement the aerodynamic model of a simulator. As a data package may contain hundreds of similar plots, the tabulating process may also be prone to random errors.

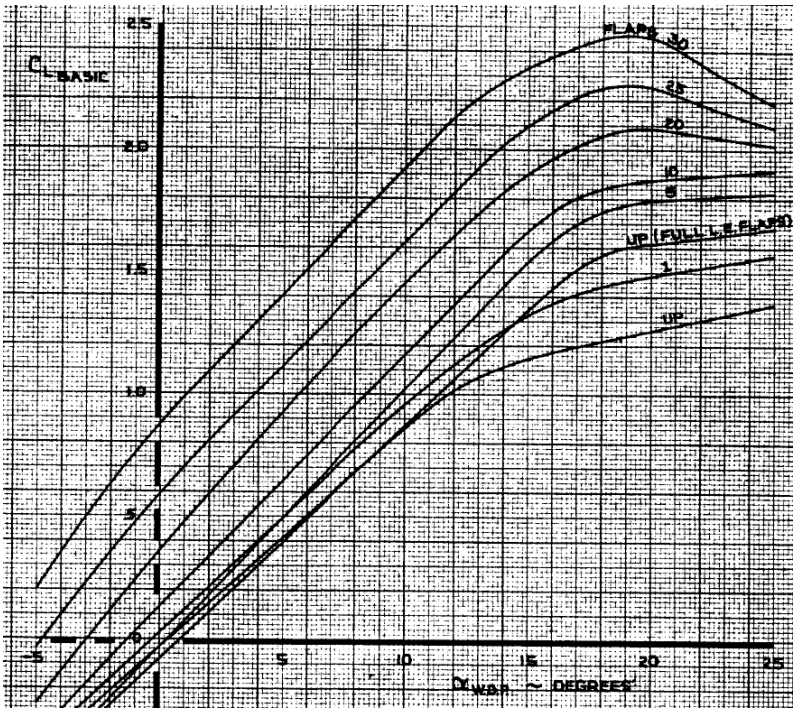

Figure 9 Boeing 747 aerodynamic data [43]

An impression of the level of complexity needed to implement an aerodynamic model may be achieved by exploring the equations of the aerodynamic forces and moments presented in chapters 5.2 through 5.7. During UPRT manoeuvres the state of the simulation may reach the outer regions of a multitude of data tables, and even if the valid range of a single table is exceeded, full realism may no longer be expected.

A much simplified approach to model lift force coefficient C_L would be to fit a linear approximation in an appropriate reference point of the plot, so that

$$C_L = a_0 + a_1\alpha \tag{12}$$

For a typical transport aircraft this method would provide decent accuracy in a wide range of normal operating conditions, and could be sufficient if for example the stall was not a relevant area for study. The effect of different flap settings could be accounted for with simple amendments to the above formula, such as

$$C_L = \left(a_0 + b_0\delta_f\right) + (a_1 + b_1\delta_f)\alpha \tag{13}$$

A more comprehensive approach would be to express the basic coefficients a_0 and a_1 in a tabular form, in relation to flap angle. The benefit of this approach is that the expression stays continuous throughout the change of flap settings. For flap angles between the tabulated values, the appropriate values of a_0 and a_1 have to be interpolated. This procedure is often referred as "table look-up" process. [41]

Given a table of values of a variable Y as a function of multiple values of X, then the value of Y for any general value X is obtained by interpolation, as illustrated in Figure 10. Thus if

$$X_2 \leq X \leq X_3 \tag{14}$$

then

$$Y = Y_2 + \left(\frac{Y_3 - Y_2}{X_3 - X_2}\right)(X - X_2) \tag{15}$$

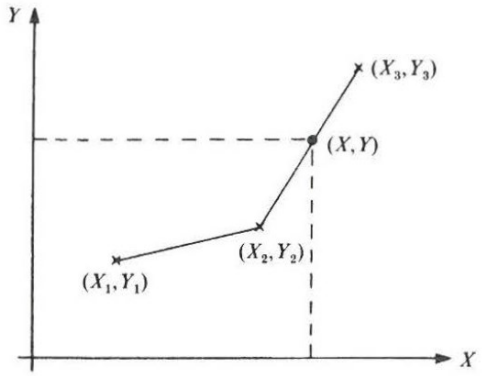

Figure 10 Illustration of linear interpolation [41]

When studying the usable operating envelope of a flight simulator, it is of particular interest how values greater than the highest or lower than the lowest tabulated values are handled in algorithms. If the value of X is outside of the tabulated range, one – rather unsophisticated – method would be to set Y at the nearest end-point value. An alternative technique would be to extend the slope of the final segment by extrapolation. [41] The first-mentioned method would be less optimal in perspective of upset training manoeuvres, as the aerodynamic model would most certainly behave erroneously in the instant when exceeding the range of the data tables. Linear extrapolation would probably grant even at least some level of continuity and a shallow buffer of a satisfactory trend beyond the available data range.

Figure 11 illustrates linear interpolation of a data set and its slope function. The left-hand curve could represent for example the relationship between pitching moment coefficient C_m and angle of attack α. Hence the slope function of the first curve, illustrated on the right, would represent the stability derivative C_{m_α} versus α, which is a primary parameter in aircraft's longitudinal stability. A notable challenge of table look-up processes is that sparse interval in X -values will quickly lead to major discontinuities in such parameters. The significance can be reduced by having denser data points, by employing a higher order interpolation technique, or by fitting a polynomial expression to the first curve. On the other hand a major advantage of table look-up processes is that at the set values of independent variables, the dependent variables match exactly the original data. [41]

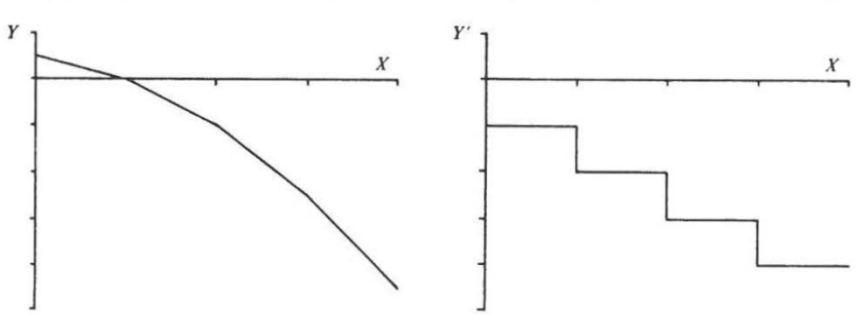

Figure 11 Linear interpolation of a data set and its slope function [41]

Figure 12 by Napolitano illustrates an example of the utilisation of the equations of motion for aeroplane simulation. At the core of the block diagram are the Conservation of the Linear and Angular Momentum equations (CLMEs and CAMEs), analogous to the total force and moment equations, as represented in Equations 3, 4 and 5. The forces and moments resolved in the previous iteration are fed as inputs to these equations. The resulting angular velocities with respect to the body axes are then translated into rates of change of the Euler attitude angles with the help of Kinematic Equations (KE), analogous to the gimbal equations, as represented in Equations 6 and 7.

Subsequently, the force effects of gravity are derived from the Gravity Equations (GE), and fed back as inputs to the CLMEs. The displacement of the aeroplane with respect to earth axes is solved with the help of Flight Path Equations (FPE), analogous to the direction cosines as represented in Equations 8, 9 and 10, and finally, the aerodynamic forces and moments acting on the aeroplane are solved as inputs for the next iteration, with the help of aerodynamic equations and table look-up processes. [44]

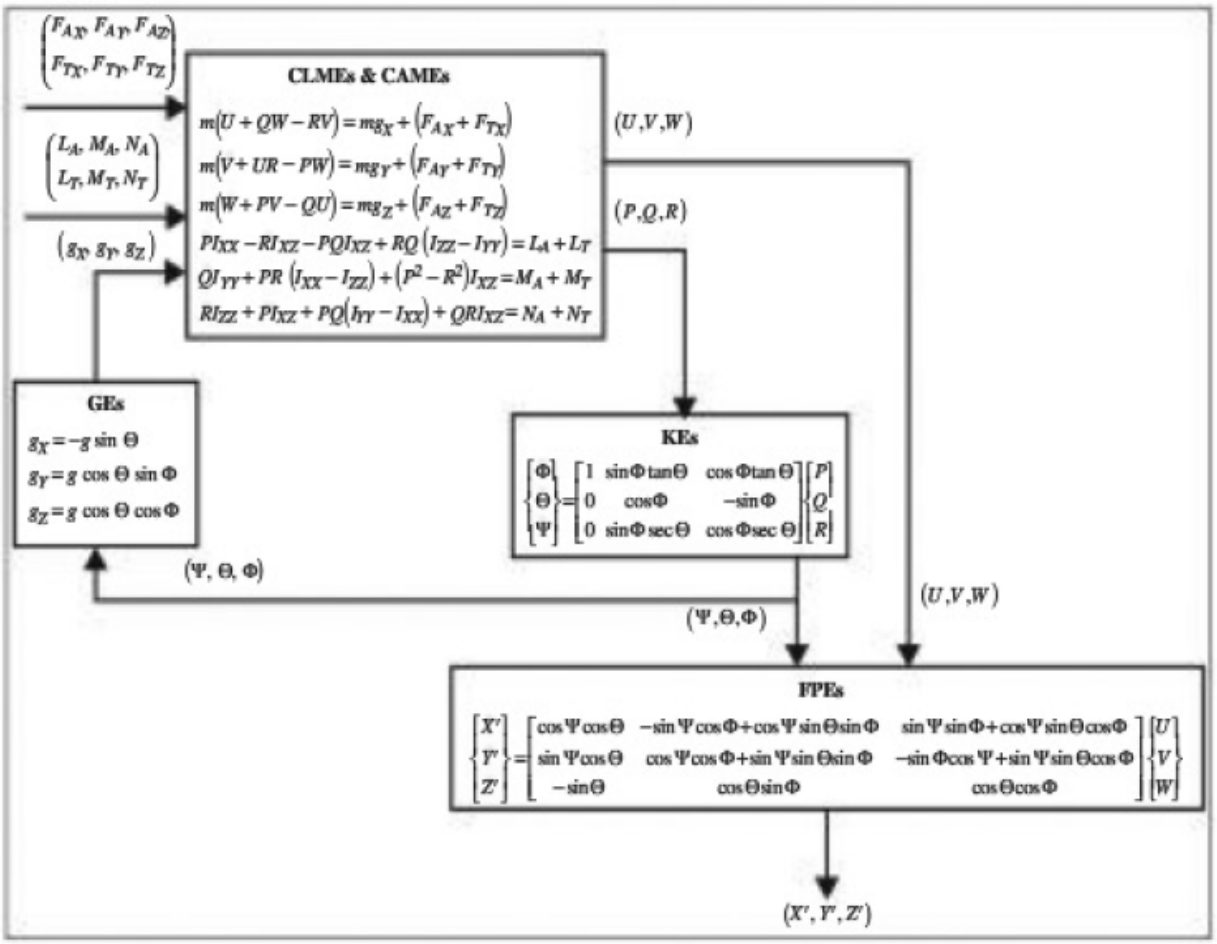

Figure 12 Utilisation of the equations of motion [44]

3.3 Data package

Different categories of data needed by simulator manufacturers and users to support their activities are listed in "Flight Simulator Design and Performance Data Requirements", published by IATA:

1. Configuration/design data: needed to construct an authentic duplicate of the flight deck and equipment of a specific aeroplane,
2. Simulation modelling data: defines the mathematical implementation of real-time simulations of the aerodynamic characteristics and the performance of various systems of the aeroplane,
3. Checkout data: to verify that the manufacturer has correctly implemented the simulator flight model and systems in accordance with the simulation modelling data,
4. Validation data: acts as a proof that the performance of the simulator corresponds to that of the actual aeroplane,
5. Proof of match data: acts as the comparison between flight test validation data and the engineering simulation by the manufacturer,
6. System verification data: contains information of functional behaviour of the simulated aircraft systems from the viewpoints of each crew member's position.

It is an established practice that the source data on which the aerodynamic model of the simulator is based on is provided in the form of a data package by the original equipment manufacturer (OEM) to be used for performance tests for demonstration of compliance. This data package contains all flight test validation data, engineering validation data, description of the mathematical equations behind the aerodynamic model, and the rationale for missing data as well as for the use of engineering data, such as data originating from wind tunnel tests or computational fluid dynamics (CFD). Validation data is furtherly discussed in the next chapter. [45]

Increasing portion of data for simulators originates from sources other than the aircraft manufacturer. Therefore it has been necessary to seek for internationally agreed upon standard processes between aircraft manufacturers, equipment vendors, simulator manufacturers and operators to streamline data provisioning within the simulator industry. These processes, addressing to procurement, configuration control, bidding, life cycle support and contractual agreements, have been described by IATA in chapter 17 of "Flight Simulator Design and Performance Data Requirements". It has been established that the terms and conditions for the supply of all data to any licensee should be equivalent under similar circumstances, documentation produced by manufacturers and vendors should be kept up to date, and engineering support should be provided throughout the life cycle of the simulator. The simulator manufacturer, aircraft manufacturer and equipment vendors should enter into separate agreements regarding the terms and conditions of the use of the data, and the subsequent right to use the data should be conferred to the operator at the time of simulator delivery. [45] However, these guidelines do not have a regulatory status, and therefore the level of compliance is varying within the industry.

3.3.1 Validation data

The validation data within the data package is typically presented in the form of graphs, such as time history tests or snapshot recordings. A snapshot recording is the presentation of one or more variables at a specific point in time, whereas a time history presents the change of variables with respect to time. Snapshot recording of aeroplane parameters should only be used in stabilised flight conditions. [45]

The sources of validation data may include flight tests and engineering data. Flight test validation data is the primary – and in many cases the only acceptable – means of validation, consisting of time histories, snapshots and graphical presentations of aeroplane flight tests, usually provided by the aeroplane manufacturer. In some cases data obtained by engineering simulation may be used as a technically valid substitution to flight tests; if certain incremental modifications, such as changed software or aerodynamically simple geometric revisions are made to a flight validated baseline model, the use of engineering data may be justified.

According to the CS-FSTD(A), aeroplane manufacturers or other validation data providers should supply, as part of the data package, a validation data roadmap (VDR) document, which describes the sources of validation data for all required qualification tests in matrix form. The VDR should also serve as guidance material for best practices on utilising the available data for QTG tests, as well as a rationale and explanation for all missing data and the use of engineering data. [46] As there is generally less available flight test validation

data from flight regions reached in upset recovery training tasks, especially if performed beyond the activation of the stall warning system, the VDR may be used to easily assess the validation data sources behind the relevant QTG tests and to estimate the level of reliability of possible engineering data covering those flight regions.

For new large aeroplane types in the EU, the type certificate applicant is obligated to provide simulator qualification data as part of the Operational Suitability Data (OSD) for the end user. The OSD is presented as mandatory and non-mandatory data, the latter which may e.g. be a recommendation or have the AMC status. The required scope of the validation source data to be included in the VDR is described in the CS-SIMD. For initial qualification of a Full Flight Simulator, the aeroplane type certificate applicant's/holders flight test data should be fundamentally used, whereas data from other sources may be used if properly justified. An OSD applicant may choose to supply validation source data from an audited engineering simulation to selectively supplement flight test data. [47]

3.4 Analysis of a flight model

The simulation space may be divided into three basic elements, as illustrated in Figure 13 by Rolfe and Staples. Starting from reality, a conceptual model is derived by analysis. It portrays reality with the use of governing relationships and equations, e.g., the equation of ΔC_L versus α. The implementation of this conceptual model via computer programming leads to the computer model, which may be related to reality through simulation. The credibility of the conceptual model is evaluated by procedures, which test that the model provides an acceptable level of agreement with reality. The computer model is tested by procedures of verification, to ensure that it constitutes an adequate representation of the conceptual model. Finally the simulation is validated by comparing the behaviour of the computer model against reality to ensure a satisfactory range of accuracy and consistence with its intended application. [41]

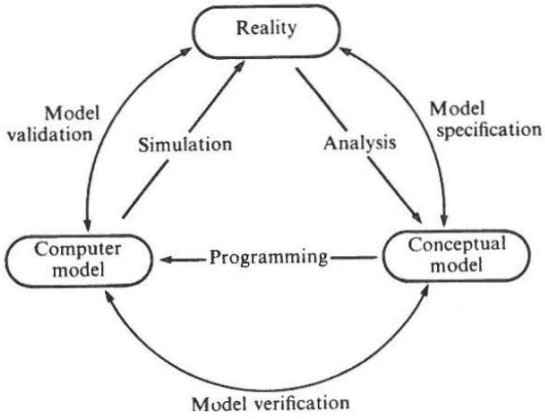

Figure 13 Basic elements of simulation space [41]

In the case of flight simulation, many systems are governed by equations that may be extremely complex and coupled. Therefore, simplifications are essential when composing the conceptual model in order to achieve a practical, yet adequately accurate solution. The

analysis process for the conceptual model may be prone to some level of uncertainty, for example due to experimental errors. Subsequently, some level of inaccuracy is inherent when implementing the conceptual model into a computer model due to technological constraints. These inaccuracies may be associated with the modelling logic or the source data, including truncation errors, random errors in data, and so forth. In the case of a simulator already in use, additional level of inaccuracy is brought by wear and tear, including for example free play or friction in the primary flight controls.

When validating a simulator flight model for upset prevention and recovery training, all of the above-listed sources of inaccuracy must be accounted for. Furtherly, the validation process itself may be prone to elements of unreliability. These may include for example measurement errors in the validation data, piloting error during validation testing, inappropriate conclusions drawn from the test results, etc. Therefore it should be recognised that the measured correspondence from validation of a flight simulator is never absolutely perfect. Focus should be placed on demonstrating an acceptable overall level of fidelity, and on the avoidance of sources of negative training.

4 Aspects of defining training envelopes for upset training

4.1 General considerations

The concept of upset prevention and recovery training is well defined by aviation authorities, and it is established that the use of simulators is essential for effective UPRT programmes. A necessity has arisen to review the capabilities of flight simulation training devices in use to ensure their compatibility with these programmes.

It may be reasoned that the useful training envelope of a flight simulator training device should be limited by those constraints that, if exceeded, could potentially lead to negative training or negative transfer of training. The critical limits should be unequivocally measurable and verifiable. Several questions arise when considering the definition of these constraints:

a) Which of the aerodynamic parameters are essential when defining the limits of sufficient fidelity?
b) Should the training envelope be based strictly on flight validated data, or may engineering data be taken into consideration?
c) How should the limits of sufficient fidelity be determined if support from the manufacturer is not readily available?

These questions are further elaborated in the following chapters.

4.2 Relevant aerodynamic parameters for the envelope

Aeroplane manoeuvrability is governed by parameters such as airspeed, load factor, angle of attack, sideslip angle, weight, air density and thrust vector. These parameters are limited by constraints, such as structural limitations, minimum speeds, critical angle of attack, buffet, thrust limits, etc., which confine a variety of operating regions, or in other words, flight envelopes. The multitude of definitions for different flight envelopes may cause confusion when assessing the capabilities of a simulator for upset training.

A common method to define a flight envelope in flight operations is the V-n diagram, which represents the airspeed V as a function of load factor n. The V-n diagram is a well-established concept among engineers, as they are used extensively in the determination of combinations of flight conditions and load factors required for structural design of an aeroplane, and in addition they are useful for determining the manoeuvring capability of an aeroplane. [48] In the context of upset training, V-n diagrams are particularly useful in giving insight on the margins of safety of a performed manoeuvre in relation to operational limits of the aeroplane.

From an aerodynamic standpoint, at relatively low airspeeds, it is preferable to study the fidelity of a simulated flight model by examining an envelope constituted by the aerodynamic angles, namely angle of attack α and sideslip angle β. Fundamentally the aerodynamic forces and moments acting on an aeroplane are dependent on the orientation

of the aeroplane with respect to the airflow. Thus, the aerodynamic derivatives in the equations of these forces and moments may be expressed as functions of angle of attack and sideslip angle, and their rates of changes.

An occasional misconception, even among pilots, is that the attitude of the aeroplane – e.g. pitch angle or bank angle – would directly affect to the aerodynamic response of the aeroplane. While the aeroplane attitude does have effect on the required forces in order to stay in a given flight path, the formation of the forces and moments about the aeroplane stability axis depends solely on the aerodynamic angles and the airspeed. However, without additional information, an α-β data plot of a performed manoeuvre only indicates how correctly the manoeuvre was replicated from an aerodynamic standpoint, and does not point out whether it was performed acceptably with respect to the aeroplane's operational limitations. As an example, a full 360 degrees barrel roll manoeuvre conducted without exceeding the validated range of the angle of attack and sideslip angle will be correctly replicated from an aerodynamic point of view. [9]

Along with angle of attack, the lift produced by a wing is also a function of the Mach number due to compressibility effects, especially when the aeroplane approaches transonic speeds, typical for cruise flight conditions. At a given airspeed, an increment in Mach number will result in higher lift and reduced critical angle of attack. Consequently, at high altitudes a swept wing jet aircraft may stall at a reduced angle of attack, and the pitch attitude experienced will be noticeably lower compared to lower altitudes. [9] The responses of aerodynamic derivatives are commonly expressed with respect to the three parameters of α, β and Ma in the validation data of the simulator. The typical threshold for taking compressibility into account lies at Mach 0.3.

Thus, the problem of determining a flight test validated envelope of an aerodynamic model of an FSTD is reduced to finding the range of available validation data for α and β with respect to airspeed, aircraft configuration and Mach number.

4.3 Regions of confidence

Flight test data is generally not available for conditions where flight testing would be hazardous, namely the post stall region and the region of high angle of attack with high sideslip angle. While stall tests including full-stalls are conducted in flight test programmes, the lateral flight controls are not fully applied in these experiments due to safety issues. For the same reason, roll and yaw rates, as well as sideslip angle are avoided, often rendering the validation of derivatives related to these terms impossible in the stall region.

Usually the aerodynamic model is, to certain extent, expanded to represent regions outside the flight tested envelope with the use of predictive methods, such as wind tunnel data or computational fluid dynamics. These methods, however, have inherent limitations and therefore cannot be considered equally reliable as flight testing. Finally, in the regions where there is no flight test data or analytical data available, the values of aerodynamic derivatives may be mathematically extrapolated.

Based on the source of the data, the aerodynamic model of a simulator may be divided into regions of confidence. The AURTA Working Group has classified three general confidence levels:
[9]

1. High: Validated by flight test data for a variety of tests and flight conditions.
2. Medium: Based on reliable predictive methods, supported by the aircraft manufacturer.
3. Low: Extrapolated.

Momentary excursions to medium confidence region during training manoeuvres may be considered acceptable, as long as the instructor has sufficient means to detect such excursions and take appropriate action. All training tasks should be carefully planned to ensure that the combination of α and β will never exceed to the low confidence region during the manoeuvre.

Figure 14 presents α-β envelopes from validation data of various types of transport aircraft with two different flap settings. The high confidence region is marked with solid line and regions of medium and low confidence are marked with dashed lines. It is noteworthy how sideslip angles are avoided at regions of high angle of attack.

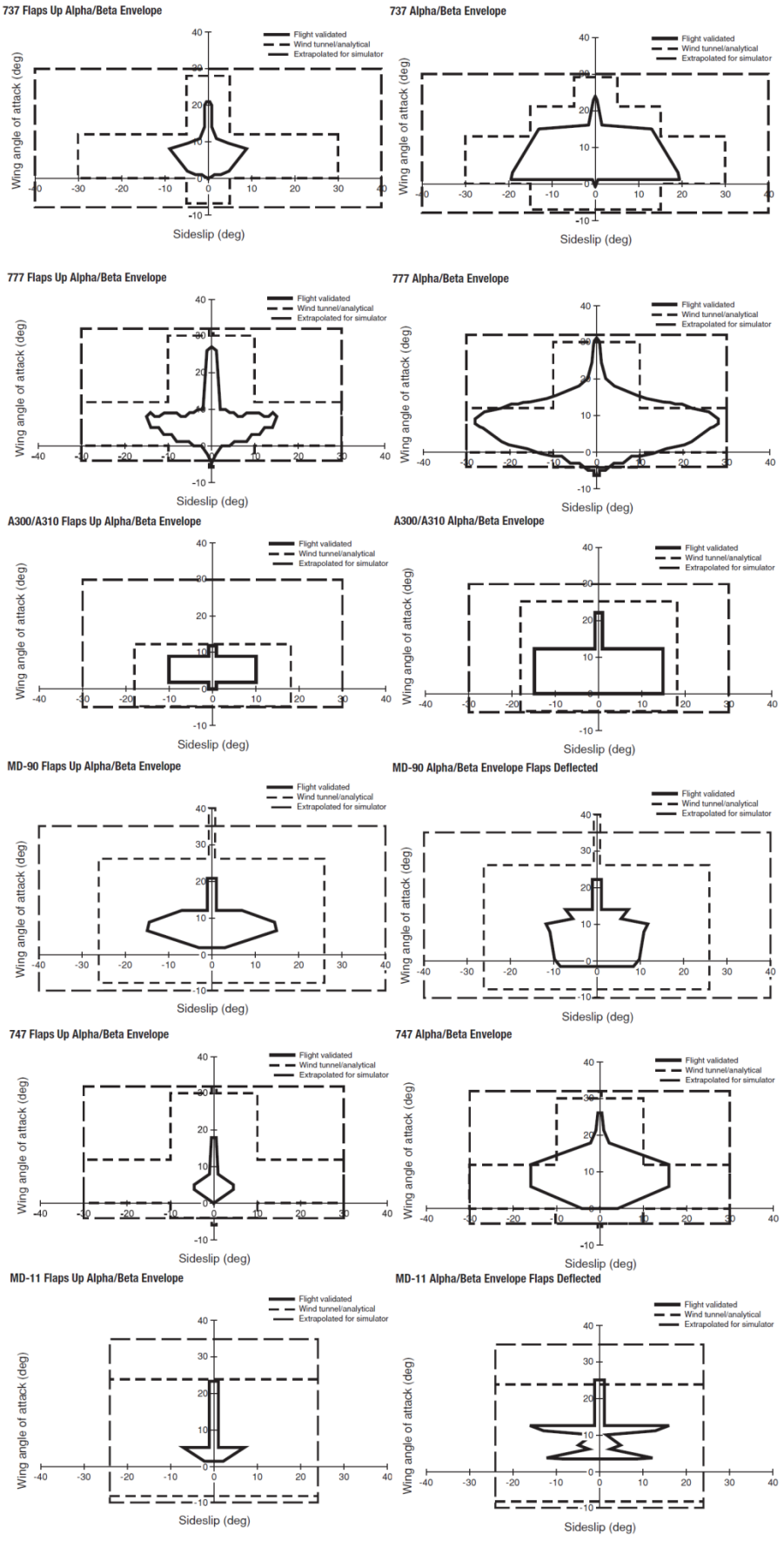

Figure 14 α-β envelopes for a variety of transport aeroplane types [9]

When simulator training is conducted outside the normal operational envelope, such as in the case of UPRT, it is essential for the instructor to have sufficient tools to observe the state of the simulation in relation to the envelopes of different confidence levels. According to the ICAO Manual on Aeroplane Upset Prevention and Recovery Training, "*instructors should have available, and be trained to effectively utilise, IOS tools that convey:*

a) when the simulator model is no longer valid,
b) when the aeroplane operational envelope has been exceeded, and
c) *when inappropriate control inputs have been used.*"

Consequently, enhancements for the instructor operating stations have become an important area of development for simulators to be utilised in UPRT. The ICAO has for example adopted a recommendation to include real-time instructor feedback during the upset event for existing simulators used in UPRT. Figure 15 illustrates an example of what an instructor feedback display of a modern simulator may look like. [9]

Top left part of the display represents the envelope with respect to angle of attack α and sideslip angle β; the green plot indicates the area of high confidence with flight test validated data, the yellow plot indicates the area of medium confidence with data based on predictive methods, and finally the red rectangle represents the area of low confidence level with estimated data. Top right part of the display represents the envelope with respect to airspeed V and aeroplane load factor n. Bottom right part of the display shows the primary flight display as seen by the pilot, and bottom left part of the display indicates control inputs and aeroplane configuration. [8]

From this kind of feedback display the instructor has access to all the necessary information to simultaneously monitor the state of the simulation and the activities of the flight crew. For example inappropriate rudder control inputs would otherwise be rather difficult to detect from the IOS position. Another valuable aspect is that the applied control inputs can be replayed to the flight crew during debriefing; if for example the pilot has adversely applied rudder in an approach-to-stall exercise, the occurrence could be pointed out from the replay, as well as the possible excursion from the high confidence region to instil the understanding that in a real aeroplane a similar input could have led to a different result.

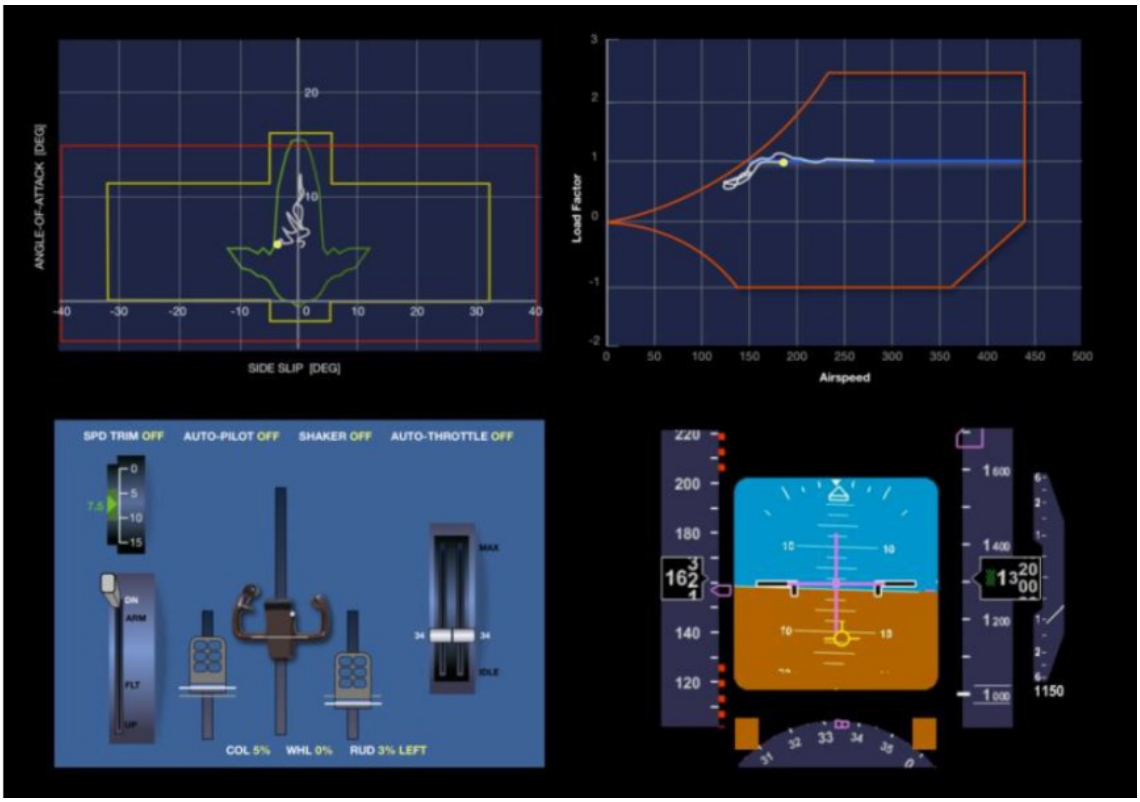

Figure 15 UPRT instructor feedback [8]

4.4 Validated Training Envelope

Defining the term Validated Training Envelope was set as one of the key objectives for the first work package of the EASA rulemaking task RMT.0196 on updating FSTD requirements, and a proposal of the definition is encompassed within the resulting NPA 2017-13, issued in July 2017. Noteworthily, the contents of the NPA mostly follow the guidelines set by the AURTA. It is proposed that the currently used term "Validated Training Envelope" would be replaced by the term "FSTD Training Envelope". Additionally a new term, "FSTD Validation Envelope", is presented. Even though the NPA is only a draft of the upcoming set of requirements, and subject of changes based on consultation, the key elements are likely to remain comparable with the final wording of the regulations. [18]

The FSTD Validation Envelope is defined as synonymous with the α-β regions of three confidence levels as classified by the ICAO, as presented in the previous chapter. Furthermore, the FSTD Training envelope is defined as the combination of high and medium confidence level regions of the FSTD Validation Envelope.

It is noteworthy, that in the above-mentioned NPA the EASA has proposed to include the region of medium confidence level to the definition of the FSTD Training Envelope. In other words, the simulation is not required to stay entirely within the flight test validated region during an UPRT manoeuvre, but instead excursions to the medium confidence region – based on predictive methods – are allowed. For continuity, the aerodynamic

model should also remain contiguous beyond the FSTD Training Envelope, to allow completion of the upset recovery tasks in all situations.

It is proposed that the FSTD Validation Envelope should be derived by the aerodynamic-data provider, or using information and data sources provided by the aerodynamic-data provider, and that the envelope should be constituted for flaps up and flaps down configurations at minimum. [18]

Similarly as presented in the previous chapter, it is proposed in the NPA that the instructor operating station should be equipped with a feedback mechanism, employing a method to display the expected fidelity of the simulation with respect to the FSTD Validation Envelope. This may be achieved by displaying an α-β cross-plot on the instructor screen, or an alternative method. The IOS should also employ methods for the instructor to evaluate the flight control inputs made during the upset recovery manoeuvre, as well as the aeroplane's flight parameters with respect to operational limits. At minimum, the IOS should display in real-time, and in a provided time history, the following parameters and limits:

- Airspeed and airspeed limits, including stall speed, maximum operating limit airspeed and maximum operating Mach number;
- Load factor and operational load factor limits;
- Angle of attack and stall identification angle of attack.

Figure 16 illustrates an example of a V-n diagram, convenient for depicting the operational limits of an aeroplane. The IOS feedback mechanism may also be a separate mobile device, provided that it is suitable for monitoring the proper execution of UPRT exercises and debriefing the crew. The instructor should have all the necessary information available to clearly establish if a manoeuvre was conducted within the FSTD Training Envelope or not. [18]

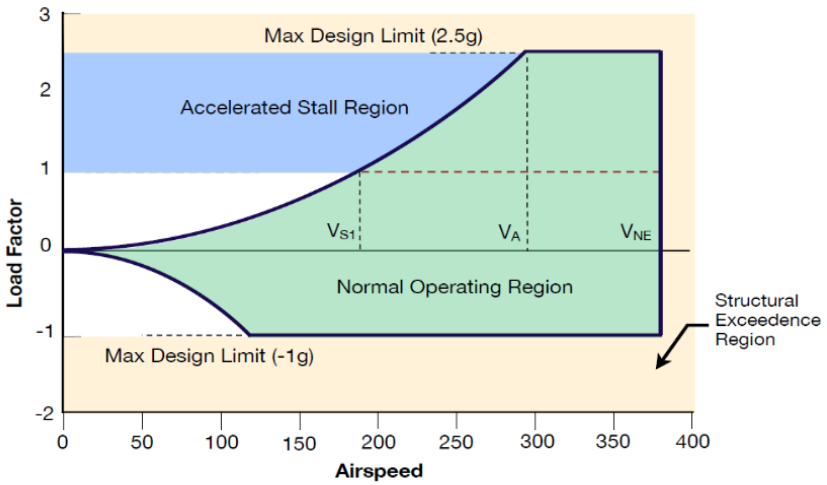

Figure 16 V-n diagram [18]

As discussed in Chapter 2.4.3, additional provisions are proposed for simulators used in upset recovery tasks conducted in angles of attack beyond the stall warning system activation. These requirements specifically address to type specific recognition cues experienced during an impending stall, and control input response from stall break to recovery. The additional qualification is partially composed of subjective testing by an SME pilot, and the results should be declared in a Statement of Compliance.

While the fundamental problem of determining the validated envelope of a simulator is the same, the means for solution for a modern simulator with all data and support from OEM readily available are very different compared to the case with an aged device, qualified under grandfathered rights and possibly having the MQTG as the sole source of flight validated data. This issue is further elaborated in the next chapter.

4.5 Methods to determine the envelope

The primary source for deriving the Validated Training Envelope should essentially be the original equipment manufacturer, and for the most modern devices, many of the necessary mechanisms for UPRT are commonly included already within the delivery. For older devices the level of support from the manufacturer may however be degraded due to varying reasons, and in such cases the simulator qualification certificate holder may have to implement alternative methods to constitute the envelope. In any case the envelope should be based on data and information originating from the OEM.

All devices are flight test validated during the qualification process to meet the minimum provisions set in the relevant Primary Reference Document. Therefore, a reasonable starting point for determining the high confidence region would be to examine the tests incorporated in the Qualification Test Guide. Depending on the provisions at the time of the initial qualification, the QTG tests may or may not display the results against angle of attack and sideslip angle. If these parameters are available, the simplest approach would be to collect α-β data points from passed QTG tests and combine them into an envelope per aeroplane configuration. At minimum, distinction should be made between flaps up and flaps down configurations.

If available, the VDR document of the simulator should be inspected to verify the sources of the validation data behind the relevant QTG tests. If any engineering data is included, a special effort should be made to estimate the level of reliability of that data.

In case the values of α and β are not printed on the validation tests of the simulator, an option would be to replicate the QTG tests and by some means record the values of those parameters. If, for example, the results of a QTG tests show a good match between simulator performance and flight test data in terms of control inputs, attitude angles, and airspeed, it may be reasoned that the aerodynamic model has calculated the aerodynamic forces and moments with good accuracy, and therefore α and β should also have a decent match. Even if the values of α and β are not included in the resulting data plots, they may still be visible in engineering displays or at least extractable via some digital interface during the execution of the test. After all, the parameters of α and β are inherently included in the computation of aerodynamic forces and moments of all Full Flight Simulators.

The high confidence region is not strictly limited to what has been tested in the QTG; if any additional flight test data is available, it could be utilised to extend the region beyond the minimum provisions covered by the QTG tests. According to NPA 2017-13, "*as long as the aerodynamics mathematical model has been conformed to the flight test results, that portion of the mathematical model is considered to be within the flight-test-validated region*". [18]

As is the case with initial qualification, the validity of the aerodynamic model can only be tested against a limited set of data points; for example QTG tests incorporating high sideslip angles are typically not replicated for both directions. Generally the combinations of aeroplane configurations and initial conditions per each test are rather limited for practical reasons. Given the assumption that the aeroplane is geometrically symmetrical about the XZ-plane, it is likely a sufficient approach to manage the envelope as symmetrical with respect to β. In reality, the rotating masses and unsymmetrical airflows of the engines (and propellers) produce moments, which may cause lopsided responses especially in stall breaks with turboprop aeroplanes. When assessing the suitability of the device for full-stall training, the validation of this kind of behaviour must be taken into account. This thesis, however, does not delve deeper into the issue, as only approach-to-stall exercises are required by the EASA.

Engineering judgement should be used when connecting data points to outline the envelope. The most straightforward approach would be to connect the α-β data points linearly. However, particular attention should be paid if two adjacent data points are far apart, and especially when working with combinations of high α and high β. Convex hull approximation may be justified for filling minor gaps, but it should nevertheless be used with caution. The closer to zero the angle of attack is, the more reasonable such simplifications are. At regions of higher α, it may be more appropriate to handle β as constant when bridging a minor gap.

It should also be noted, that initial conditions have effect on the aerodynamic response of the aeroplane. For example, some aerodynamic stability derivatives, such as aeroelastic effects and load factor effects on lift factor, are functions of atmospheric density. This may cause some inconsistencies when combining data points from tests conducted at considerably different altitudes. For practical reasons the loading conditions and CG position may vary between tests conducted during the flight test programme. The influence of ground effect becomes relevant in tests conducted at the very lowest altitudes, such as in the side wind landing QTG test. This returns to the fact that a 100 % validation is practically not possible, but nevertheless the goal is to attain sufficiently high confidence.

In order to assess the medium confidence level region, two matters must be resolved:

1. What regions of simulation are covered by aerodynamic data in the aerodynamic model?
2. Which part of that data is based on reliable methods, i.e. not extrapolated?

The preferred sources for the analysis would be the aerodynamic data package, any software descriptions by the manufacturer, and the source code of the aerodynamic model, if available. Depending on the technical implementation, these may be found in very different formats.

The main element that should be addressed for is the table look-up process, as the ranges of data contained in the look-up tables provide a good frame of reference for questions 1 and 2. Fundamentally the medium confidence region should be the region that is not out of range of any existing look-up table. Neglecting the effects of any stability or control derivatives should be a carefully reasoned decision.

Some of the aerodynamic parameters may be expressed in the form of functions instead of look-up tables, which introduces a challenge when attempting to determine the validity range of those parameters. When such is the case, the overall importance of those parameters should be taken into account. Chapter Five addresses this issue in more detail.

5 Case study of a Boeing 747 data package

One of the rare simulation data packages made available in the public domain is originally prepared by the Boeing Company and published as a NASA contractor report in 1971. This report contains mathematical models and extensive aerodynamic data to simulate the flying qualities and characteristics of the Boeing 747 jet airliner for the NASA Flight Simulator for Advanced Aircraft. The report is divided into two volumes. Volume I includes a description of the work performed under the contract, generalised equations and approximations for simulation, the form of the data and nomenclature. Volume II is composed as a summary of the 747 aerodynamic data, including a general description of the aircraft, aerodynamic characteristics in terms of lift, drag, pitching moment, rolling moment, yawing moment, and side force coefficients, control characteristics, descriptions of high lift system, propulsion system and landing gear, and finally, results of the simulation checkout. [43]

As a base rule set for the NASA simulation programme, flaps-up and flaps-down data was to be incorporated into one computer program to enable simulation capability throughout the whole flight envelope of the aircraft. The significant stability derivatives, including control derivatives were to be modified by multiplication factors during simulation. System malfunctions, such as asymmetric flaps and floating control surfaces are included in the provided data. [49]

The Boeing 747 is a very large four-engine intercontinental jet airliner, first flown in 1969. Modern variants of the aircraft are still manufactured, and the total production number is over 1500. [50] As a conventional, swept wing design, it may be presumed that the aerodynamic characteristics of the airframe are adequately comparable to a generic modern wide-body jet airliner, even though the aerodynamic data is originating from an early 747-100 variant. The scope of the included aerodynamic data is extensive.

The aerodynamic coefficients for the six above-mentioned forces and moments acting on the airframe are presented in their own chapters, containing the main equation for the variable, and the associated stability and control derivatives in forms of graphs. Usually, for slow airspeeds, the stability derivatives are presented per flap or spoiler configuration as functions of aerodynamic angles, equivalent airspeed, rate of change of orientation angles, load factor, or control surface deflection. For high airspeeds the stability derivatives are presented in flaps up condition, usually as functions of Mach number and aerodynamic angles, pressure altitude, rate of change of orientation angles, load factor, or control surface deflection. The division between low speed and high speed occurs at Mach 0.3. The dimensionless force and moment coefficients are further converted into forces and moments to obtain six degree of freedom airframe response.

The aerodynamic data in Volume II of the report is based on flight tests, engineering simulation by Boeing, analytical extrapolation and aeroplane flight manual (AFM). The ranges of analytically extrapolated data are marked as dashed lines in contrast to solid lines, presenting validated data in the data plots. For even higher values than the highest analytically extrapolated, only linear extrapolation is advised to be used. [49] As an example, Figure 17 illustrates the relation between the lifting force coefficient and the drag force coefficient at high airspeeds, with the extrapolated region shown as dashed lines.

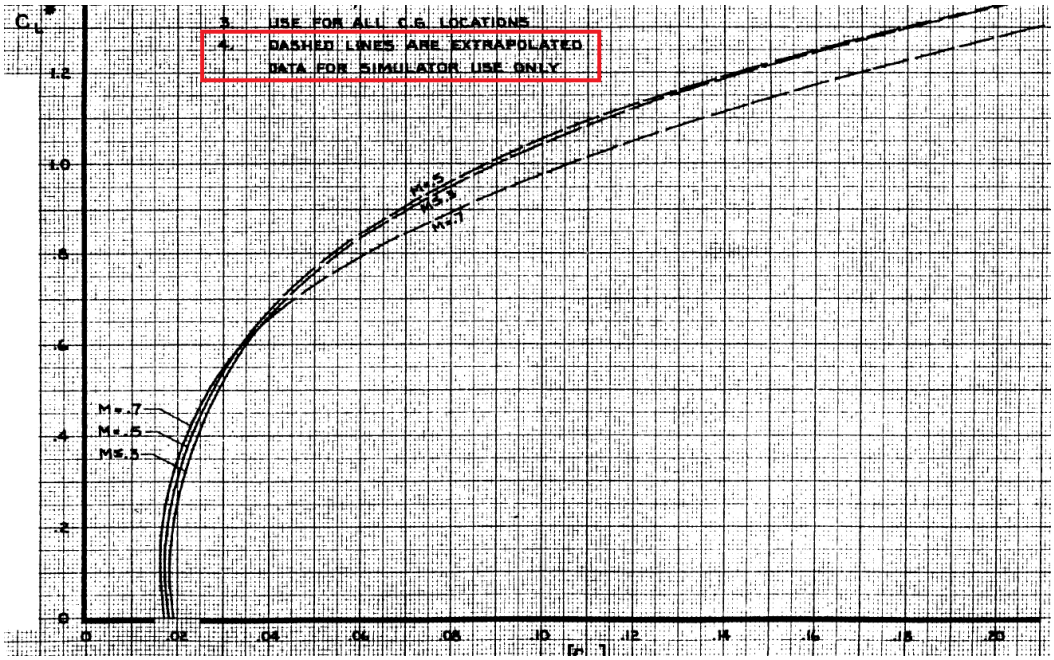

Figure 17 Boeing 747 aerodynamic data [43]

In this case study the aerodynamic data encompassed within the Volume II of the documentation was examined in an attempt to outline an envelope. The composition of the six aerodynamic forces and moments, and their individual sub-components, were studied, and data for these sub-components was interpolated and calculated from selected flight conditions, in order to get an understanding of their relative significance in the context of their relevant stability axis. Point of comparison for the results was also sought from the literature.

5.1 Research methods

The main objectives of this case study were to examine the relative significance of different aerodynamic stability and control derivatives, and to outline a medium confidence level region with respect to the aerodynamic angles of α and β. This case was assumed to be comparable to the situation of the simulator operator attempting to resolve the medium confidence envelope by examining an aerodynamic data package. As there are typically only a limited amount of resources to be dispatched for such a task, while the amount of data may be immense, prioritisation must be made on basis of the importance of the derivatives.

The medium confidence region may be based on reliable predictive methods, whereas extrapolated region is considered as low confidence. In order to outline the medium confidence level α-β envelope, the data plots of all available aerodynamic derivatives were examined in order to locate the regions of experimental data and extrapolated data. Values of individual derivatives at selected flight conditions were interpolated from the data plots in order to get a picture of their influence. Two flight conditions representing high speed at high altitude, and low speed at low altitude, as listed in Table 5, were colour coded to help

with comparison. Selected samples from the interpolations were presented as tables in Appendix 1.

Table 5 Colour coded flight conditions

Mach number	Pressure altitude	Flap position
0.30	Sea Level	Up
0.80	40 000 ft	Up

As the individual sub-components of the equations are heavily coupled, it was found impractical to compare the individual components of the relevant stability axis to each other within a given flight condition. For example in the context of lift force, it would have been possible to compare only a subset of the components, given if a stabilised flight condition would have been assumed, and all the dynamic components, such as the effect of pitch rate, would have been neglected. However this kind of analysis would not have provided very valuable information in the context of simulating UPRT related manoeuvres, which commonly introduce rough attitudes and high angle rates.

Thus, attention was focused in the order of magnitude of the effects that each sub-component brings about to the relevant aerodynamic force or moment. For the interpolation and calculation of the dynamic components, representative values of angle rates, airspeed, etc. were sought from the literature.

Ground operations and malfunctions leading to asymmetrical flight conditions were excluded from this case study. Additionally, several effects related to control derivatives, spoilers, landing gear and ground effect were considered as marginal with respect to the whole picture, and were therefore excluded.

5.2 Lift force coefficient

At a given wing datum plane angle of attack ($\propto_{\text{W.D.P}}$) the lift coefficient is expressed as:

(16)

$$C_L = C_{L_{Basic}} + (\Delta C_L)_{\alpha_{W.D.P.}=0} + \Delta\left(\frac{dC_L}{d\alpha}\right)\alpha_{W.D.P.} + \frac{dC_L}{d\hat{\alpha}}\left(\frac{\dot{\alpha}\bar{c}}{2V}\right) + \frac{dC_L}{d\hat{q}}\left(\frac{q\bar{c}}{2V}\right) + \frac{dC_L}{dn_z}n_z + K_\alpha\frac{dC_L}{d\eta}\eta_{F.R.L.} + K_\alpha\frac{dC_L}{d\delta_{e_l}}\delta_{e_l} + K_\alpha\frac{dC_L}{d\delta_{e_o}}\delta_{e_o} + \Delta C_{L_{spoilers}} + \Delta C_{L_{outboard\ ailerons}} + \Delta C_{L_{landing\ gear}} + \Delta C_{L_{ground\ effect}}$$

The separate terms are defined below:

1. $C_{L_{Basic}}$ — Basic lift coefficient for the rigid aeroplane with neutral stabiliser in free air and with the landing gear retracted
2. $(\Delta C_L)_{\alpha_{W.D.P.}=0}$ — Change in lift coefficient at $\alpha_{W.D.P.} = 0$ due to aeroelasticity
3. $\Delta\left(\frac{dC_L}{d\alpha}\right)\alpha_{W.D.P.}$ — Change in lift coefficient due to the aeroelastic effect on the aeroplane's basic lift curve slope
4. $\frac{dC_L}{d\hat{\alpha}}\left(\frac{\dot{\alpha}\bar{c}}{2V}\right)$ — Change in lift coefficient due to rate of change of angle of attack
5. $\frac{dC_L}{d\hat{q}}\left(\frac{q\bar{c}}{2V}\right)$ — Change in lift coefficient due to pitch rate
6. $\frac{dC_L}{dn_z}n_z$ — Change in lift coefficient due to aeroelastic inertia relief caused by normal load factor
7. $K_\alpha\frac{dC_L}{d\eta}\eta_{F.R.L.}$ — Change in lift coefficient due to change in stabiliser angle from $\eta_{F.R.L.} = 0°$
8. $K_\alpha\frac{dC_L}{d\delta_{e_i}}\delta_{e_i}$ — Change in basic lift coefficient due to inboard elevator deflection from $\delta_{e_i} = 0°$
9. $K_\alpha\frac{dC_L}{d\delta_{e_o}}\delta_{e_o}$ — Change in basic lift coefficient due to outboard elevator deflection from $\delta_{e_o} = 0°$
10. $\Delta C_{L_{component}}$ — Change in basic lift coefficient due to different components

The basic lift coefficient $C_{L_{Basic}}$ itself is defined by a set of data plots – as a function of angle of attack and flap angle at low airspeeds, and as a function of angle of attack and Mach number at high airspeeds. Free air is assumed, stabiliser and elevators are set in neutral angle, landing gear is retracted and thrust effects are excluded.

The available data for basic lift coefficient at low airspeeds ranges from $\propto_{\text{W.D.P}} = -5°$ to $\propto_{\text{W.D.P}} = +25°$, with the maximum demonstrated value of $C_{L_{Basic}} = 2.47$ occurring at $\propto_{\text{W.D.P}} = +19°$ with maximum flap extension of 30 degrees. The data plots for flap settings of 20 degrees and higher demonstrates a developing aerodynamic stall, as the maximum basic lift coefficient occurs before reaching the highest measured angle of attack. The highest demonstrated value with flaps retracted occurs at $\propto_{\text{W.D.P}} = +25°$, where $C_{L_{Basic}} = 1.37$. Values of $C_{L_{Basic}}$ at low airspeeds are listed in Table A1.1 of Appendix 1.

The data plots for high airspeeds range from Mach 0.30 to Mach 0.97. Flaps are in retracted position in all of the high speed data plots. The upper limit of the angle of attack is reduced from +25° to +10° toward higher Mach numbers. Aerodynamic stall is not demonstrated in the high speed data, as the maximum values of $C_{L_{Basic}}$ are measured at the high end of α in each data plot. Upwards from Mach 0.50 the data plots are also extrapolated up to $\propto_{\text{W.D.P}} = +25°$ as dashed lines. It is further elaborated on the data sheet that the dashed lines are for simulator use only, and that only linear extrapolation should be used if a higher value of $\propto_{\text{W.D.P}}$ is required. Values of $C_{L_{Basic}}$ at high airspeeds are listed in Table A1.2.

Interpolated values of lift force related terms from selected flight conditions are listed in Table A1.3. In order to study the trends associated with terms #4 and #5, deliberately high values of pitch rate and rate of change of angle of attack were used. For a wings level steady state pull-up, the pitch rate can be obtained from:

$$q = \frac{180}{\pi}\frac{g}{V}(n-1) \tag{17}$$

where the maximum operational limit for load factor n = 2.5. Thus, the maximum imaginable pitch rate would be in the order of 10 degrees per second.

Maximum demonstrated lift coefficients and initial buffet boundary with flaps up, gear up and in a trimmed symmetrical flight condition are listed in Table A1.4. [43]

5.3 Drag force coefficient

At a given $\propto_{\text{W.D.P}}$ the drag coefficient is expressed as:

$$C_D = K\left[C_{D_{Basic}} + \frac{dC_D}{d\eta}\eta_{F.R.L.}\right] + [1-K][C_D]_M + \Delta C_{D_{spoilers}} + \Delta C_{D_{landing\ gear}} + \Delta C_{D_{ground\ effect}} + \Delta C_{D_{sideslip}} + \Delta C_{D_{rudders}} + \Delta C_{D_{flap\ failure}} \quad (18)$$

where K = 0 for flaps up, and K = 1 for all other flap settings.

The separate terms are defined below:

1. $C_{D_{Basic}}$ — Basic drag coefficient for the rigid aeroplane with neutral stabiliser in free air and with the landing gear retracted
2. $\frac{dC_D}{d\eta}\eta_{F.R.L.}$ — Change in basic drag coefficient due to change in stabiliser angle from $\eta_{F.R.L.} = 0°$
3. $[C_D]_M$ — Drag coefficient in Mach number M
4. $\Delta C_{D_{component}}$ — Change in drag coefficient due to different components

If the flaps are extended, the drag resulting from the airframe is expressed as a sum of the basic drag coefficient, and the effect due to change of stabiliser angle. Both of these terms are expressed as functions of angle of attack and flap angle, and they have data available in the range of $\propto_{\text{W.D.P}} = -5°$ to $\propto_{\text{W.D.P}} = +25°$. Free air is assumed, landing gear is retracted, thrust effects are excluded and tests are conducted at low airspeed. Extremums for these terms are tabulated in Table A1.5 for a selection of flap settings. Maximum demonstrated value for basic drag coefficient occurs at $\propto_{\text{W.D.P}} = +25°$ in each data plot.

If the flaps are fully retracted, the drag of the airframe is expressed as a function of the lift coefficient, and the Mach number. The data range for demonstrated airframe drag is limited by the lift coefficient. The data plots for each Mach number are extrapolated as dashed lines, to cover higher values of the lift coefficient for simulator use. Unlike with the data sheet of basic lift coefficient, the data sheet of airframe drag coefficient does not contain an advice to extend the data range by linear extrapolation. Values of the basic drag coefficient are listed in Table A1.6.

The drag increment due to extended landing gear is plotted as a function of angle of attack and flap setting. For low airspeeds the data ranges from $\propto_{\text{W.D.P}} = -5°$ to $\propto_{\text{W.D.P}} = +25°$. For high airspeeds the multiplier for Mach number effect is plotted on a separate single graph up to the maximum extension speed of Mach 0.82. The maximum and minimum drag increments due to landing gear are listed in Table A1.7.

The drag increment due to sideslip is plotted as a function of sideslip angle and flap setting. The available data ranges from $\beta = 0°$ to $\beta = \pm 15°$. Values of drag due to sideslip for different flap configurations at $\beta = \pm 15°$ are listed in Table A1.8. [43]

The drag effects of control surfaces, spoilers and ground effect were briefly assessed, but not included in the tables, as they were considered insignificant for this case study.

5.4 Pitching moment coefficient

At a given $\propto_{\text{W.D.P}}$ the pitching moment coefficient is expressed as:

$$C_{m_{C.G.}} = C_{m_{.25_{Basic}}} + \left(\Delta C_{m_{.25}}\right)_{\alpha_{W.D.P.=0°}} + \Delta\left(\frac{dC_{m_{.25}}}{d\alpha}\right)\alpha_{W.D.P.} + C_L(C.G.-.25) + \frac{dC_m}{d\hat{\alpha}}\left(\frac{\dot{\alpha}\bar{c}}{2V}\right) + \frac{dC_{m_{.25}}}{d\hat{q}}\left(\frac{q\bar{c}}{2V}\right) + \frac{dC_{m_{.25}}}{dn_z}n_z + K_\alpha\frac{dC_{m_{.25}}}{d\eta}\eta_{F.R.L.} + K_\alpha\frac{dC_{m_{.25}}}{d\delta_{e_i}}\delta_{e_i} + K_\alpha\frac{dC_{m_{.25}}}{d\delta_{e_o}}\delta_{e_o} + \Delta C_{m_{.25_{spoilers}}} + \Delta C_{m_{.25_{inboard\ ailerons}}} + \Delta C_{m_{.25_{outboard\ ailerons}}} + \Delta C_{m_{.25_{landing\ gear}}} + \Delta C_{m_{.25_{ground\ effect}}} + \Delta C_{m_{.25_{sideslip}}} + \Delta C_{m_{.25_{rudders}}} + \Delta C_{m_{.25_{flap\ failure}}} \tag{19}$$

The separate terms are defined below:

1. $C_{m_{.25_{Basic}}}$ — Basic pitching moment coefficient for the rigid aeroplane with neutral stabiliser in free air and with the landing gear retracted and with the C.G. = 25% M.A.C.
2. $\left(\Delta C_{m_{.25}}\right)_{\alpha_{W.D.P.=0°}}$ — Change in basic pitching moment coefficient at $\alpha_{W.D.P.} = 0$ due to aeroelasticity
3. $\Delta\left(\frac{dC_{m_{.25}}}{d\alpha}\right)\alpha_{W.D.P.}$ — Change in basic pitching moment coefficient due to the aeroelastic effect on the rigid aeroplane basic pitching moment coefficient curve slope
4. $C_L(C.G.-.25)$ — Change in pitching moment coefficient due to centre of gravity variation from 25% M.A.C.
5. $\frac{dC_m}{d\hat{\alpha}}\left(\frac{\dot{\alpha}\bar{c}}{2V}\right)$ — Change in basic pitching moment coefficient due to rate of change of angle of attack
6. $\frac{dC_{m_{.25}}}{d\hat{q}}\left(\frac{q\bar{c}}{2V}\right)$ — Change in basic pitching moment coefficient due to pitch rate
7. $\frac{dC_{m_{.25}}}{dn_z}n_z$ — Change in basic pitching moment coefficient due to aeroelastic inertia relief caused by normal load factor

8. $K_\alpha \frac{dC_{m_{.25}}}{d\eta} \eta_{F.R.L.}$ Change in basic pitching moment coefficient due to change in stabiliser angle from $\eta_{F.R.L.} = 0°$

9. $K_\alpha \frac{dC_{m_{.25}}}{d\delta_{e_i}} \delta_{e_i}$ Change in basic pitching moment coefficient due to inboard elevator deflection from $\delta_{e_i} = 0°$

10. $K_\alpha \frac{dC_{m_{.25}}}{d\delta_{e_o}} \delta_{e_o}$ Change in basic pitching moment coefficient due to outboard elevator deflection from $\delta_{e_o} = 0°$

11. $\Delta C_{m_{.25_{component}}}$ Change in basic pitching moment coefficient due to different components

The basic pitching moment coefficient is given as a function of flap position and angle of attack at low airspeeds, and as a function of Mach number and angle of attack at high airspeeds. Free air is assumed, stabiliser and elevators are set in neutral angle, landing gear is retracted and thrust effects are excluded. The centre of gravity is set at 25% MAC.

Interpolated values for the basic pitching moment coefficient are listed in Table A1.9 for low airspeeds, and in Table A1.10 for high airspeeds. At high airspeeds, the range of available flight test data gradually decreases toward higher Mach numbers: at Mach 0.91 the maximum available angle of attack is 10 degrees. These values are further extrapolated at high airspeeds.

Interpolated values of pitching moment related terms from selected flight conditions are listed in Table A1.11. All values were derived with the centre of gravity set at 25% MAC. [43]

5.5 Rolling moment coefficient

At a given $\propto_{W.D.P}$ the rolling moment coefficient is expressed as:

$$C_l = \frac{dC_l}{d\beta}\beta + \frac{dC_l}{d\hat{p}}\frac{p_s b}{2V} + \frac{dC_l}{d\hat{r}}\frac{r_s b}{2V} + \Delta C_{l_{spoilers}} + \Delta C_{l_{inboard\ ailerons}} + \Delta C_{l_{outboard\ ailerons}} + \Delta C_{l_{rudders}} + \Delta C_{l_{flap\ failure}} + \Delta C_{l_{L.E.failure}} \quad (20)$$

The separate terms are defined below:

1. $\frac{dC_l}{d\beta}\beta$ — Rolling moment coefficient due to the angle of sideslip β
2. $\frac{dC_l}{d\hat{p}}\frac{p_s b}{2V}$ — Rolling moment coefficient due to the roll rate about the stability axis x_s
3. $\frac{dC_l}{d\hat{r}}\frac{r_s b}{2V}$ — Rolling moment coefficient due to the yaw rate about the stability axis z_s
4. $\Delta C_{l_{component}}$ — Rolling moment coefficient due to different components

The rolling moment coefficient is composed of the effects of sideslip angle, roll rate, yaw rate, and control derivatives. Interpolated values for the stability derivatives from selected flight conditions are listed in Table A1.12. The components of the rolling moment coefficient do not contain any extrapolated data. All values were derived with the centre of gravity set at 25% MAC. It is noteworthy, that angular rates are expressed with radians and velocity with feet per second in the documentation, as well as in Table A1.12. [43]

5.6 Yawing moment coefficient

At a given $\propto_{W.D.P}$ the yawing moment coefficient is expressed as:

$$C_{n_{C.G.}} = \frac{dC_n}{d\beta}\beta + \frac{dC_n}{d\hat{\dot{\beta}}}\frac{\dot{\beta}b}{2V} + \frac{dC_n}{d\hat{p}}\frac{p_s b}{2V} + \frac{dC_n}{d\hat{r}}\frac{r_s b}{2V} + \Delta C_{n_{spoilers}} + \Delta C_{n_{inboard\ ailerons}} + \Delta C_{n_{outboard\ ailerons}} + \Delta C_{n_{rudders}} + \Delta C_{n_{flap\ failure}} + \Delta C_{n_{L.E.failure}} \quad (21)$$

The separate terms are defined below:

1. $\frac{dC_n}{d\beta}\beta$ — Yawing moment coefficient due to the angle of sideslip β
2. $\frac{dC_n}{d\hat{\dot{\beta}}}\frac{\dot{\beta}b}{2V}$ — Yawing moment coefficient due to rate of change of sideslip angle
3. $\frac{dC_n}{d\hat{p}}\frac{p_s b}{2V}$ — Yawing moment coefficient due to the roll rate about the stability axis x_s
4. $\frac{dC_n}{d\hat{r}}\frac{r_s b}{2V}$ — Yawing moment coefficient due to yaw rate about the stability axis z_s
5. $\Delta C_{n_{component}}$ — Yawing moment coefficient due to different components

The yawing moment coefficient is composed of the effects of sideslip angle, sideslip rate, roll rate, yaw rate, and control derivatives. Interpolated values for the stability derivatives from selected flight conditions are listed in Table A1.13. The components of the yawing moment coefficient do not contain any extrapolated data. All values were derived with the centre of gravity set at 25% MAC. As previously, angular rates are expressed with radians and velocity with feet per second. [43]

5.7 Side force coefficient

At a given $\propto_{W.D.P}$ the side force coefficient is expressed as:

$$C_Y = \frac{dC_Y}{d\beta}\beta + \frac{dC_Y}{d\hat{p}}\frac{p_s b}{2V} + \frac{dC_Y}{d\hat{r}}\frac{r_s b}{2V} + \Delta C_{Y_{spoilers}} + \Delta C_{Y_{rudders}} + \Delta C_{Y_{flap\ failure}} + \Delta C_{Y_{L.E.failure}} \quad (22)$$

The separate terms are defined below:

1. $\frac{dC_Y}{d\beta}\beta$ — Side force coefficient due to the angle of sideslip β
2. $\frac{dC_Y}{d\hat{p}}\frac{p_s b}{2V}$ — Side force coefficient due to the roll rate about the stability axis x_s
3. $\frac{dC_Y}{d\hat{r}}\frac{r_s b}{2V}$ — Side force coefficient due to the yaw rate about the stability axis z_s
4. $\Delta C_{Y_{component}}$ — Side force coefficient due to different components

Finally, the side force coefficient is composed of the effects of sideslip angle, roll rate, yaw rate and control derivatives. Values interpolated for the stability derivatives are listed in Table A1.14. The components of the side force coefficient do not contain any extrapolated data. [43]

5.8 Results

5.8.1 Relative importance of stability derivatives

Based on extracts from the data, for longitudinal stability the basic terms $C_{L_{Basic}}$ and $C_{m.25_{Basic}}$ have by far the most influential role. The aeroelastic effects become significant at flaps-down configurations, as well as at the highest transonic cruise speeds. Concerning the pitching moment, the effects of pitch rate have a greater influence than the effects of the angle of attack rate. The drag force coefficient is mostly coupled with the lift force coefficient. With regards to lateral stability, the sideslip related effects have a major influence. Roll rate is significant with respect to the rolling moment coefficient, whereas yaw rate is to the yawing moment coefficient.

These results are well in line with Napolitano, who has grouped the relative importance of the longitudinal and lateral control stability derivatives as presented in the following table:

Table 6 The relative importance of aerodynamic stability derivatives [44]

Relative importance group		Stability derivatives
#1	Very important	c_{L_α}, c_{m_α}, c_{l_β}, c_{n_β}
#2	Important	$c_{m_{\dot{\alpha}}}$, c_{m_q}, c_{l_p}, c_{n_r}
#3	Moderately important	c_{D_0}, c_{D_α}
#4	Moderately to marginally important	c_{L_0}, c_{m_0}
#5	Moderately to marginally important	$c_{L_{\dot{\alpha}}}$, c_{L_q}
#6	Marginally important to insignificant	c_{Y_β}, c_{Y_p}, c_{Y_r}, c_{n_p}, c_{l_r}
#7	Insignificant	$c_{D_{\dot{\alpha}}} \approx 0$, $c_{D_q} \approx 0$, $c_{Y_{\dot{\beta}}} \approx 0$, $c_{l_{\dot{\beta}}} \approx 0$, $c_{n_{\dot{\beta}}} \approx 0$

The stability derivatives listed as group #1 describe the effects of α to lift force and pitching moment, and the effects of β to rolling moment and yawing moment. These are the most important aerodynamic coefficients – acting as key elements of aerodynamic design, defining to a large extent the dynamic stability of the aeroplane.

Whereas the group #1 stability derivatives affect the overall stability of the aeroplane, the derivatives listed as group #2 principally affect to the handling qualities and dynamic characteristics as perceived by the pilot. The drag related coefficients listed as group #3 do not directly affect the stability of the aeroplane, but have a major influence on the overall drag at trimmed states, and consequently the necessary thrust force to obtain steady state flight. The coefficients listed as group #4 are longitudinal bias terms, which have effect on the trimmability of the aeroplane.

The coefficients listed as groups #5, #6 and #7 have moderate to insignificant importance, with coefficients listed as group #7 being virtually negligible for most aeroplanes. [44]

Thus, it may be deduced that the most attention should be paid on the following aerodynamic stability terms contained in a data package of this kind:

Table 7 Significant lift force related stability terms

Term	Definition	Order of magnitude
$C_{L_{Basic}}$	Basic lift coefficient as a function of α and aeroplane configuration (component of c_{L_α})	0 to -1 or less
$(\Delta C_L)_{\alpha_{W.D.P.}=0}$	Change in lift coefficient at $\alpha_{W.D.P.} = 0$ due to aeroelasticity	-1 to -3 or less
$\Delta\left(\frac{dC_L}{d\alpha}\right)\alpha_{W.D.P.}$	Change in lift coefficient due to the aeroelastic effect on the aeroplane's basic lift curve slope (component of c_{L_α})	-1 to -3 or less

Table 8 Significant pitching moment related stability terms

Term	Definition	Order of magnitude
$C_{m_{.25}Basic}$	Basic pitching coefficient as a function of α and aeroplane configuration (component of c_{m_α})	-1 to -2 or less
$\left(\Delta C_{m_{.25}}\right)_{\alpha_{W.D.P.=0°}}$	Change in basic pitching moment coefficient at $\alpha_{W.D.P.} = 0$ due to aeroelasticity	-2 to -3 or less
$\Delta\left(\frac{dC_{m_{.25}}}{d\alpha}\right)\alpha_{W.D.P.}$	Change in basic pitching moment coefficient due to the aeroelastic effect on the rigid aeroplane basic pitching moment coefficient curve slope (component of c_{m_α})	-1 to -3 or less
$\frac{dC_m}{d\hat{\alpha}}\left(\frac{\dot{\alpha}\bar{c}}{2V}\right)$	Change in basic pitching moment coefficient due to rate of change of angle of attack (component of $c_{m_{\dot{\alpha}}}$)	-2 to -3 or less
$\frac{dC_{m_{.25}}}{d\hat{q}}\left(\frac{q\bar{c}}{2V}\right)$	Change in basic pitching moment coefficient due to pitch rate (component of c_{m_q})	-1 to -3 or less

Table 9 Significant rolling moment related stability terms

Term	Definition	Order of magnitude
$\frac{dC_l}{d\beta}\beta$	Rolling moment coefficient due to the angle of sideslip β (component of c_{l_β})	-2 to -4 or less
$\frac{dC_l}{d\hat{p}}\frac{p_s b}{2V}$	Rolling moment coefficient due to the roll rate about the stability axis x_s (component of c_{l_p})	-2 to -4 or less

Table 10 Significant yawing moment related stability terms

Term	Definition	Order of magnitude
$\frac{dC_n}{d\beta}\beta$	Yawing moment coefficient due to the angle of sideslip β (component of c_{n_β})	-2 to -4 or less
$\frac{dC_n}{d\hat{r}}\frac{r_s b}{2V}$	Yawing moment coefficient due to yaw rate about the stability axis z_s (component of c_{n_r})	-2 to -4 or less

Even though the effect of drag force is rather important especially with respect to the required thrust force, it has marginal significance with respect to the dynamic stability of the aeroplane. In addition, the total drag force is heavily coupled with the total lift force. Hence, it is justified to leave the terms related to drag force to less attention than the terms listed above. Of the six aerodynamic forces and moments, the side force is of least importance. In addition to the groups #1 and #2 listed in Table 6, the aeroelasticity-induced offset derivatives were found to be significant especially in low-speed situations with flaps-down configuration, and were therefore included in tables 7 and 8.

5.8.2 Medium confidence level region

At low airspeeds all of the α-dependent derivatives, excluding ground effect, were found to contain analytical or flight test data in the range between -5 and 25 degrees. Ground effect related derivatives contain data in the range between 0 and 15 degrees, and separate ground effect control factors in the range between 0 and 14 degrees, as listed in Table 11.

Table 11 Ranges of α for aerodynamic variables, low speed

Derivative	$\boldsymbol{\alpha_{min}}$	$\boldsymbol{\alpha_{max}}$
$C_{L_{Basic}}$, $C_{L_{spoilers}}$, $\Delta C_{L_{ailerons}}$, $\Delta C_{L_{landing\ gear}}$, $C_{D\,Basic}$, $\Delta C_{D_{landing\ gear}}$, $C_{m_{.25_{Basic}}}$, $\Delta C_{m_{.25_{spoilers}}}$, $\Delta C_{m_{.25_{ailerons}}}$, $\Delta C_{m_{.25_{landing\ gear}}}$, $\frac{dC_l}{d\beta}$, $\frac{dC_l}{d\hat{p}}$, $\frac{dC_l}{d\hat{r}}$, $\Delta C_{l_{spoilers}}$, $\Delta C_{l_{ailerons}}$, $\Delta C_{l_{rudders}}$, $\frac{dC_n}{d\beta}$, $\frac{dC_n}{d\hat{\dot{\beta}}}$, $\frac{dC_n}{d\hat{p}}$, $\frac{dC_n}{d\hat{r}}$, $\Delta C_{n_{spoilers}}$, $\Delta C_{n_{ailerons}}$, $\Delta C_{n_{rudders}}$, $\frac{dC_Y}{d\beta}$, $\frac{dC_Y}{d\hat{p}}$, $\frac{dC_Y}{d\hat{r}}$, $\Delta C_{Y_{spoilers}}$, $\Delta C_{Y_{rudders}}$	-5°	25°
$\Delta C_{L_{ground\ effect}}$, $\Delta C_{D_{ground\ effect}}$, $\Delta C_{m_{.25_{ground\ effect}}}$	0°	15°
F_D, $F_{m_{GE}}$, F_l, F_{l_β}, F_n, F_{n_β}, F_{Y_β}	0°	14°

All β-dependent derivatives are plotted in the range of ±15 degrees, as listed in Table 12.

Table 12 Ranges of β for aerodynamic variables, low speed

Derivative	$\boldsymbol{\beta}$
$\Delta C_{D_{sideslip}}$, $\Delta C_{D_{rudders}}$, $\Delta C_{m_{.25_{sideslip}}}$, $\Delta C_{m_{.25_{rudders}}}$, $\frac{dC_l}{d\beta}$	±15°

Thus, it would be justified to declare that the medium confidence region at low airspeeds and outside of ground effect is in the range of $\propto = -5°\ to\ 25°$ and $\beta = \pm 15°$. For ground effect the range of $\propto$ would be reduced to 0° to 15°. The region of medium confidence is outlined in Figure 18.

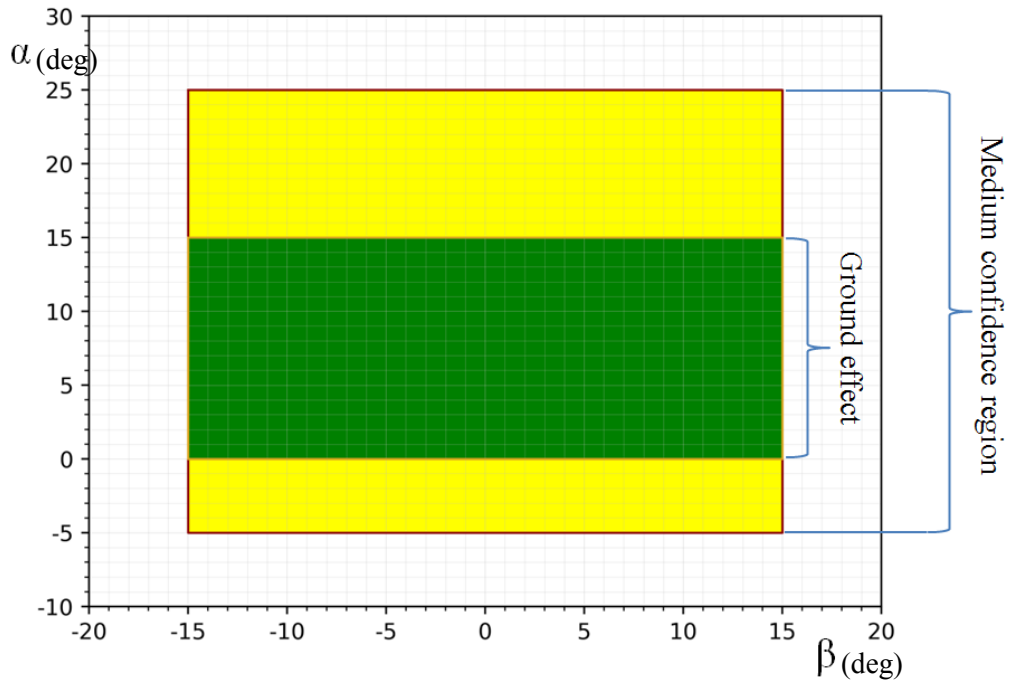

Figure 18 Region of medium confidence for low airspeed

At high airspeeds the upper range of α is reduced toward higher Mach numbers. This is likely due to the effect of aerodynamic buffeting, which restrains flight testing at high values of α. The ranges of all available variables that are plotted with respect to angle of attack and Mach number are illustrated in Figure 19. The basic lift coefficient is plotted as dark red, basic pitching moment as dark blue, and spoiler effects on side force coefficient as green. Sideslip effects on lift coefficient and sideslip effects on rolling moment coefficient have identical ranges; hence both are plotted as yellow. Additionally, the slopes of several other variables are expressed with respect to the Mach number and some other variable than α.

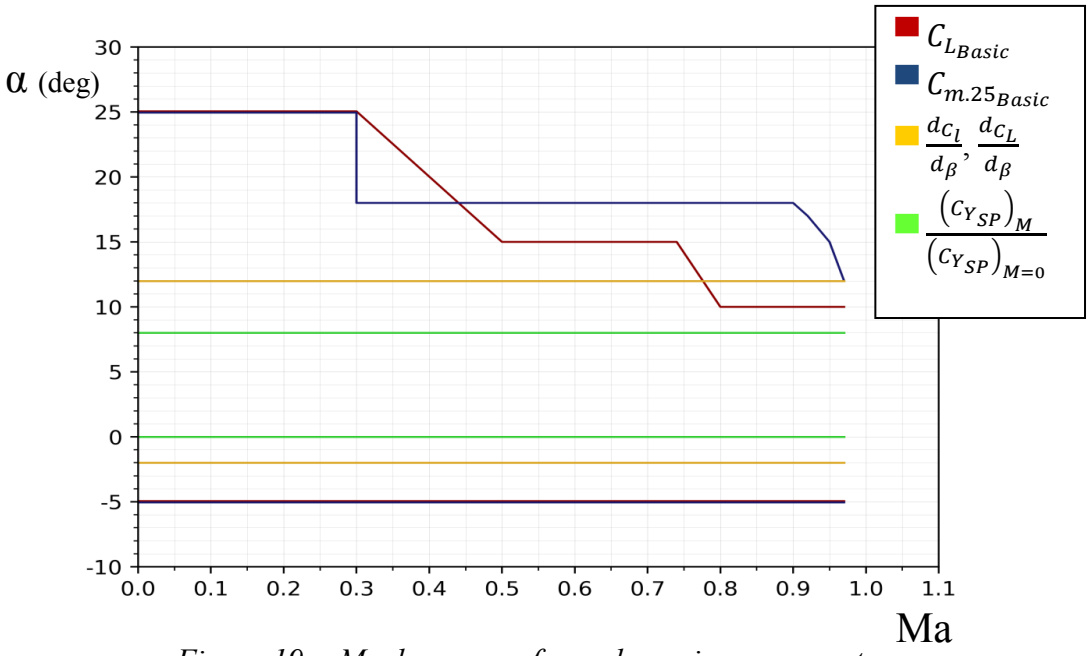

Figure 19 α-Mach ranges of aerodynamic components

5.9 Conclusions of the Boeing 747 case study

At an early stage it became apparent, that even though this data package contains to a large extent data originating from actual flight tests, separate plots for each derivative are insufficient for estimating the simultaneous values of α and β experienced during individual tests. However, the region of medium confidence level for low airspeeds could be determined with reasonable effort. The coverage of the encompassed aerodynamic data is extensive and likely representative even when compared to modern simulators.

It was discovered that the distinction between the regions of medium and low confidence levels is not always a clear cut, as some components may be extrapolated earlier than others. For example, in this data package, the extrapolated regions of the basic lift coefficient and the basic pitching moment coefficient started at different values of α at high airspeeds. When such is the case, the significance of the individual components should be taken into consideration. Based on this, when considering the amount of fidelity, the regions of medium and low confidence levels should not be regarded as binary; the closer the simulation gets to the extrapolated region, the less fidelity can be expected.

Toward higher Mach numbers, less flight test data was available for high angles of attack. This may likely be attributed to the effect of aerodynamic buffet. Thus, it may be reasonable to consider constituting the α-β training envelope as dynamic with respect to the Mach number, especially if the aeroplane is able to operate at high subsonic or transonic speeds.

Only a few data plots were found to depict the sideslip angle directly. Instead, the majority of the sideslip related effects are plotted with respect to other variables, with the results expressed as slope functions per sideslip angle. In addition, there are numerous coupling effects related to the sideslip angle. Consequently, the task of assessing the confidence level with respect to β had to be based on a notably less amount of source material. The aerodynamic database of a simulator based on this data package would likely contain a rather limited amount of tabulated data with respect to the sideslip angle.

Descriptions for the thresholds for activation of stall warning system and stall buffet are provided in the data package. However, any specific plots depicting the effects of flow separation or adverse behaviour during aerodynamic stall were not found to be encompassed.

Even though the high confidence region could not be determined from the available data, the resulting medium confidence envelope would still provide some level of additional value to the simulator operator. As discussed in Chapter 4.4, the FSTD training envelope is proposed to be composed of the high and medium confidence level regions, and momentary training is allowed within the medium confidence region, as long as the resulting implications are taken into account. The Boeing 747 is comparable to the aeroplane types listed in Figure 14 (Chapter 4.3), and the achieved range of the medium confidence level region is on par with the α-β envelopes as presented in Figure 14.

It may be generally concluded, that when assessing the aerodynamic data of a simulator, particular attention should be paid to the stability derivatives as listed in groups #1 and #2 of Table 6. If the non-extrapolated data ranges of these derivatives could be uncovered, one

would have a solid foundation for the medium confidence level envelope of the simulator. However, the omission of any stability or control derivative from the evaluation of the medium confidence region should always be carefully reasoned on case by case basis.

6 Case study of a Super King Air 300 simulator

A simulator of the Beechcraft Super King Air 300 was chosen as the second case study. The device was put into operation in the early 1990s, and initially approved as a Level C Full Flight Simulator with the FAA AC 120-40A as the PRD. Currently the simulator is in active service in flight training organisation environment, qualified as a Level CG Full Flight Simulator. As type-specific simulators of the King Air 300 are rather few in numbers, while the actual aircraft type is in widespread active service, this device serves as an example of an older simulator which would still be reasonable to adapt for the new upset training provisions. Typically in this age class the support from manufacturer is no longer self-evident, possibly leaving the qualification certificate holder on its own to face the challenge of demonstrating compliance.

The King Air 300 is a pressurised twin-turboprop business and utility aircraft with a capacity of 6 to 14 passengers. First flown in 1983, the King Air 300 is part of the Super King Air family, which has the longest production run of any civilian turboprop aircraft in its class, with variants still in production. Typical cruise condition for this aircraft is at medium to high altitude and fairly low Mach number; the maximum operational Mach number is 0.58. [51] The King Air 300 has a straight and tapered wing planform, typical for a turboprop aircraft. The aircraft has a retractable undercarriage and a four segment fowler type flap system, with three positions: up, approach (14°) and landing (35°).

The primary goals for this case study were to outline two envelopes for the simulator – a flight validated envelope for flaps-down configuration, and an envelope for medium confidence level, and to study which regions of the envelope require the most attention. In principle the envelopes were composed and studied in terms of the aerodynamic angles of α and β, but the consistency of airspeed and load factor was also taken into consideration.

6.1 Research methods and limitations

This case was presumed to correspond to the problematics faced by simulator qualification certificate holders possessing older devices, without readily available support from the manufacturer. The research was conducted accordingly, with the available manufacturer's original documentation and the MQTG as the primary sources of information, and hands-on testing as supporting measures. The manufacturer's documentation consisted of software detail documentation, including source code and look-up data, and the aircraft flight manual.

The software detail documentation was studied to get a general overview of the composition of the aerodynamic model, and particular interest was paid to the available data range of the look-up tables and the handling of greater than tabulated values of variables. As such, the look-up tables do not disclose the original source of the data, or which portion of it is flight validated, but they may still be utilised to outline an envelope for medium confidence level. The aircraft data plots from the QTG tests were the only source of data points for the high confidence level flight test validated envelope. The operational limits, speeds and loading conditions needed for tests were extracted from the aeroplane flight manual.

There were three objectives set for hands-on testing: to study the range of values of the aerodynamic angles typically achieved during upset-related manoeuvres, to duplicate tests listed in the MQTG while recording additional aerodynamic parameters in order to obtain validated data points for the Validated Training Envelope, and finally to vary tests listed in the MQTG to study the effects of different aircraft configuration.

Tested manoeuvres were performed by flying and by performing QTG tests, while parameters were recorded in both of these cases. All manual flying was performed by an experienced flight instructor. The main purpose of the tests performed by flying was to study the range of the aerodynamic angles achievable during different manoeuvres. Some of the QTG tests were run in automatic mode, in order to accurately record additional parameters to those included in the MQTG in selected data points. Finally, some QTG tests were also run in varied flap settings in order to study how well the results may be generalised between different configurations.

The testing setup consisted of video cameras recording the pilot's flight control inputs and instrument readings, and live parameters from the instructor operating station. Additionally, the simulator operator had constructed an ad hoc enhancement to the IOS, which enabled real-time capture of the aerodynamic angles and several other parameters in a digital format. The results from QTG tests and varied QTG tests were also taken as printouts from the system.

Effects of compressible aerodynamics were neglected in this case study. In addition, ground operations and control surface malfunctions were excluded from the scope of this study. The effects of icing and ground effect were covered on the most general level.

6.2 Software documentation

The software detail documentation of the aerodynamic model by the manufacturer was found to contain extracts from the source code, as well as look-up table data and descriptions of labels. The aerodynamic model is implemented by FORTRAN 77 programming language, consisting of interactive modules for tasks such as calculating aerodynamic forces, atmospheric conditions, control responses, weight and balance, ground handling, malfunctions, special effects etc. [52]

6.2.1 General overview of the aerodynamic module

The aerodynamic model of the simulator utilises conventional equations of motion, where the translations and rotations of the aeroplane are resolved from six aerodynamic force and moment coefficients with respect to the aeroplane stability axes. Orientation of the aeroplane with respect to earth axis is computed by means of quaternions, direction cosines and the Euler attitude angles.

The aerodynamic coefficients are calculated in the aerodynamic module, and sent to the equations of motion module to be transformed into forces and moments, and furtherly into accelerations acting on the aeroplane. The aerodynamic moments in the stability axes are converted to moments into the body axes with reference to the centre of gravity of the aeroplane.

The total lift coefficient of the aeroplane is formed as a sum of effects of the lift at zero angle of attack, angle of attack, elevator deflection, icing, landing gear position, ground effect, rate of change of angle of attack, and pitch rate.

Similarly as in Equation 13 (Chapter 3.2), the basic lift coefficient is expressed in a linear form. For each of the three flap positions, the lift at zero angle of attack and the slope of the basic lift coefficient line can be found in the data tables. Lift effects of thrust are summed to the lift at zero angle of attack.

The lift effect of the elevator deflection angle is expressed as a linear function. The lift effect of icing is calculated as a product of average icing build-up factor from both wings and a constant multiplier. The lift effect of landing gear is dependent on flap position and thrust. The ground effect is given as a constant coefficient, which is gradually washed out, until altitude reaches 50 feet. The lift effects of angle of attack rate and pitch rate are expressed in terms of their respective constant coefficients, and true airspeed. The lift coefficient effects of asymmetric thrust and load factor caused inertia relief are neglected.

The total drag coefficient of the aeroplane is formed as a sum of effects of basic drag coefficient, landing gear position, elevator deflection, rudder deflection, sideslip angle, and icing.

The basic drag coefficient is composed of forward thrust component and angle of attack dependent drag component. Values for both of these components are tabulated for each of the three flap positions. The drag effect of the landing gear position is given as a constant per each flap position, whereas the drag effects of elevator and rudder are expressed as linear functions of respective deflection angles. The drag effect of sideslip is not tabulated, but handled as a linear function instead. The drag effect of icing is calculated from ice build-up factors of each wing and body, using separate multipliers for wing and body. The drag coefficient effect of ground effect is neglected.

The total side force coefficient is formed as a sum of the effects of sideslip angle, rudder deflection, yaw rate and roll rate. The side force effects of side slip angle and rudder deflection are handled as linear functions with constant coefficients for each flap positions. The side force effects of roll and yaw rate are composed of respective linear coefficients, multiplied by airspeed dependent damping terms.

The total pitching moment coefficient is formed as a sum of basic pitching moment and the effects of elevator deflection angle, ground effect, elevator trim position, angle of attack rate, pitch rate and landing gear position.

The basic pitching moment is furtherly composed of thrust dependent component, flap position component and angle of attack dependent component. Of these, the first and last components are in tabulated form per each flap position. The pitching effect of elevator and elevator trim tab are composed of several tabulated components, describing the elevator effectiveness per deflection angle, angle of attack and stall condition. The pitching moment caused by ground effect is given in tabular form per altitude for up to 50 feet. The pitching effect of landing gear position is composed of tabulated components dependent on angle of attack and flap position.

The pitching effect of angle of attack rate is given as a linear coefficient, multiplied by an airspeed dependent damping term. The effect of pitch rate is composed of tabulated components per thrust effect and flap position, multiplied by an airspeed dependent damping term. The pitching moment effect of load factor caused inertia relief is neglected.

The total rolling moment coefficient is formed as a sum of effects of aileron and aileron tab deflection angles, rudder deflection angle, sideslip angle, roll rate, yaw rate, differential flaps and differential thrust.

The rolling effect of ailerons is composed of tabulated components per flap position and angle of attack. The rolling effect of sideslip is handled as linear functions per flap position. The rolling effect of rudder deflection is composed of several tabulated components, describing the rudder effectiveness per deflection angle, flap position and angle of attack. The rolling effects of roll rate and yaw rate are handled as linear functions per flap positions, multiplied by respective airspeed dependent damping terms.

The total yawing moment coefficient is formed as a sum of effects of sideslip angle, rudder and rudder tab deflection angles, roll rate, yaw rate, and differential flaps.

The yawing effect of sideslip is expressed as linear functions per flap position. The yawing effect of rudder deflection is handled as tabulated components, describing rudder effectiveness per deflection angle and angle of attack. The yawing effect of roll rate is given as a linear coefficient, multiplied by an airspeed dependent damping term. The yawing effect of yaw rate is handled as linear functions per flap position, multiplied by an airspeed dependent damping term. The effect of adverse yaw induced by aileron deflection is neglected. [52]

6.2.2 Stall module

The implementation of the stall characteristics of the simulator is in line with the conventional solution as described in Section 2c of the Aeroplane Flight Simulator Evaluation Handbook by the RAeS. Wing flow separation occurs differently than the reattachment of the flow, and therefore hysteresis increments to the basic data need to be calculated. A simple first-order lag filter function to lag the angle of attack is used to derive these hysteresis increments. As the angle of attack decreases after stall-break, the simulation begins calculation of the lagged body angle of attack. The stall hysteresis increments are a function of the difference between the angle of attack and the reattachment angle of attack, and they return to zero when the flow reattaches the wing. Thus, the simulation of the stall behaviour utilises separate special aerodynamic models, which are not used in other flight regimes. [53]

In the King Air simulator the effects of aerodynamic stall are constituted in a separate module. When a stall condition is detected, additional increments for pitching, rolling and lift coefficients are calculated and sent to the aerodynamic module. It is noteworthy, that the presence of a stall condition is deduced from airspeed instead of angle of attack. The stall speed is calculated per each flap position, taking into account the effects of gross weight, load factor, icing and thrust. [52]

Stall warning activation and buffeting are also triggered by airspeeds, which are derived from the calculated stall speed and an added increment. The increment for stall warning is tabulated per each flap position, and multiplied by an ice build-up factor of the left-hand wing stall sensor vane. The increment for buffeting speed is simply tabulated per each flap setting.

The weight dependent component of stall speed is composed as a sum of basic stall speed and gross weight multiplied by a weight factor. The basic stall speed and the weight factor are tabulated per each flap position. The effect of load factor is expressed as a function of lagged load factor and the calculated weight dependent component of stall speed. The effect of icing is handled as a linear function of wing ice build-up factor. The reducing effect of thrust on stall speed is derived from power setting, constrained by a limit function; the maximum reducing effect of thrust on stall speed is mathematically limited to 15 knots.

During each iteration, the stall module analyses the state of the aeroplane with the help of two flags set in the previous iteration: one to indicate a stalled state, and another to indicate a recovery-from-stall state. If both of these flags are set to false, the aeroplane has been in unstalled condition in the previous iteration, and the module then compares the indicated airspeed to the calculated stall speed. In case the airspeed is lower than the calculated stall speed, a stall break is initiated, where the stall flag is set to true, and increments of pitching moment and rolling moment are sent to the aerodynamic module. The stall break increment of pitching moment is tabulated per flap position, whereas the stall break increment of rolling moment coefficient is tabulated per sideslip angle.

If the stall flag is set to true and the recovery flag is set to false, the aeroplane is in a stalled state, and a stall increment of pitching moment is added. If the angle of attack has reduced from the last iteration, the stall increment of lift force coefficient is set to zero. In the opposite case, the change of lift is proportionate to the square of delta angle of attack. During a stalled state, no changes are added to the rolling moment by the stall module. Finally, if the delta angle of attack is greater than or equal to -2 degrees, and the indicated airspeed has risen above the calculated stall speed, the stall recovery flag is set to true.

In case both of the flags are set to true, the aeroplane is in a state of recovery from stall – the airspeed has risen above the calculated stall speed, and the reduction of angle of attack has been eased. In this case, stall hysteresis increments of pitching moment and rolling moment are added. If the change of pitching moment calculated by the stall module reaches a negative value, both the stall flag and the recovery flag are set to false, and the hysteresis increments for lift, pitching moment and rolling moment are set to zero. Hence, the aeroplane has once again reached an unstalled condition.

The increments of lift, pitching moment and rolling moment, induced by the stall module, are constrained by limit functions to not fall below defined minimum values. In addition, the change of rolling moment during stall recovery is limited to have only negative or zero values.

To summarise, depending on the condition, the changes induced by the stall module for the three coefficients are handled differently per stall break, stalled state and recovery-from-stall state:

1. During stall break the change of rolling moment is proportional to the sideslip angle, and the change of pitching moment to the flap position,
2. During stall the rolling moment stays unchanged, the pitching moment has a constant stall delta, and the lift force delta is a function of the rate of angle of attack squared,
3. During recovery the rolling moment and pitching moment have constant hysteresis increments.

The effect of negative roll response caused by opposite aileron inputs during full-stall condition is not included in the stall module. [52]

6.2.3 Table look-up process

The table look-up process is composed of an external function written in assembly language. From the available information, it could be deduced that the process manages three separate cases:

1. The X value matches exactly to a tabulated X value
2. The X value does not match to a tabulated value, but is in range of the table
3. The X value is outside the range of the table

In case #1 the corresponding Y value is selected from the table. In case #2, an offset for Y is calculated from the nearest tabulated value, in accordance with Equation 15 (Chapter 3.2). Finally, in case #3 the nearest tabulated value for Y is selected, and the offset is set as zero.

The discovery of case #3 leads to the conclusion that when the range of a look-up table is exceeded, the simulation will most likely not continue to be representative for the parameter in question.

6.3 Master Qualification Test Guide

The Master Qualification Test Guide of the simulator is based on the original FAA Approval Test Guide, composed in accordance with the Phase II simulator requirements set in the FAA AC 120-40A. The included tests are grouped by subject into twelve chapters. For this study, the chapters for longitudinal control, lateral control, take-off and landing were considered relevant.

Each test is presented in a similar format, beginning with a narrative of the objective and test procedure to replicate flight test data. Parameter tolerances as set in the AC 120-40A and additional notes and calculations are provided as required. The narrative is followed by a list of simulator and aircraft conditions, such as gross weight, centre of gravity, pressure altitude, flap position, pitch trim, etc. to be initialised as the simulator is set up for the test. Finally, time history data plots of the simulator's performance and of the corresponding

flight test are presented. The plots consist of a possible total of six parameters against time. The aircraft data traces and the simulator data traces are provided on the same plot for ease of comparison and analysis.

For the purpose of recurrent evaluations, the simulator software contains scripts that are used to initialise the parameters for the tests and to record data regardless whether the test is performed automatically (i.e. flown by the software script), or manually (i.e. flown by a human pilot). It is possible to run the tests with differing initial conditions. [54]

As such, the QTG data plots turned out to be insufficient for the purpose of the objectives of this study, due to limited parameters available in the test prints. Instead of aerodynamic angles, the motion of the aircraft is generally plotted in terms of attitude angles, such as pitch and roll angle. Therefore it was necessary to simultaneously record the values of the aerodynamic angles from alternative sources, and afterwards match their values to the QTG plots, in order to obtain validated data points for the aerodynamic angles.

6.4 Testing

6.4.1 Tests performed by flying

A total of 32 operational tests were performed. Of these, 18 tests were performed by flying in order to assess the regions achievable by moderate to severe control abuse. All manual flying was performed by an experienced flight instructor, familiar with the device and holding a valid pilot license for this type. The conducted tests performed by flying are listed in Table 13 and the initial conditions of these tests are listed in Table 14.

Table 13 Conducted test manoeuvres

Test	Description
FF.1	Level flight stall, clean configuration
FF.2	Level flight stall, clean configuration, simulated unintentional yaw
FF.3	Level flight stall, clean configuration, simulated unintentional yaw
FF.4	Level flight stall, clean configuration, simulated unintentional yaw
FF.5	Level flight stall, approach configuration
FF.6	Level flight stall, approach configuration
FF.7	Level flight stall, approach configuration, simulated unintentional yaw
FF.8	Level flight stall, landing configuration
FF.9	Level flight stall, landing configuration, simulated unintentional yaw
FF.10	Emergency descent according to standard procedure
FF.11	Emergency descent, clean configuration
FF.12	Emergency descent, clean configuration, simulated unintentional yaw
FF.13	Maximum sideslip, landing configuration, near stall speed, centre of gravity at aft limit
FF.14	Maximum sideslip, clean configuration, near stall speed, centre of gravity at aft limit
FF.15	Maximum sideslip, clean configuration, maximum manoeuvring speed, centre of gravity at aft limit
FF.16	Wake vortex scenario, hands off flight controls (free response)
FF.17	Wake vortex scenario, controlled
FF.18	60 degrees steep turn, clean configuration

Table 14 Initial conditions of the tests

Test	CG (%MAC)	Mass (lbs)	Altitude (ft MSL)	V (KIAS)
FF.1, FF.2, FF.3, FF.4, FF.5, FF.6, FF.7, FF.8, FF.9	22.49	12887	12000	n/a
FF.10, FF.11, FF.12	22.49	12887	28000	280
FF.13, FF.14	29.64	12887	3000	n/a
FF.15	29.64	12887	3000	181 (V_A)
FF.16, FF.17, FF.18	29.64	12887	2000	n/a

For comparability, the initial conditions and aircraft loading of the stall tests were set to match the QTG stall test in approach configuration. The stall tests were carried out through full aerodynamic stall and recovery. At the discretion of the flight instructor, sideslip was intentionally added prior to stall break in some tests, in order to replicate such unintentional yaw and bank that can be expected due to out-of-trim condition or inappropriate control inputs by the trainee.

Emergency descent tests from cruise flight conditions were carried out to study the low-end values of angle of attack. One of these tests was conducted according to standard operational procedures, where flaps are extended at the initiation of descent, and other tests were conducted by performing immediate dive with flaps up configuration. One test was performed with added sideslip.

Sideslip tests were conducted for the purpose of finding the maximum achievable sideslip angle at different angles of attack. To obtain the least directional stability for these tests, the loading condition of the aeroplane was set so, that the centre of gravity was positioned at the aft limit. To achieve high sideslip angles at low angles of attack, maximum cross control was applied at maximum manoeuvring speed. For high angles of attack, tests were conducted near stall speed with maximum cross control inputs – some of these tests were carried through stall break.

The simulator has a preconfigured wake vortex scenario, which was tested with and without flight control inputs. Finally, the last test included a 60 degree bank steep turn, with the purpose of examining the relation between bank angle and load factor.

6.4.2 QTG Tests

The purpose of the performed QTG tests was to act as the primary source of information for outlining the flight test validated envelope of the simulator. These tests were selected with the intention of discovering data points of the highest available values of angle of attack and sideslip angle. The conducted QTG tests and the validated parameters are listed in Table 15. After each test these parameters were plotted against flight test data and received as printouts. Additional parameters were recorded during execution via digital interface and from the real-time screen of the IOS.

Table 15 Conducted QTG tests

Test	Description
QTG.1	Standard V_{MCA} test, manual control
QTG.2	Standard V_{MCA} test, manual control
QTG.3	V_{MCA} test with varied configuration (full flaps), manual control
QTG.4	V_{MCA} test with varied configuration (flaps up), manual control
QTG.5	Standard V_{MCA} test, automatic control
QTG.6	Standard stall test in approach configuration, automatic control
QTG.7	Standard stall test in landing configuration, automatic control
QTG.8	Standard cross control test in approach configuration, automatic control

QTG.9	Standard crosswind landing test, automatic control
QTG.10	Standard crosswind take-off test, automatic control
QTG.11	Standard engine-out take-off test, automatic control
QTG.12	Standard stick force per g test in clean configuration, automatic control
QTG.13	Standard stick force per g test in approach configuration, automatic control
QTG.14	Standard stick force per g test in landing configuration, automatic control
Test	**Validated parameters**
QTG.1 QTG.2 QTG.3 QTG.4 QTG.5	- Pitch attitude θ (°) - Roll attitude φ (°) - Heading ψ (°) - Indicated airspeed (kts) - Left engine torque (%) - Right engine torque (%)
QTG.6 QTG.7	- Stall warning (on/off) - Pitch attitude θ (°) - Roll attitude φ (°) - Heading ψ (°) - Indicated airspeed (kts) - Left engine torque (%) - Right engine torque (%)
QTG.8	- Roll attitude φ (°) - Heading ψ (°) - Wheel position (°) - Pedal position (in) - Y-Axis acceleration (g)
QTG.9	- Pitch attitude θ (°) - Roll attitude φ (°) - Heading ψ (°) - Indicated airspeed (kts) - Altitude (ft) - Stick position (in) - Wheel position (°) - Pedal position (in) - Left engine torque (%) - Right engine torque (%)
QTG.10 QTG.11	- Pitch attitude θ (°) - Roll attitude φ (°) - Heading ψ (°) - Indicated airspeed (kts) - Pressure altitude (ft) - Stick position (in) - Wheel position (°) - Pedal position (in) - Left engine torque (%) - Right engine torque (%)

QTG.12 GTG.13 GTQ.14	- Pitch attitude θ (°) - Roll attitude φ (°) - Stick force (lbs) - Load factor (g)

The QTG test for minimum control speed in air (V_{MCA}) was carried out several times. V_{MCA} is defined in certification specifications (CS-23) as "*the calibrated airspeed at which, when the critical engine is made suddenly inoperative, it is possible to maintain control of the aeroplane, with that engine still inoperative, and thereafter maintain straight flight at the same speed with an angle of bank not more than 5 degrees*". [55] This test was conducted both in automatic and manual control mode, and additionally with varied aeroplane configurations. Varied configurations were used with the intention of clarifying the effect of different flap positions, and furtherly the applicability of the results between configurations. The rationale behind focusing on the V_{MCA} test was, that of the QTG tests, it was presumed to provide the highest values of sideslip angle at high angles of attack.

The QTG stall tests for approach and landing configurations were selected as sources of validated data points for the highest values of angle of attack. The QTG tests for crosswind landing, crosswind take-off and engine-out take-off were selected in order to discover the highest validated sideslip angles at angles of attack below stall break. Finally, the stick-force-per-G tests at different configurations were selected to study the consistency of the aerodynamic model with respect to the load factor.

6.5 Results

6.5.1 Document study

The aerodynamic model of the simulator was found to commonly encompass slope functions for components of the aerodynamic coefficients. This in itself is not an indication of the quality of the simulation, but it complicates analysis, as there are no cues about at which ranges of values the linear fit becomes invalid.

The basic lift coefficient, which is the dominating component of the total lift coefficient, is expressed as a linear function of angle of attack, with the slope given per flap position. Hence, the relation between lift and angle of attack is strongly linear all the way up to the point where the stall module initiates a stall break.

There were found to be look-up tables for five different ranges of angle of attack in the aerodynamic source data. These five tables are utilised to solve a total of six variables, as listed in Table 16.

Table 16 Look-up tables containing angle of attack

Variable	Range of tabulated data (α)
ΔC_{D_α}	-12°, -8°, -7°, -6°, -5°, -4°, -3°, -2.5°, -2°, -1.5°, -1°, -0.5°, 0°, 0.5°, 1°, 1.5°, 2°, 2.5°, 3°, 3.5°, 4°, 4.5°, 5°, 6°, 7°, 8°, 10°, 12°, 20°
ΔC_{m_α}	-20°, -10°, -8°, -6°, -4°, -2°, -1°, 0° 0.5°, 1°, 1.5°, 2°, 2.5°, 3°, 4°, 6°, 8°, 10°, 20°
$\Delta C_{m_{gear}}$	0°, 1.5°, 3.5°
$\Delta C_{m_{elevator}}$	7°, 9°, 10°, 11°, 15°
$\Delta C_{l_{aileron}}$	4°, 10°, 15°
$\Delta C_{n_{rudder}}$	4°, 10°, 15°

The sideslip angle has effect on the coefficients of drag, side force, rolling moment and yawing moment. All of these effects are handled as linear functions by the aerodynamic module, i.e. there is no indication of the valid range available. The only sideslip-dependent variable that is tabulated is the rolling moment caused by sideslip on stall break, which has data from the range presented in Table 17.

Table 17 Look-up tables containing sideslip angle

Variable	Range of tabulated data (β)
$\Delta C_{r_{StallBreak}}$	-4°, -2°, -1°, -0.5°, 0 0.5°, 1°, 2°, 4°

The value ranges of all tabulated aerodynamic data are illustrated in Figure 20. Values related to pitching moment coefficient are marked as dark blue, those related to drag

coefficient as dark red, and finally those related to effects of landing gear and control surfaces as light green.

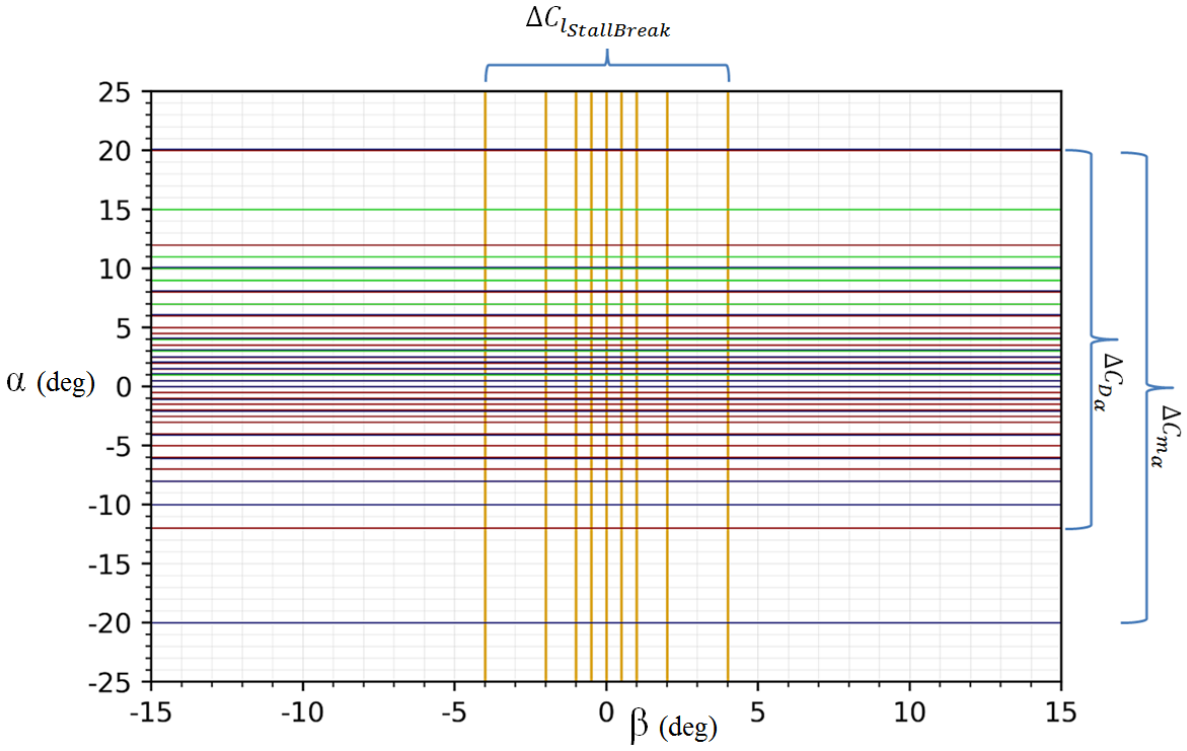

Figure 20 Ranges of tabulated aerodynamic data

6.5.2 Tests performed by flying

A selection of data points from tests performed by flying are illustrated in Figure 21, grouped by the type of the test:

1. Stall breaks at various aircraft configurations and sideslip angles;
2. Maximum sideslips, near stalling speed;
3. Maximum sideslips at manoeuvring speed;
4. Emergency descents.

Of all conducted tests performed by flying, the outermost values of α and β were achieved during these four types of tests. These data points outline the uttermost region which a trainee could reasonably reach. In the following chapters, with the help of QTG tests, an effort is made to determine which part of this region may be considered as flight test validated. The obtained region is further illustrated in Figure 22.

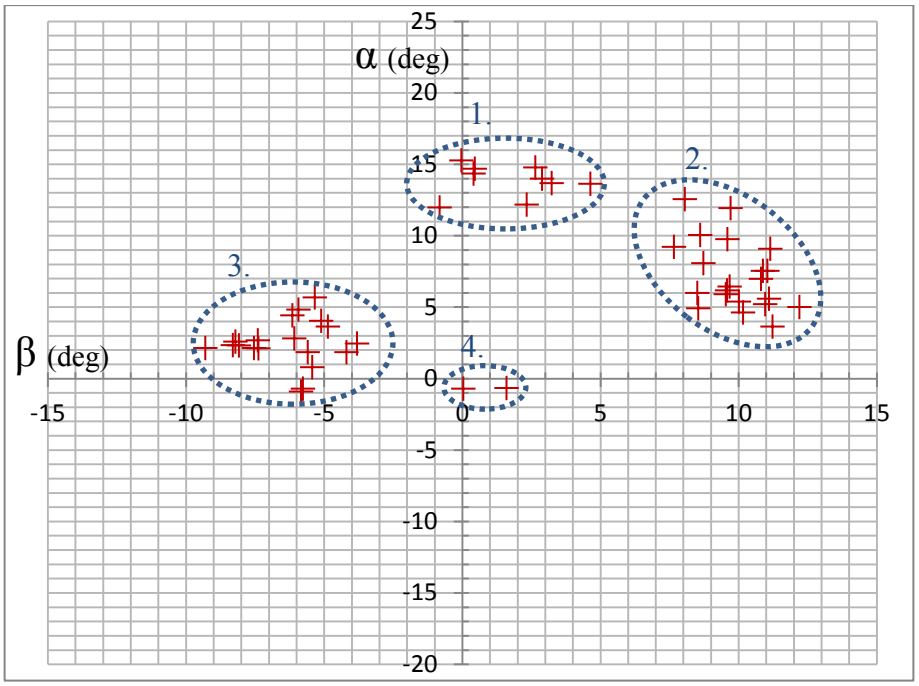

Figure 21 α-β data points from tests performed by flying

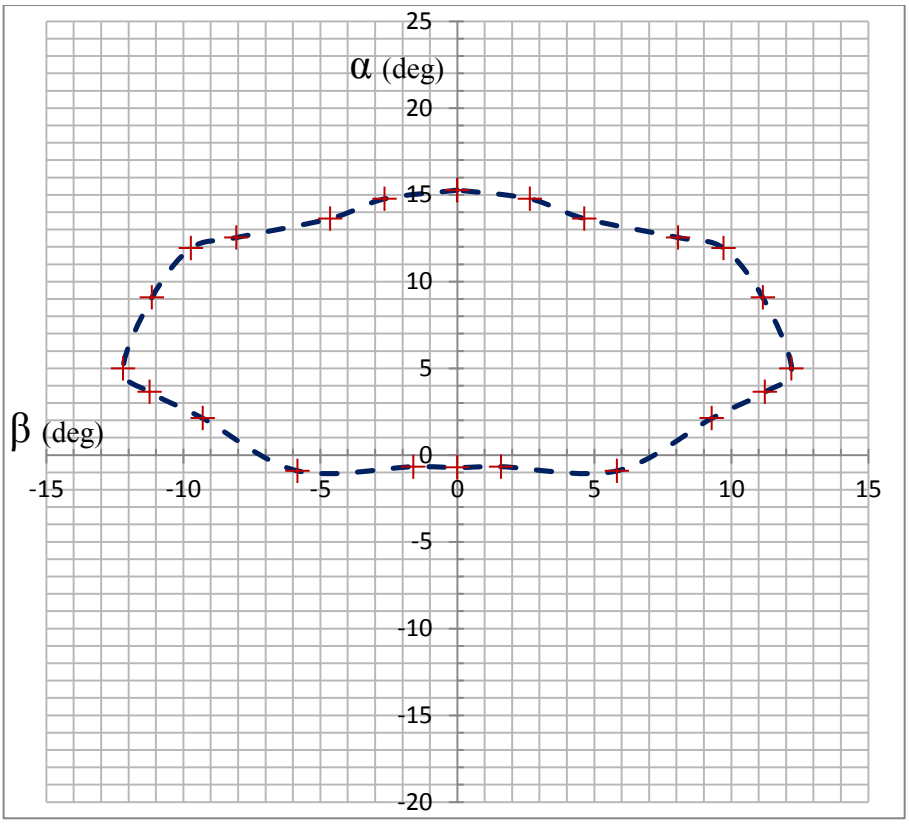

Figure 22 Region obtained during testing

The highest value of angle of attack α = 15.3° was achieved with straight, level stall in clean configuration. In approach and landing configurations the highest values of α were achieved with level stalls and slight sideslips: α = 14.8°, β = 2.7° and α = 12.2°, β = 2.3°

respectively. Straight stalls with flaps down configurations presented slightly lower angles of attack at stall break.

The highest value of sideslip angle $\beta = 12.2°$ was achieved with full cross control deflections at slow speed in clean configuration and centre of gravity set in the aft limit. The highest value of sideslip angle achieved at maximum manoeuvring speed V_A with full cross controls, clean configuration and centre of gravity in the aft limit was $\beta = 9.3°$. The maximum achieved sideslip angle at stall break occurred at $\alpha = 11.9°$ and $\beta = 9.7°$.

To examine the consistency of the simulation of the load factor, a steady 60 degrees steep turn was conducted. As expected, a 2g turn was achieved with a good accuracy (e.g. 2.02 g's at 60.7° bank angle).

6.5.3 QTG tests

Data plots of the aerodynamic angles recorded from conducted QTG tests are illustrated in Figure 23. All of these tests were run in automatic control mode. The data plots represent time histories from the whole duration of each test, excluding post-stall and wheels on-the-ground conditions. Generally the results of the conducted tests were found display a good match between the simulator and flight test data with respect to the validated parameters listed in Table 15. Therefore, each time instance from each test may be considered to validate the aerodynamic model, as comparison is made against flight test data of the actual aeroplane during the entirety of the time histories. Contrary to the original assumption, the highest values of sideslip angle were recorded from crosswind landing and crosswind take-off tests, instead of engine-out situations. The maximum recorded sideslip angle of $\beta = -9.7°$ occurred at crosswind landing flare, during which the rudder is used to align the nose with the runway centreline.

Based on these data plots a symmetrical envelope was outlined for flaps down envelope, as illustrated in Figure 24.

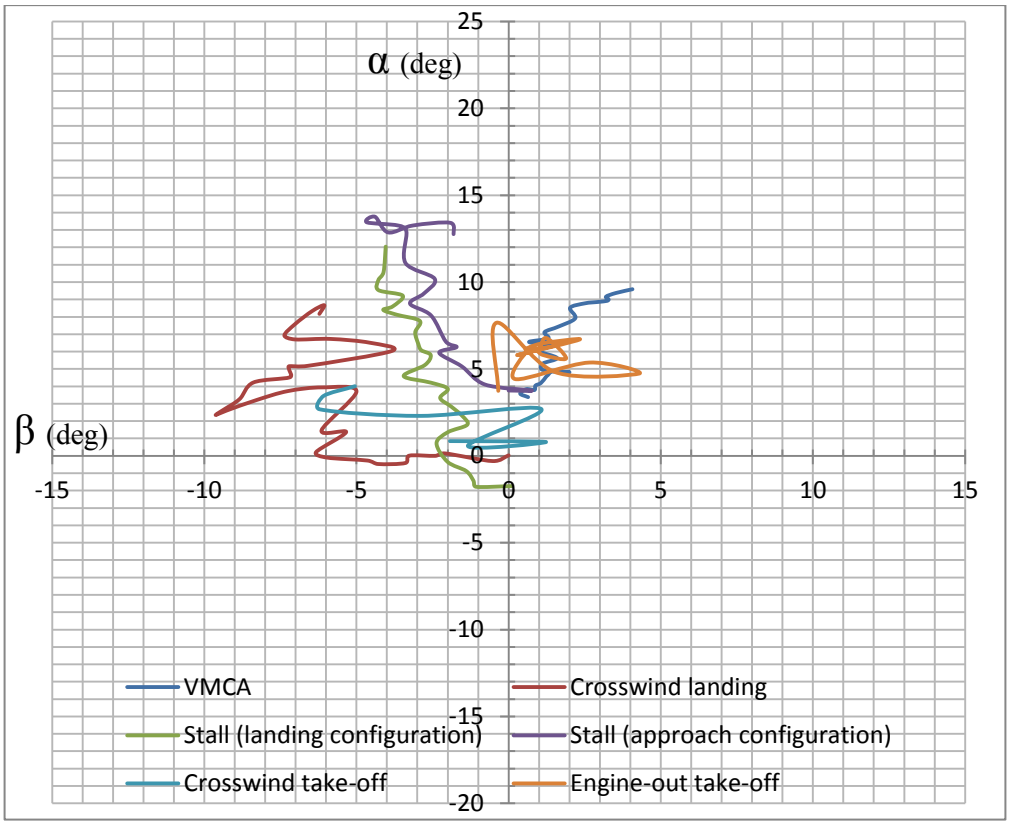

Figure 23 α-β data plots from automatic QTG tests

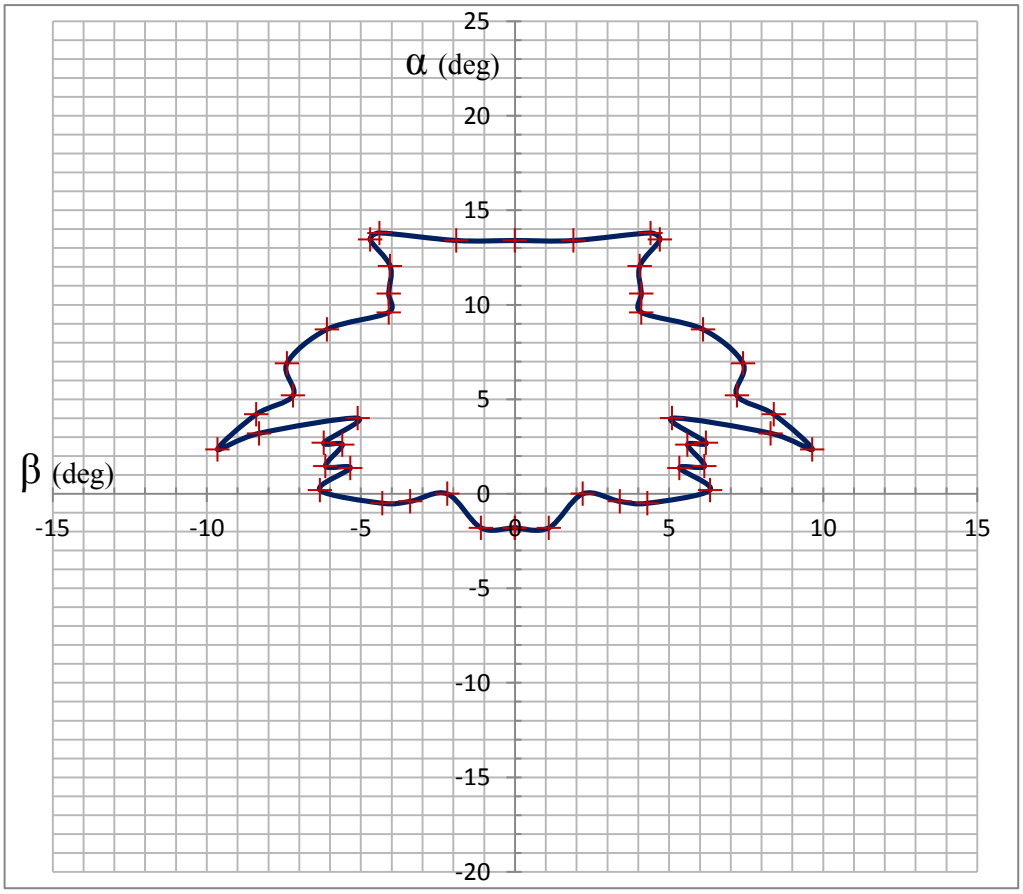

Figure 24 Outlined envelope from automatic QTG tests

In order to assess the validated region of the load factor, stick force per g tests were conducted in three configurations. In these tests the g forces are achieved by means of steady banking turns. The maximum achieved load factors are listed in Table 18.

Table 18 Maximum achieved load factors from "stick force per g" QTG tests

QTG Test	Maximum demonstrated load factor
Stick force per g, clean configuration	1.55
Stick force per g, approach configuration	1.84
Stick force per g, landing configuration	1.63

6.5.4 Modified QTG tests

In addition to the tests executed in automatic mode, the standard V_{MCA} QTG test was carried out in varied configurations in manual control mode. The standard test is conducted in approach configuration. Data plots of the aerodynamic angles from these manual tests are illustrated in Figure 25.

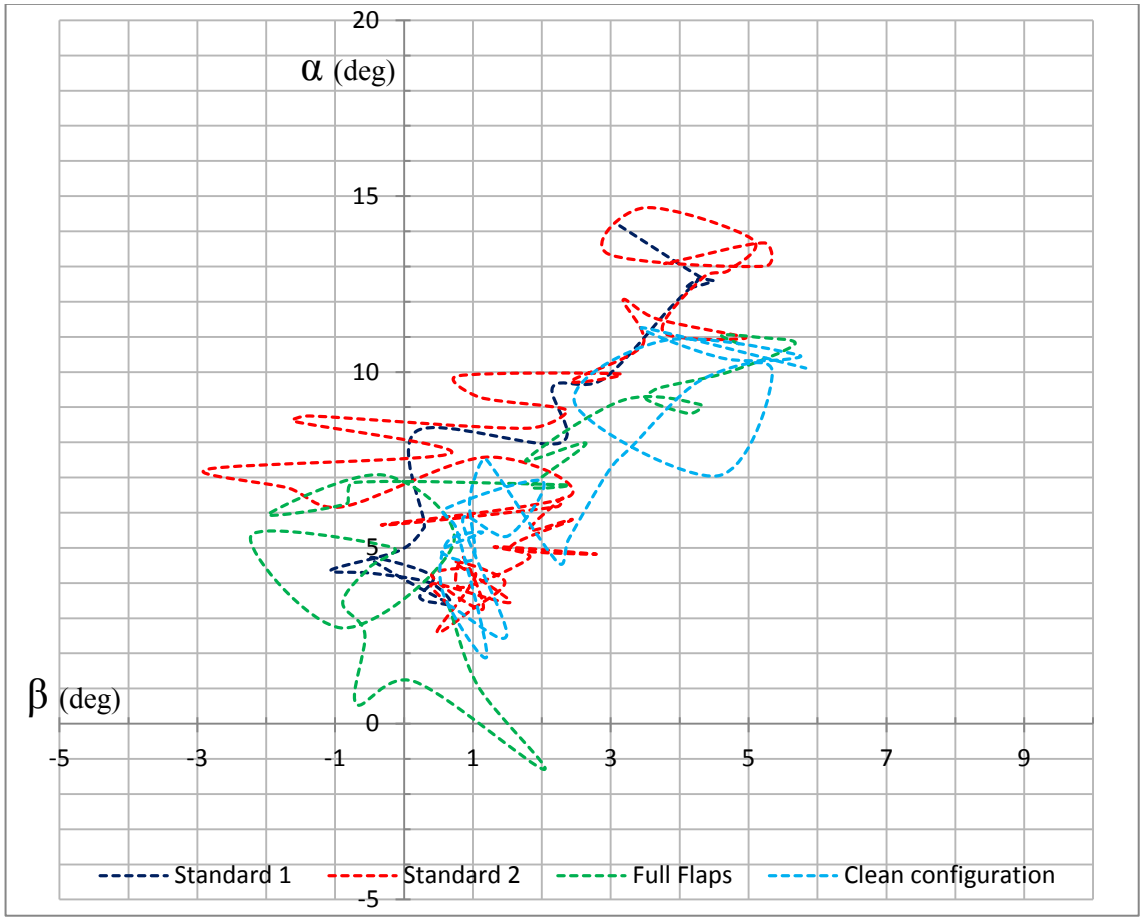

Figure 25 Manually flown V_{MCA} tests in different configurations

The results of the roll attitude angle ϕ could not be validated from the manually conducted V_{MCA} tests, due to diverging plots on the printout. Additional test runs would have likely been sufficient to achieve a more settled roll attitude. As a manoeuvre performed in an unsymmetrical flight condition coupled with high angle of attack, the V_{MCA} test is conducted at the very limits of the directional stability of the aeroplane, and is therefore highly challenging to execute manually in a repeated manner. This in its part will inevitably account for some level of fluctuations and random errors in the end results.

However, the rest of the flight test validated parameters showed correct trends in the context of the test in question. When comparing the tests conducted in different configurations with each other, the maximum angles of attack occurred in an unexpected order with respect to the flap configurations; presumption was that the results would have displayed the maximum angles of attack one below another per flap configuration, as an increment in flap angle typically causes an increment in $C_{L_{max}}$, and a decrement in α_{max}. It should be noted though, that the V_{MCA} test is not continued up to the critical angle of attack (i.e. stall break). The cause of this may simply be a type-specific flying quality in that particular flight condition, or it may have to do with the handling style of the pilot. More testing would have been required to refine these results.

Based on these partially mixed results, it would seem feasible to furtherly study the possibility to execute QTG tests in modified configurations in order to outline the validated flaps-up envelope.

6.6 Conclusions of the Super King Air 300 case study

Based on the conducted tests, a symmetrical flight validated envelope for flaps down configuration was constituted, as shown in Figure 24. It should be mentioned, that the outlined envelope is a combination of data plots obtained from tests, which were conducted by using varying initial conditions and aircraft configurations. The crosswind landing test was carried out in landing configuration, whereas the rest of the tests in approach configuration.

The shape of the envelope gives grounds to consider if some smoothing could be performed for the high confidence envelope. Figure 26 illustrates a convex hull approximation of the envelope, with possible simplifications numbered as 1 to 5.

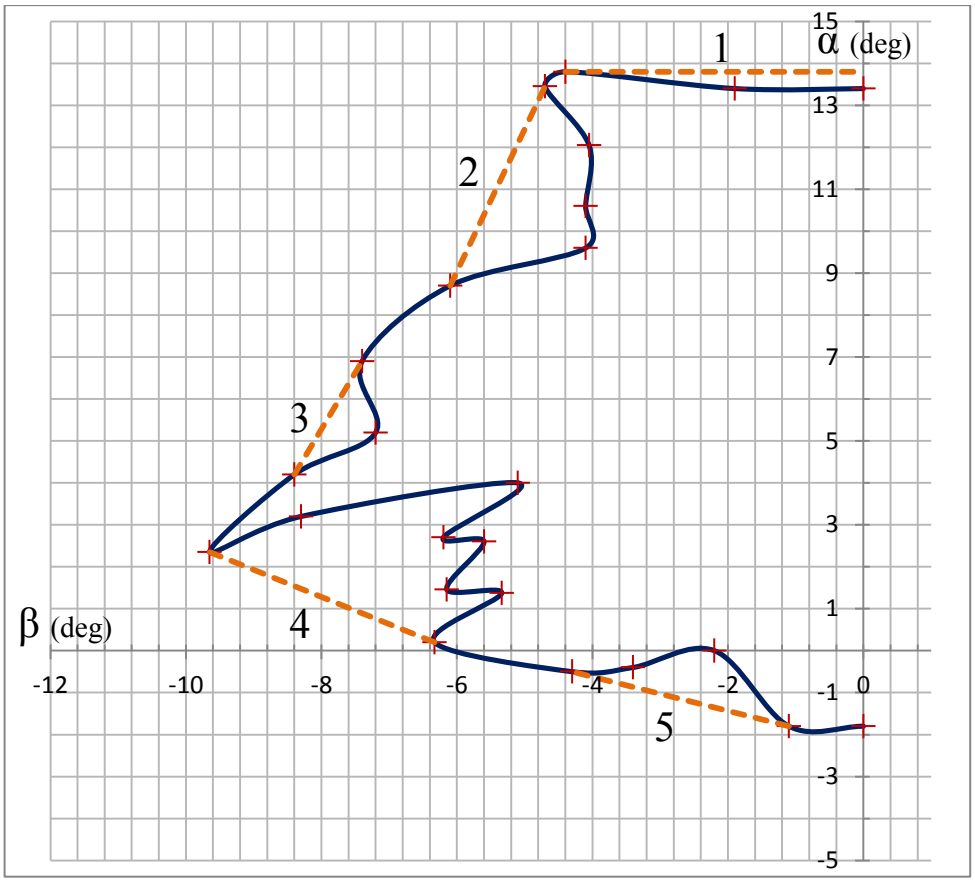

Figure 26 Convex hull approximation of the envelope

The highest angle of attack occurred with a moderate sideslip angle, and all of the high-α data points originated from the same stall test. It may be reasoned, that if a data point validates the aerodynamic model at a given position of α and β, the model is then also validated at smaller values of β with the same α. Therefore simplification #1 may be considered justified.

Simplification #2 is located in the critical region of high-α and high-β, and hence, is not advisable. Although, it may be argued that the reduction of α with fixed β from the top corner is toward safer direction, and therefore justified.

The simplifications from #3 to #5 are located in the region of low to medium α, and their trends are strongly supported by the surroundings. These simplifications may therefore be considered as justified.

Based on this, the following flaps-down envelope is proposed as the high confidence region:

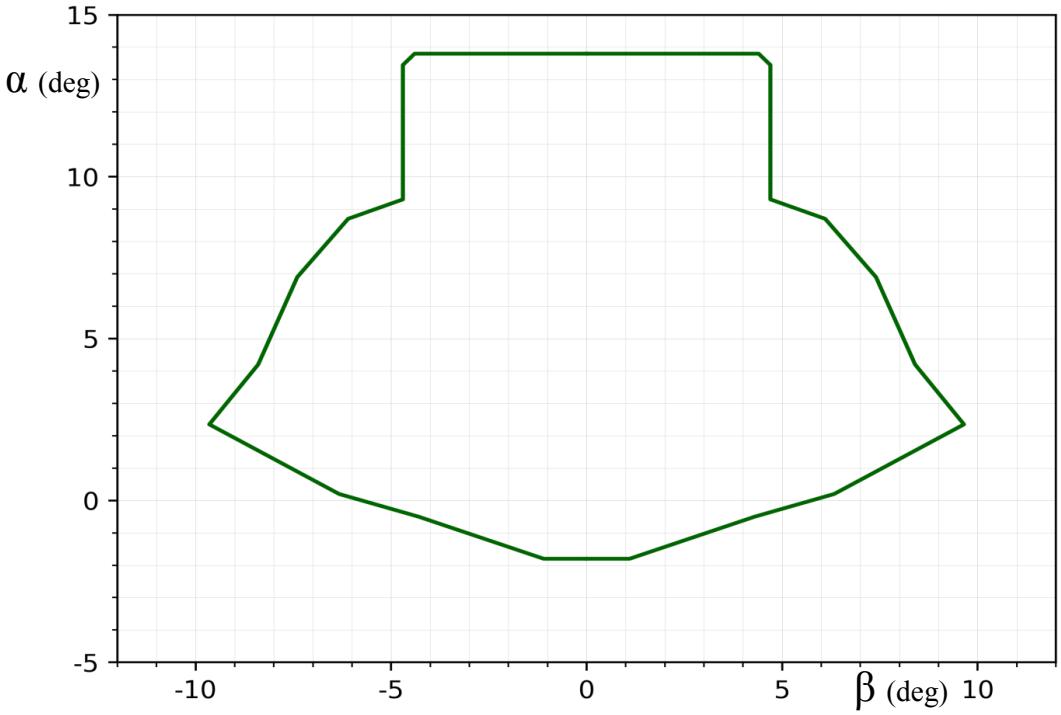

Figure 27 Proposed high confidence flaps down envelope for the simulator

The ranges of available look-up data and the proposed high confidence region were combined in Figure 28, to further demonstrate the density regions of the look-up tables.

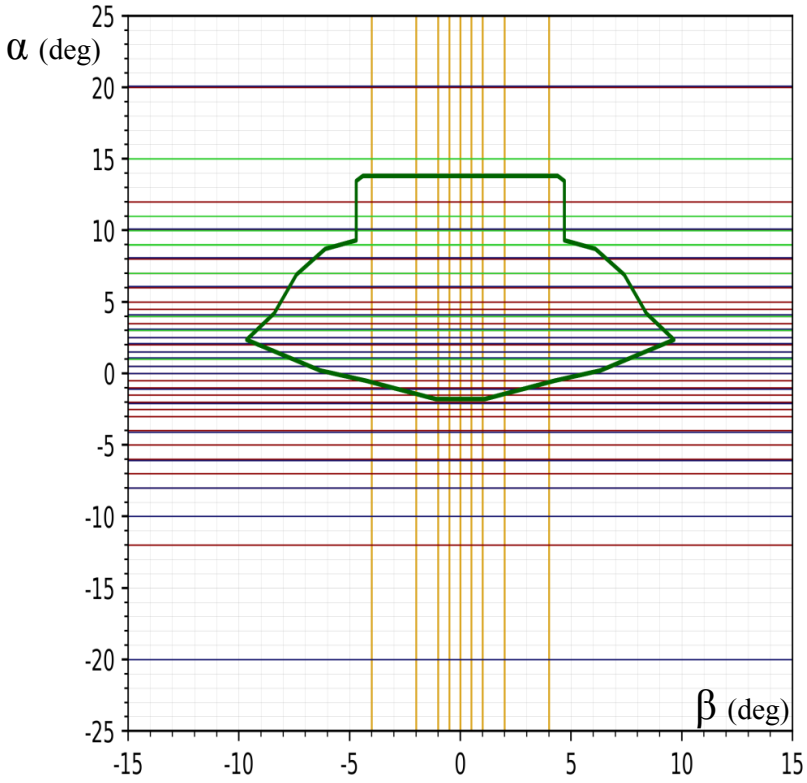

Figure 28 Proposed high confidence flaps down envelope illustrated with the ranges of tabulated aerodynamic data

The proposed FSTD training envelope is shown in Figure 29.

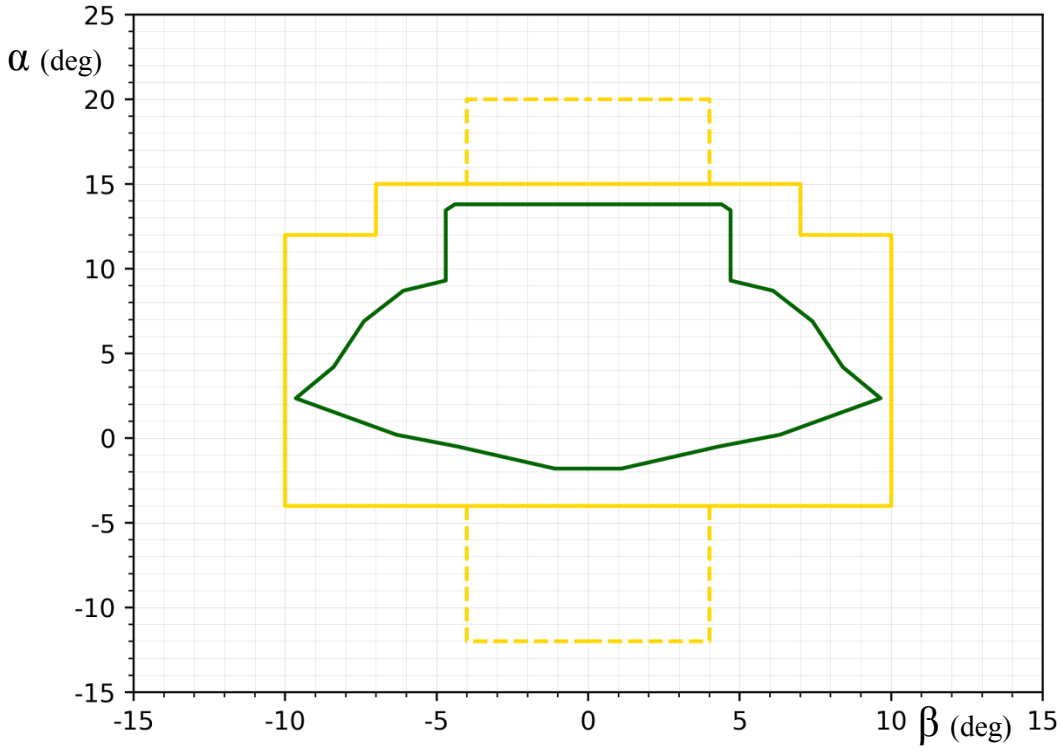

Figure 29 Proposed flaps down FSTD training envelope for the simulator

The high confidence level region is plotted as a green line, and could be furtherly extended by validation against any additional flight test data.

The proposed medium confidence level is illustrated as a solid yellow line. All of the stability and control derivatives, excluding the effects of landing gear, contain look-up data in this range with respect to α. The range of tabulated α-dependent effects of flight control derivatives, such as effect of α on aileron effectiveness, begins at 4 degrees α. Hence, these effects are negligible at lower angles of attack. The α-dependent effects of control derivatives are not tabulated for negative angles of attack. As a simplification, the threshold of significance for these effects was considered to be symmetric with respect to α, and therefore the lower border of the medium confidence envelope was set to -4 degrees α. The effect of landing gear on pitching moment was considered to be insignificant at higher-than-tabulated angles of attack, and was therefore neglected.

In addition, both of the tabulated stability derivatives, namely pitching moment and drag coefficient, are tabulated up to 20 degrees α. However, the range of the look-up tables for the control derivatives ends at 15 degrees α. Due to the nature of the table-look-up process, as described in Chapter 6.2.3, the response of the flight control inputs will likely not be representative at angles of attack beyond 15 degrees.

The analysis with respect to the sideslip angle is considerably more challenging, as it is mainly handled with linear functions in the aerodynamic model. The only applicable look-up table is related to the roll effect on stall-break, and has a rather limited range of data ($\beta = \pm 4°$). The furthest flight test validated data point with respect to β was achieved in the crosswind landing QTG test, located in $\alpha = 2.4°$, $\beta = -9.7°$. Therefore, based on engineering judgement, the side border of the medium confidence envelope was set in ±10 degrees β, in the range between $\alpha = -4°$ and $\alpha = 12°$; this range contains densely populated data with respect to α.

In the range between $\alpha = 12°$ and $\alpha = 15°$, the position of the side border of the envelope was reduced to $\beta = \pm 7°$. This was an estimation based on the reduced density of data in the look-up tables of α. Due to the linear nature of the modelling of the sideslip angle, much of the reasoning behind the estimation of side borders of the medium confidence envelope had to be based on engineering judgement.

An additional region is illustrated with a dashed yellow line. This region contains at least some aerodynamic data, but the consistency of the simulation in this region could not be doubtlessly verified on the basis of the available information. The upper dashed line region is out of range of the control derivative look-up tables.

The region obtained by testing performed by flying is illustrated with respect to the proposed FSTD training envelope in Figure 30. These tests were conducted with severe control abuse, and with the centre of gravity at the aft limit for minimum directional stability. It should also be noted, that momentary excursions to the medium confidence level region will likely be allowed during upset training. When such is the case, the instructor should be able to detect the excursion, to understand the possible limitations, and take appropriate action, such as explaining the occurrence to the trainee. Any training outside the high confidence level region should be conducted only at the discretion of the instructor. The closer the state of the simulation gets to the outer limits of the medium confidence level envelope, the less fidelity can be expected. An approximate threshold of stall warning system activation in approach configuration was added with a red dashed line.

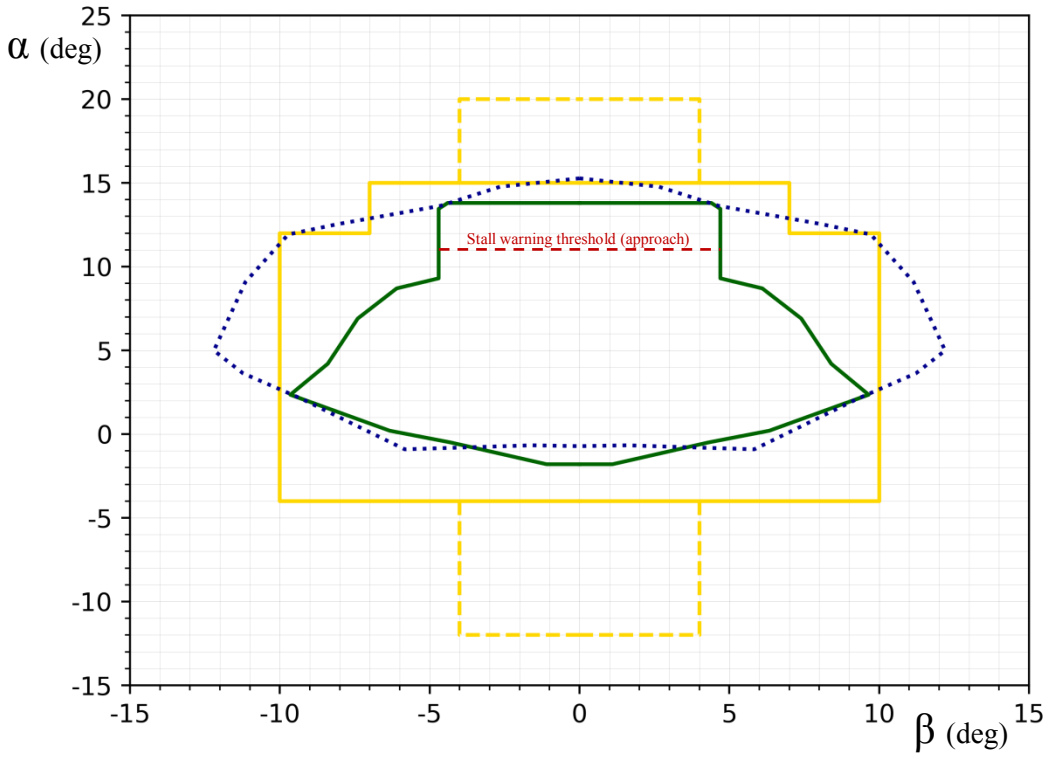

Figure 30 Conducted tests performed by flying (blue) illustrated with the proposed FSTD training envelope, and an approximate stall warning threshold in approach configuration (red)

The conducted 60 degree bank steep turns and stick force per g QTG tests support the impression that the simulation of the load factor is accurate at least up to 2 g's.

The proportions of the determined envelope are roughly in line with those represented for larger aeroplane types in Figure 14 (Chapter 4.3). Many of the flight validated envelopes in Figure 14 show a narrow region at highest angles of attack. Similar spike is missing from the determined high confidence level region due to the fact that there is no QTG test for maximum α at zero β for this simulator.

Based on the findings from the document study, it cannot be verified that the fidelity of the aerodynamic model of this simulator is sufficient for full-stall recovery training. Even though the stall algorithm does induce an adverse rolling moment at stall break, there is no indication that the unexpected effects of opposite aileron input are taken into account during full stall condition. The stall module does not incorporate randomisation, which likely contributes to predictability. In addition, the initiation of a stall break is deduced from airspeed instead of angle of attack, which likely leads to unrepresentative simulation of the effects of dynamic stall. The stall validation tests contained in the QTG are carried out through full aerodynamic stall, but these tests are conducted with rather mild lateral control inputs. These observations could be revised by a statement from an SME pilot, familiar with the stall characteristics of the particular aeroplane type. However, full-stall training is not included in the current EASA provisions, as all upset recovery training tasks

should be carried out solely as approach-to-stall exercises within the Validated Training Envelope.

The fidelity seems to be sufficient to a large extent for upset prevention training, as well as upset recovery training from the initiation of the stall warning. An approximate threshold of stall warning system activation in approach configuration is illustrated with the red dashed line, to give an impression of the relevant region. The actual activation angle may vary with respect to aeroplane configuration and flight condition.

The level of inaccuracy in the process of determining the flight test validated envelope was likely slightly higher than the tolerances set in the MQTG. Possible sources of error were at least the partially manual process of handling the collected data, time-offset in the synchronisation of simultaneously recorded video footages and rounding-off of results. The crosswind landing QTG test was conducted with full flaps configuration, and the highest data point of β achieved from that test was recorded in the influence of ground effect. All the other QTG tests used to outline the flight test validated envelope were conducted in approach configuration.

Due to the nature of employing linear functions in the modelling of effects of the sideslip angle, the width of the medium confidence envelope had to be partially based on engineering judgement. The level of inaccuracy inherited in this process is rather difficult to estimate. These conclusions could be further strengthened by a statement from an SME pilot, especially in part of the behaviour of the simulator in the most extreme sideslip angles.

7 Discussion

As a reaction to the adverse trend of LOC-I accidents, the provisions for upset related training and Full Flight Simulator qualification have been in a global state of transition in the 2010's. The Federal Aviation Administration of the United States has issued comprehensive UPRT requirements ahead of the European Aviation Safety Agency. At the time being, the EASA is in the process of expanding the scope of its corresponding set of regulations, as well as harmonising the regulatory framework with respect to the FAA. This intercontinental harmonisation is of great advantage for the FSTD industry, as well as for the training organisation industry.

The most fundamental difference between the provisions set by the aforementioned two agencies is, that in foreseeable near future the FAA will begin to require simulator conducted full-stall training starting in 2019, whereas the upcoming provisions set by the EASA will require exercises only from approach-to-stall situations.

In order to avoid negative training, it has been commonly recognised, that all simulator based upset prevention and recovery training should unquestionably be conducted within the technical capabilities of the device, providing sufficient fidelity throughout each exercise. The region of sufficient fidelity should essentially be founded on validation against actual flight test data. The current EASA regulations for air operators uses the term Validated Training Envelope for such a region, however the definition of that term is not encompassed within the technical qualification standards. The FAA uses the term FSTD training envelope, that which the EASA is in the process of adapting for its own regulations.

The entire domain in which a flight simulator can be flown, may be roughly divided into three subdivisions – or regions, based on the degree of reliability of the aerodynamic data behind the state of the simulation; the high confidence level region is based strictly on flight test data, the medium confidence level region may be based on reliable predictive methods supported by the aeroplane manufacturer, and finally the low confidence region consists of extrapolated data. These regions are commonly expressed as envelopes of the aerodynamic angles, namely the angle of attack α and the sideslip angle β, which fundamentally determine the aerodynamic forces and moments acting on the aeroplane.

By definition, the FSTD training envelope is a composition of the high and medium confidence level α-β envelopes. All training should primarily be conducted within the high confidence level region, although momentary excursions to the medium confidence level region are allowed, as long as the instructor is aware of the occurrence and the implications to the outcome of the training are properly taken into account. In such occurrences the expertise of the instructor is of particular importance in order to avoid negative training. The low confidence region should not be entered in any training task. To address the problematics involved, additional provisions are issued by the FAA and proposed by the EASA to incorporate feedback tools to the instructor operating stations, enabling the instructor to monitor all necessary information from the state and validity of the simulation, as well as from the inputs by the trainee.

To incorporate already qualified devices to training programmes conformant to the novel UPRT provisions, the qualification certificate holder may in some cases be forced to

determine the FSTD training envelope by itself. In such cases the analysis should principally be founded on all available flight test data from the OEM, software documentation by the simulator manufacturer, and any supporting material, such as the VDR document, if available.

A reasonable starting point for the determination of the high confidence level region are the tests incorporated in the QTG. If the simulator originates from an era when the values of α and β were not required to be included in the QTG test printouts, an alternative method has to be derived in order to solve them. These variables are inherently incorporated in the calculations of aerodynamic forces and moments of all Full Flight Simulators, and therefore they should be extractable at least via some digital interface. In order to determine the high confidence level region, those QTG tests should be selected that reach the highest values of α and β. A solid point of reference would be the sections concerning longitudinal and lateral stability/control, as well as take-off and landing. For the simulator in question for the second case study of this thesis, the most relevant QTG tests were found to be the following:

- stall in approach configuration,
- crosswind landing,
- crosswind take-off,
- minimum control speed (air).

When deriving the α-β region from these tests, distinction should be made between flaps-up and flaps-down configurations at minimum. If the VDR document is available, it should be studied in order to estimate the reliability of any possible engineering data that is employed in the QTG tests.

In order to determine the medium confidence level region, one should resolve the ranges and classify the sources of the look-up data behind the aerodynamic model of the simulator. It is impossible to provide universal instructions for the process, as the technical implementations of the aerodynamic models of simulators differ from each other, as well as the documentation by the simulator manufacturers come in a variety of formats. In the case of the simulator studied in the second case study of this thesis, the software detail design documentation in written form, provided by the manufacturer, turned out the be the most valuable source of reference. When assessing the source data and source code of the aerodynamic modelling, attention should be paid particularly to the stability derivatives listed as groups #1 and #2 in Table 6 (Chapter 5.8.1). However, the omission of any component of the aerodynamic model in the analysis should be a carefully reasoned decision. As a ground rule, the medium confidence level region should be that region that is not out of range of any existing look-up table.

Due to practical reasons, it is not possible to validate a confidence region fully at 100 percent. When outlining the envelopes – both the flight test validated high confidence level envelope and the analytical data based medium confidence level envelope – engineering judgement should be used when connecting the data points. Simplifications should be avoided in the regions of combination of high α and high β. Finally, it should be recognised, that when considering the fidelity of the simulation, the difference between medium and low confidence level regions is not always a clear cut, and therefore they

should not be regarded as binary; the closer the simulation gets to the extrapolated region, the less fidelity can be expected.

References

[1] National Transportation Safety Board, “Loss of Control on Approach, Colgan Air, Inc., Operating as Continental Connection Flight 3407, Bombardier DHC-8-400, N200WQ, Clarence Center, New York, February 12, 2009,” Washington D.C., The United States of America, 2010.

[2] Bureau d’Enquêtes et d’Analyses pour la sécurité de l’aviation civil, “Final Report on 1st June 2009 to the Airbus A330-203 registered F-GZCP operated by Air France flight AF 447 Rio De Janeiro - Paris,” 2012.

[3] International Civil Aviation Organization, “ICAO Safety Report 2015 Edition,” Montreal, Quebec, Canada, 2015.

[4] B. Crawford, *Unusual Attitudes and the Aerodynamics of Maneuvering Flight,* Flightlab Inc., 2009.

[5] International Civil Aviation Organization, *Doc 10011 Manual on aeroplane upset prevention and recovery training,* Montreal, Quebec, Canada, 2014.

[6] ICAO, Airbus, ATR, Boeing, Bombardier, Embraer, “Airplane Upset Prevention and Recovery Training Aid for Transport Category Airplanes, Revision 3,” 2 2017. [Online]. Available: https://www.icao.int/safety/LOCI/AUPRTA/index.html. [Accessed 1 10 2017].

[7] International Civil Aviation Organization, *Doc 10011 Manual on aeroplane upset prevention and recovery training,* 2014.

[8] S. K. Advani and J. A. Schroeder, *Global Implementation of Upset Prevention & Recovery Training,* American Institute of Aeronautics and Astronautics, 2015.

[9] AURTA Working Group, *Airplane Upset Recovery Training Aid, Revision 2,* 2008.

[10] Jacobson, Steven R., NASA Dryden Flight Research Center, ”Aircraft Loss of Control Causal Factors and Mitigation Challenges,” American Institute of Aeronautics and Astronautics, California, the United States of America, 2010.

[11] The Boeing Company, “Statistical Summary of Commercial Jet Airplane Accidents - Worldwide Operations 1959-2015,” 2016.

[12] International Air Transport Association, “Loss of Control In-Flight Accident Analysis Report 2010 - 2014,” Montreal, Quebec, Canada, 2015.

[13] European Aviation Safety Agency, *Terms of Reference for a rulemaking task: Loss of Control Prevention and Recovery Training, RMT.0581 and RMT.0582, Issue 2,* 2015.

[14] International Civil Aviation Organization, *Amendment No. 3 to the Procedures for Air Navigation Services - Training (PANS-TRG, Doc 9868),* Montreal, Quebec, Canada, 2014.

[15] European Aviation Safety Agency, *Explanatory Note to Decision 2015/012/R - Upset Prevention and Recovery Training,* 2015.

[16] European Aviation Safety Agency, *NPA 2015-13 Loss of control prevention and recovery training,* 2015.

[17] European Aviation Safety Agency, *Terms of Reference for a rulemaking task: Update of Flight Simulation Training Devices requirements, RMT.0196, Issue 1,* 2016.

[18] European Aviation Safety Agency, *NPA 2017-13 Update of flight simulation training devices requirements,* 2017.

[19] U.S. Department of Transportation, Federal Aviation Administration, *Advisory Circular 120-111 Upset Prevention and Recovery Training,* 2017.

[20] U.S. Department of Transportation, Federal Aviation Administration, *Advisory Circular 120-109A Stall Prevention and Recovery Training,* 2015.

[21] Federal Government of the United States, *Code of Federal Regulations, Title 14, Appendix A to Part 60, Qualification Performance Standards for Airplane Full Flight Simulators,* 2016.

[22] European Aviation Safety Agency, *Acceptable Means of Compliance (AMC) and Guidance Material (GM) to Annex III - Part-ORO Issue 2 Amendment 2,* 2015.

[23] European Aviation Safety Agency, *Commission Regulation (EU) No 965/2012 on Air Operations,* 2012.

[24] European Aviation Safety Agency, *Certification Specifications for Aeroplane Flight Simulation Training Devices,* 2012.

[25] U.S. Department of Transportation, Federal Aviation Administration, *Advisory Circular 120-40A Airplane Simulator and Visual System Evaluation,* 1986.

[26] U.S. Department of Transportation, Federal Aviation Administration, *National Simulator Program FSTD Qualification Guidance Bulletin NSP GB 14-01,* 2016.

[27] U.S. Department of Transportation, Federal Aviation Administration, *National Simulator Program FSTD Qualification Guidance Bulletin NSP GB 11-05,* 2016.

[28] Federal Government of the United States, *14 CFR Part 60 NSP Consolidated Version,* 2016.

[29] S. J. Advani ja J. N. Field, ”Upset Prevention and Recovery Training in Flight Simulators,” National Aerospace Laboratory NLR, Amsterdam, The Netherlands, 2011.

[30] National Transportation Safety Board, ”In-Flight Separation of Vertical Stabilizer American Airlines Flight 587 Airbus Industrie A300-605R, N14053 Belle Harbor, New York, November 12, 2001,” Washington D.C., The United States of America, 2004.

[31] International Air Transport Association, *Guidance Material and Best Practices for the Implementation of Upset Prevention and Recovery Training,* 1st Edition ed., Montreal, Quebec, Canada, 2015.

[32] P. J. Bolds-Moorehead, V. G. Chaney, T. Lutz and S. Vaux, “Stalling Transport Aircraft,” Royal Aeronautical Society, 2013.

[33] M. E. Beyers, M. Mamou, A. P. Brown and Y. Mebarki, “Computational Fluid Dynamics and Experimental Investigation of Airplane Stall Dynamics with Wing Contamination,” International Congress of the Aeronautical Sciences, 2008.

[34] Z. Yang, H. Igarashi, M. Martin ja H. Hu, ”An Experimental Investigation on Aerodynamic Hysteresis of a Low-Reynolds Number Airfoil,” American Institute of Aeronautics and Astronautics, Reno, Nevada, the United States of America, 2008.

[35] A. D. Woodrow and J. T. Webb, “Handbook of Aerospace and Operational Physiology,” Air Force Research Library, 2011.

[36] Bahrain Ministry of Transportation, “Final Report on A320 (A40-EK) Aircraft Accident (Gulf Air Flight 072),” 2002.

[37] European Aviation Safety Agency, *NPA 2017-06 Loss of control or loss of flight path during go-around or other flight phases,* 2017.

[38] D. Allerton, Principles of Flight Simulation, John Wiley & Sons, Ltd, 2009.

[39] *Qualification Test Guide Airbus A350 Full Flight Simulator Level D,* 2017.

[40] R. L. Page, *Brief history of flight simulation,* Sydney, Australia: The SimTechT 2000 Organizing and Technical Committee, 2000.

[41] J. M. Rolfe and K. J. Staples, Flight Simulation, Cambridge University Press, 1986.

[42] Airbus S.A.S, *A318/A319/A320/A321 Flight Crew Operating Manual,* 2015.

[43] C. R. Hanke and D. R. Nordwall, "The Simulation of a Jumbo Jet Transport Aircraft Volume II: Modeling Data," The Boeing Company, 1971.

[44] M. R. Napolitano, Aircraft Dynamics: From Modeling to Simulation, John Wiley & Sons Inc., 2012.

[45] International Air Transport Association, *Flight Simulator Design and Performance Data Requirements, 6th Edition,* Montreal, Quebec, Canada, 2000.

[46] International Civil Aviation Organization, *Doc 9625 Manual of Criteria for the Qualification of Flight Simulators,* Montreal, Quebec, Canada, 2003.

[47] European Aviation Safety Agency, *Certification Specifications and Guidance Material for Simulator Data CS-SIMD,* 2014.

[48] J. Roskam and C.-T. E. Lan, Airplane Aerodynamics and Performance, Kansas, USA: DARcorporation, 1997.

[49] C. R. Hanke and D. R. Nordwall, "The Simulation of a Large Jet Transport Aircraft Volume I: Mathematical Model," The Boeing Company, 1971.

[50] The Boeing Company, "Historical Snapshot: 747 Commercial Transport," 2017. [Online]. Available: http://www.boeing.com/history/products/747.page. [Accessed 2017].

[51] Raytheon Aircraft, *Aircraft Flight Manual for Beechcraft Super King Air 300.*

[52] *King Air 300 Simulator, Software Detail Design Document,* 1990.

[53] Royal Aeronautical Society, Aeroplane Flight Simulator Evauation Handbook, Third Edition, London, the United Kingdom, 2005.

[54] *Qualification Test Guide King Air 300/200, Full Flight Simulator JAA Level CG,* 1990.

[55] European Aviation Safety Agency, *Certification Specifications for Normal, Utility, Aerobatic and Commuter Category Aeroplanes CS-23,* 2003.

Attachments

Attachment 1. Extracts from the Boeing 747 aerodynamic data

Attachment 1. Extracts from the Boeing 747 aerodynamic data

Lift force coefficient

Table A1.1 Basic lift coefficient at low airspeeds

Flap setting	$C_{L_{Basic}}$ at $\propto_{W.D.P} = -5°$	Maximum demonstrated $C_{L_{Basic}}$	$\propto_{W.D.P}$ at maximum demonstrated $C_{L_{Basic}}$
Flaps up	-0.48	1.37	+25°
Flaps up, full slats extended	-0.55	1.68	+25°
Flaps 1°	-0.43	1.57	+25°
Flaps 5°	-0.55	1.82	+25°
Flaps 10°	-0.40	1.92	+25°
Flaps 20°	-0.26	2.09	+20°
Flaps 25°	-0.04	2.26	+19°
Flaps 30°	+0.20	2.47	+19°

Table A1.2 Basic lift coefficient at high airspeed

Mach number	Range of $\propto_{W.D.P}$	Minimum value of $C_{L_{Basic}}$	Maximum value of $C_{L_{Basic}}$
0.30	-5° to +25°	-0.30	1.37
0.50	-5° to +15°	-0.42	1.12
0.74	-5° to +15°	-0.39	1.18
0.80	-5° to +10°	-0.38	1.03
0.84	-5° to +10°	-0.40	1.07
0.86	-5° to +10°	-0.43	1.15
0.88	-5° to +10°	-0.45	1.13
0.90	-5° to +10°	-0.46	1.17
0.92	-5° to +10°	-0.44	1.08
0.95	-5° to +10°	-0.40	1.02
0.97	-5° to +10°	-0.40	0.93

Table A1.3 Lift force terms

Term	Flight condition	ΔC_L
$(\Delta C_L)_{\alpha_{W.D.P.}=0}$	Flaps up, Mach 0.30, Sea Level	-0.002
	Flaps up, Mach 0.80, 40 000 ft	-0.022
	Flaps up, Mach 0.88, 10 000 ft (Maximum measured absolute value with flaps up)	-0.056
	Flaps 30°, 250 kts EAS (Maximum measured absolute value with flaps extended)	-0.240

$\Delta\left(\frac{dC_L}{d\alpha}\right)$	Flaps up, Mach 0.30, Sea Level	-0.0065 / deg $\propto_{\text{W.D.P}}$
	Flaps up, Mach 0.80, 40 000 ft	-0.0350 / deg $\propto_{\text{W.D.P}}$
	Flaps up, Mach 0.97, 10 000 ft (Maximum measured absolute value with flaps up)	-0.0475 / deg $\propto_{\text{W.D.P}}$
	Flaps 20°, 250 kts EAS (Maximum measured absolute value with flaps extended)	-0.0148 / deg $\propto_{\text{W.D.P}}$
$\frac{dC_L}{d\hat{\alpha}}\left(\frac{\dot{\alpha}\bar{c}}{2V}\right)$	Flaps up, Mach 0.30, Sea Level, $\dot{\propto}_{\text{W.D.P}} = 5\frac{deg}{s}$	-0.024
	Flaps up, Mach 0.30, Sea Level, $\dot{\propto}_{\text{W.D.P}} = 10\frac{deg}{s}$	-0.048
	Flaps up, Mach 0.30, Sea Level, $\dot{\propto}_{\text{W.D.P}} = 15\frac{deg}{s}$	-0.072
	Flaps up, Mach 0.80, 40 000 ft, , $\dot{\propto}_{\text{W.D.P}} = 5\frac{deg}{s}$	-0.008
$\frac{dC_L}{d\hat{q}}\left(\frac{q\bar{c}}{2V}\right)$	Flaps up, Mach 0.30, Sea Level, $\text{q} = 5\frac{\text{deg}}{s}$, $\text{C.G} = 0.25\ \text{MAC}$	0.019
	Flaps up, Mach 0.30, Sea Level, $\text{q} = 10\frac{\text{deg}}{s}$, $\text{C.G} = 0.25\ \text{MAC}$	0.039
	Flaps up, Mach 0.30, Sea Level, $\text{q} = 15\frac{\text{deg}}{s}$, $\text{C.G} = 0.25\ \text{MAC}$	0.058
	Flaps up, Mach 0.80, 40 000 ft, $\text{q} = 5\frac{\text{deg}}{s}$, $\text{C.G} = 0.25\ \text{MAC}$	0.010
$\frac{dC_L}{dn_z}$	Flaps up, Mach 0.30, Sea Level	$0.0231 * \text{n}_{z_{max=2.5}}$
	Flaps up, Mach 0.80, 40 000 ft	$0.0278 * \text{n}_{z_{max=2.5}}$
	Flaps up, Mach 0.87, 40 000 ft (Maximum measured value with flaps up)	$0.0297 * \text{n}_{z_{max=2.5}}$

$K_\alpha \frac{dC_L}{d\eta}$	All flap settings, Mach 0.30, Sea Level, $\propto_{W.D.P} < +15°$	0.0132 / deg $\eta_{F.R.L.}$
	All flap settings, Mach 0.86, 40 000 ft, $\propto_{W.D.P} < +15°$ (Maximum measured absolute value)	0.0153 / deg $\eta_{F.R.L.}$
$K_\alpha \frac{dC_L}{d\delta_{e_i}}$	All flap settings, Mach 0.30, Sea Level, $\propto_{W.D.P} < +15°$	0.0026 / deg δ_{e_i}
	All flap settings, Mach 0.60, 40 000 ft, $\propto_{W.D.P} < +15°$ (Maximum measured absolute value)	0.0036 / deg δ_{e_i}
$K_\alpha \frac{dC_L}{d\delta_{e_o}}$	All flap settings, Mach 0.30, Sea Level, $\propto_{W.D.P} < +15°$	0.0028 / deg δ_{e_o}
	All flap settings, Mach 0.40, 40 000 ft, $\propto_{W.D.P} < +15°$ (Maximum measured absolute value)	0.0039 / deg δ_{e_o}
$\Delta C_{L_{outboard\ ailerons}}$	Per aileron, Flaps up, $\propto_{W.D.P} = 10°$	0.0180 ($\delta_{oa} = -15°$) -0.0460 ($\delta_{oa} = +25°$)
	Per aileron, Flaps 30°, $\propto_{W.D.P} = 10°$	0.0200 ($\delta_{oa} = -15°$) -0.0650 ($\delta_{oa} = +25°$)
$\Delta C_{L_{landing\ gear}}$	Flaps 30°, Mach < 0.30, $\propto_{W.D.P} = +6°$ (Maximum measured absolute value with full flaps extended)	-0.030
	Flaps up, Mach < 0.30, $\propto_{W.D.P} = -5°$ (Maximum measured absolute value with flaps up)	0.046

Table A1.4 Total lift force coefficients

Mach number	Maximum demonstrated C_L	C_L of initial buffet boundary
<0.30	1.12	0.87
0.30	1.06	0.86
0.50	1.01	0.84
0.70	0.96	0.80
0.80	0.90	0.73
0.90	0.76	0.58
0.97	0.59	0.32

Drag force coefficient

Table A1.5 Basic drag coefficient at low airspeeds

Flap setting	$C_{D_{Basic}}$ at $\propto_{W.D.P} = -5°$	Minimum demonstrated $C_{D_{Basic}}$	$\propto_{W.D.P}$ at minimum demonstrated $C_{D_{Basic}}$	Maximum demonstrated $C_{D_{Basic}}$	Range of $\frac{dC_D}{d\eta}\eta_{F.R.L.}$, per degree of stabiliser angle ($\propto_{W.D.P} = -5 - +25°$)
1°	0.091	0.028	+3°	0.448	-0.0031 – 0.0047
10°	0.120	0.042	+3°	0.459	-0.0031 – 0.0041
25°	0.092	0.070	0°	0.623	-0.0043 – 0.0032
30°	0.146	0.115	-1°	0.688	-0.0051 – 0.0034

Table A1.6 Basic drag coefficient at high airspeeds

Mach number	Upper limit of C_L	Demonstrated $[C_D]_M$ at the upper limit of C_L	Upper extrapolation limit of C_L	Upper extrapolated value for $[C_D]_M$
0.30	0.70	0.0430	1.37 (extrapolated)	0.2090
0.50	0.70	0.0420	1.36 (extrapolated)	0.2080
0.70	0.70	0.0457	1.31 (extrapolated)	0.2100
0.80	0.60	0.0353	0.77 (extrapolated)	0.0661
0.84	0.60	0.0369	0.76 (extrapolated)	0.0679
0.86	0.60	0.0405	0.74 (extrapolated)	0.0696
0.88	0.60	0.0471	0.70 (extrapolated)	0.0718
0.90	0.60	0.0577	0.67 (extrapolated)	0.0729
0.92	0.60	0.0675	0.63 (extrapolated)	0.0759
0.95	0.60	0.0780	N/A	N/A
0.97	0.53	0.0778	N/A	N/A

Table A1.7 Maximum and minimum values of landing gear drag increment

Condition	$\Delta C_{D_{landing\ gear}}$
Flaps up, Mach 0.82, $\propto_{W.D.P} = +5°$	0.0344
Flaps 30°, Low speed, $\propto_{W.D.P} = +12°$	0.0070

Table A1. 8 Maximum values for drag increment due to sideslip

Condition	$\Delta C_{D_{sideslip}}$ at $\beta = \pm 15°$
Flaps up, 1°, 5°, 10°, 20°	0.023
Flaps 25°	0.028
Flaps 30°	0.031

Pitching moment coefficient

Table A1.9 Basic pitching moment coefficient at low airspeeds

Flap setting	$C_{m_{.25_{Basic}}}$ at $\propto_{W.D.P} = -5°$	$C_{m_{.25_{Basic}}}$ at $\propto_{W.D.P} = +25°$
Flaps up	0.270	-0.535
Flaps up, full slats extended	0.270	-0.750
Flaps 1°	0.230	-0.525
Flaps 5°	0.265	-0.645
Flaps 10°	0.280	-0.855
Flaps 20°	0.190	-0.670
Flaps 25°	0.145	-0.765
Flaps 30°	0.120	-0.950

Table A1.10 Basic pitching moment coefficient at high airspeeds

Mach number	Range of $\propto_{W.D.P}$	$C_{m_{.25_{Basic}}}$ at minimum $\propto_{W.D.P}$	$C_{m_{.25_{Basic}}}$ at maximum $\propto_{W.D.P}$	$\propto_{W.D.P}$ at upper extrapolation limit	Upper extrapolated value for $C_{m_{.25_{Basic}}}$
0.30	-5° to +18°	0.268	-0.159	N/A	N/A
0.50	-5° to +15°	0.247	-0.139	+18° (extrapolated)	-0.323
0.74	-5° to +15°	0.225	-0.223	+18° (extrapolated)	-0.374
0.80	-5° to +15°	0.225	-0.239	+18° (extrapolated)	-0.368
0.84	-5° to +12°	0.238	-0.161	+18° (extrapolated)	-0.370
0.86	-5° to +12°	0.247	-0.162	+18° (extrapolated)	-0.350
0.88	-5° to +12°	0.244	-0.161	+18° (extrapolated)	-0.331
0.90	-5° to +10°	0.245	-0.135	+18° (extrapolated)	-0.303
0.92	-5° to +10°	0.279	-0.146	+17° (extrapolated)	-0.263
0.95	-5° to +10°	0.318	-0.152	+15° (extrapolated)	-0.233
0.97	-5° to +10°	0.356	-0.156	+12° (extrapolated)	-0.200

Table A1.11 Pitching moment terms

Term	Flight condition	ΔC_m
$(\Delta C_{m_{.25}})_{\alpha_{W.D.P.=0°}}$	Flaps up, Mach 0.30, Sea Level	-0.0075
	Flaps up, Mach 0.80, 40 000 ft	-0.0045
	Flaps up, Mach 0.92, 10 000 ft (Maximum measured absolute value with flaps up)	-0.0680
	Flaps 30°, 250 kts EAS (Maximum measured absolute value with flaps extended)	0.0260
$\Delta\left(\frac{dC_{m_{.25}}}{d\alpha}\right)$	Flaps up, Mach 0.30, Sea Level	0.0045 / deg $\propto_{W.D.P}$

	Flaps up, Mach 0.80, 40 000 ft	0.0072 / deg $\propto_{\text{W.D.P}}$
	Flaps up, Mach 0.97, 10 000 ft (Maximum measured absolute value with flaps up)	0.0288 / deg $\propto_{\text{W.D.P}}$
	Flaps 30°, 250 kts EAS (Maximum measured absolute value with flaps extended)	0.0084 / deg $\propto_{\text{W.D.P}}$
$\frac{dC_m}{d\hat{\alpha}}\left(\frac{\dot{\alpha}\bar{c}}{2V}\right)$	Flaps up, Mach 0.30, Sea Level, $\dot{\propto}_{\text{W.D.P}} = 5\frac{\text{deg}}{s}$, $\text{C.G} = 0.25\ \text{MAC}$	-0.011
	Flaps up, Mach 0.30, Sea Level, $\dot{\propto}_{\text{W.D.P}} = 10\frac{\text{deg}}{s}$, $\text{C.G} = 0.25\ \text{MAC}$	-0.023
	Flaps up, Mach 0.30, Sea Level, $\dot{\propto}_{\text{W.D.P}} = 15\frac{\text{deg}}{s}$, $\text{C.G} = 0.25\ \text{MAC}$	-0.034
	Flaps up, Mach 0.80, 40 000 ft, , $\dot{\propto}_{\text{W.D.P}} = 5\frac{deg}{s}$, $\text{C.G} = 0.25\ \text{MAC}$	-0.010
$\frac{dC_{m_{.25}}}{d\hat{q}}\left(\frac{q\bar{c}}{2V}\right)$	Flaps up, Mach 0.30, Sea Level, $\text{q} = 5\frac{\text{deg}}{s}$	-0.072
	Flaps up, Mach 0.30, Sea Level, $\text{q} = 10\frac{\text{deg}}{s}$	-0.145
	Flaps up, Mach 0.30, Sea Level, $\text{q} = 15\frac{\text{deg}}{s}$	-0.217
	Flaps up, Mach 0.80, 40 000 ft, $\text{q} = 5\frac{\text{deg}}{s}$	-0.037
$\frac{dC_{m_{.25}}}{dn_z}n_z$	Flaps up, Mach 0.30, Sea Level	$-0.0225 * \text{n}_{z_{max=2.5}}$
	Flaps up, Mach 0.80, 40 000 ft	$-0.0258 * \text{n}_{z_{max=2.5}}$
	Flaps up, Mach 0.87, 40 000 ft (Maximum measured value with flaps up)	$-0.0264 * \text{n}_{z_{max=2.5}}$
$K_\alpha \frac{dC_{m_{.25}}}{d\eta}\eta_{F.R.L.}$	All flap settings, Mach 0.30, Sea Level, $\propto_{\text{W.D.P}} < +15°$	-0.0495 / deg $\eta_{\text{F.R.L.}}$
	All flap settings, Mach 0.86, 40 000 ft, $\propto_{\text{W.D.P}} < +15°$ (Maximum measured absolute value)	-0.0570 / deg $\eta_{\text{F.R.L.}}$

$K_\alpha \frac{dC_{m_{.25}}}{d\delta_{e_i}} \delta_{e_i}$	All flap settings, Mach 0.30, Sea Level, $\propto_{\text{W.D.P}} < +15°$, $\text{C.G} = 0.25$ MAC	-0.0110 / deg δ_{e_i}
	All flap settings, Mach 0.60, 40 000 ft, $\propto_{\text{W.D.P}} < +15°$, $\text{C.G} = 0.25$ MAC (Maximum measured absolute value)	-0.0140 / deg δ_{e_i}
$K_\alpha \frac{dC_{m_{.25}}}{d\delta_{e_o}} \delta_{e_o}$	All flap settings, Mach 0.30, Sea Level, $\propto_{\text{W.D.P}} < +15°$, $\text{C.G} = 0.25$ MAC	-0.0110 / deg δ_{e_o}
	All flap settings, Mach 0.40, 40 000 ft, $\propto_{\text{W.D.P}} < +15°$, $\text{C.G} = 0.25$ MAC (Maximum measured absolute value)	-0.0154 / deg δ_{e_o}
$\Delta C_{m_{.25_{landing\ gear}}}$	Flaps 30°, Mach < 0.30, $\propto_{\text{W.D.P}} = +23°$ (Maximum measured absolute value with full flaps extended)	-0.066
	Flaps up, Mach < 0.30, $\propto_{\text{W.D.P}} = +25°$ (Maximum measured absolute value with flaps up)	0.023

Rolling moment coefficient

Table A1.12 Rolling moment terms

Term	Flight condition	ΔC_l
$\frac{dC_l}{d\beta}\beta$	Flaps up, Mach 0.30, $\propto_{W.D.P} = +22°$, $\beta = 3°$	-0.00339
	Flaps up, Mach 0.30, $\propto_{W.D.P} = +22°$, $\beta = 15°$	-0.00814
	Flaps 30°, Mach 0.30, $\propto_{W.D.P} = +18°$, $\beta = 7°$	-0.04463
	Flaps 30°, Mach 0.30, $\propto_{W.D.P} = +18°$, $\beta = 15°$	-0.07554
	Flaps up, Mach 0.80, $\propto_{W.D.P} = +7°$, $\beta = 3°$	-0.01461
	Flaps up, Mach 0.80, $\propto_{W.D.P} = +7°$, $\beta = 15°$	-0.03506
$\frac{dC_l}{d\hat{p}}\frac{p_s b}{2V}$	Flaps up, Mach 0.80, $\propto_{W.D.P} = +7°$	$-0.304\frac{1}{rad}\left(\frac{p_s b}{2V}\right)$
	Flaps up, Mach 0.30, $\propto_{W.D.P} = +22°$	$-0.142\frac{1}{rad}\left(\frac{p_s b}{2V}\right)$
	Flaps 30°, Mach 0.30, $\propto_{W.D.P} = +18°$	$-0.427\frac{1}{rad}\left(\frac{p_s b}{2V}\right)$
	Flaps 30°, Mach 0.30, $\propto_{W.D.P} = +8°$	$-0.510\frac{1}{rad}\left(\frac{p_s b}{2V}\right)$
$\frac{dC_l}{d\hat{r}}\frac{r_s b}{2V}$	Flaps up, Mach 0.80, $\propto_{W.D.P} = +7°$	$-0.499\frac{1}{rad}\left(\frac{r_s b}{2V}\right)$
	Flaps up, Mach 0.30, $\propto_{W.D.P} = +22°$	$-0.294\frac{1}{rad}\left(\frac{r_s b}{2V}\right)$
	Flaps 30°, Mach 0.30, $\propto_{W.D.P} = +18°$	$-0.263\frac{1}{rad}\left(\frac{r_s b}{2V}\right)$
	Flaps 30°, Mach 0.30, $\propto_{W.D.P} = +8°$	$-0.171\frac{1}{rad}\left(\frac{r_s b}{2V}\right)$

Yawing moment coefficient

Table A1.13 Yawing moment terms

Term	Flight condition	ΔC_n
$\frac{dC_n}{d\beta}\beta$	Flaps up, Mach 0.30, $\propto_{W.D.P} = +22°$, $\beta = 3°$	0.00747
	Flaps up, Mach 0.30, $\propto_{W.D.P} = +22°$, $\beta = 15°$	0.03735
	Flaps 30°, Mach 0.30, $\propto_{W.D.P} = +18°$, $\beta = 7°$	0.02870
	Flaps 30°, Mach 0.30, $\propto_{W.D.P} = +18°$, $\beta = 15°$	0.06150
$\frac{dC_n}{d\hat{\beta}}$	All flap settings, Mach 0.30, $\propto_{W.D.P} = -5°$	$-0.0310\frac{1}{rad}\left(\frac{\dot{\beta}b}{2V}\right)$
	All flap settings, Mach 0.30, $\propto_{W.D.P} = +25°$	$-0.0148\frac{1}{rad}\left(\frac{\dot{\beta}b}{2V}\right)$
$\frac{dC_n}{d\hat{p}}$	Flaps 30°, Mach 0.30, $\propto_{W.D.P} = +14°$	$-0.260\frac{1}{rad}\left(\frac{p_s b}{2V}\right)$
	Flaps 30°, Mach 0.30, $\propto_{W.D.P} = +22°$	$-0.054\frac{1}{rad}\left(\frac{p_s b}{2V}\right)$
	Flaps up, Mach 0.80, $\propto_{W.D.P} = +7°$	$-0.049\frac{1}{rad}\left(\frac{p_s b}{2V}\right)$
	Flaps up, Mach 0.90, $\propto_{W.D.P} = +11°$	$0.092\frac{1}{rad}\left(\frac{p_s b}{2V}\right)$
$\frac{dC_n}{d\hat{r}}$	Flaps 30°, Mach 0.30, $\propto_{W.D.P} = -5°$, C. G $= 0.25$ MAC	$-0.275\frac{1}{rad}\left(\frac{r_s b}{2V}\right)$
	Flaps 30°, Mach 0.30, $\propto_{W.D.P} = +25°$, C. G $= 0.25$ MAC	$-0.480\frac{1}{rad}\left(\frac{r_s b}{2V}\right)$
	Flaps up, Mach 0.30, $\propto_{W.D.P} = -5°$, C. G $= 0.25$ MAC	$-0.180\frac{1}{rad}\left(\frac{r_s b}{2V}\right)$
	Flaps up, Mach 0.30, $\propto_{W.D.P} = +25°$, C. G $= 0.25$ MAC	$-0.295\frac{1}{rad}\left(\frac{r_s b}{2V}\right)$

Side force coefficient

Table A1.14 Side force terms

Term	Flight condition	ΔC_Y
$\frac{dC_Y}{d\beta}\beta$	Flaps up, Mach 0.30, $\propto_{W.D.P} = +22°$, $\beta = 3°$	-0.045
	Flaps up, Mach 0.30, $\propto_{W.D.P} = +22°$, $\beta = 15°$	-0.225
	Flaps 30°, Mach 0.30, $\propto_{W.D.P} = +18°$, $\beta = 7°$	-0.140
	Flaps 30°, Mach 0.30, $\propto_{W.D.P} = +18°$, $\beta = 15°$	-0.300
	Flaps up, Mach 0.80, $\propto_{W.D.P} = +7°$, $\beta = 3°$	-0.047
	Flaps up, Mach 0.80, $\propto_{W.D.P} = +7°$, $\beta = 15°$	-0.233
$\frac{dC_Y}{d\hat{p}}$	Flaps up, $\propto_{W.D.P} = +22°$	$1.31\frac{1}{rad}\left(\frac{p_s b}{2V}\right)$
	Flaps 30°, $\propto_{W.D.P} = +18°$	$1.26\frac{1}{rad}\left(\frac{p_s b}{2V}\right)$
	Flaps up, $\propto_{W.D.P} = -5°$	$-0.36\frac{1}{rad}\left(\frac{p_s b}{2V}\right)$
$\frac{dC_Y}{d\hat{r}}$	Flaps up, $\propto_{W.D.P} = +22°$	$-0.095\frac{1}{rad}\left(\frac{r_s b}{2V}\right)$
	Flaps 30°, $\propto_{W.D.P} = +18°$	$0.067\frac{1}{rad}\left(\frac{r_s b}{2V}\right)$
	Flaps up, $\propto_{W.D.P} = -5°$	$0.295\frac{1}{rad}\left(\frac{r_s b}{2V}\right)$